Normandie Université

UNIVERSITÉ DE ROUEN NORMANDIE

THÈSE

Pour obtenir le diplôme de doctorat

Spécialité **INFORMATIQUE**

Préparée au sein de l'**Université de Rouen Normandie**

Adressing data Incest for Cooperative Localization in Multi-sensor Multi-vehicle Systems

Présentée et soutenue par

XIAOYU SHAN

Thèse soutenue le 17/09/2024

devant le jury composé de :

M. HOUCINE CHAFOUK	Professeur des Universités - ESIGELEC ROUEN	Directeur de thèse
M. ADNANE CABANI	Chargé de Recherche - ESIGELEC ROUEN	Co-directeur de thèse
M. ABDELAZIZ BENSRHAIR	Professeur des Universités - INSA de Rouen Normandie	Membre du jury
M. MALALATIANA RANDRIAMASY	-	Membre du jury
M. NACER M'SIRDI	Professeur des Universités - Aix-Marseille université	Rapporteur du jury
M. ABDELHAMID RABHI	Professeur des Universités - UNIVERSITE AMIENS PICARDIE JULES VERNE	Rapporteur du jury

Thèse dirigée par **HOUCINE CHAFOUK** (INSTITUT DE RECHERCHE EN SYSTEMES ELECTRONIQUES EMBARQUES) et **ADNANE CABANI** (ESIGELEC ROUEN)

ESIGELEC

MIIS

irseem UR 4353

Normandie Université

THÈSE

Pour obtenir le diplôme de doctorat

Spécialité Informatique

Préparée au sein de l'Université de Rouen

Addressing Data Incest for Cooperative Localization in Multi-sensor Multi-vehicle Systems

Présentée et soutenue par
Xiaoyu SHAN

Thèse soutenue publiquement le 17/09/2024 devant le jury composé de		
Abdelhamid RABHI	Professeur à l'Université de Picardie Jules Veme	Rapporteur
Nacer MSIRDI	Professeur à l'Université Aix-Marseille	Rapporteur
Abdelaziz BENSRHAIR	Professeur à l'INSA de Rouen Normandie	Examinateur
Malalatiana RANDRIAMASY	Docteure à SANEF Groupe	Examinateur
Houcine CHAFOUK	Professeur à l'ESIGELEC de Rouen	Directeur de thèse
Adnane CABANI	Professeur à l'ESIGELEC de Rouen	Codirecteur de thèse

Thèse dirigée par Houcine CHAFOUK et Adnane CABANI, laboratoire IRSEEM

UNIVERSITÉ DE ROUEN NORMANDIE

MIIS

ESIGELEC Rouen
INGÉNIEUR.E.S GÉNÉRALISTES
SYSTÈMES INTELLIGENTS ET CONNECTÉS

irseem
EA 4353

Acknowledgments

Firstly, I would like to express my gratitude to my supervisors, professor Houcine CHAFOUK and professor Adnane CABANI, for their academic guidance and daily life support throughout my doctoral journey of over three years.

Next, thanks to the members of CSI, professor Maan EL BADAOUI EL NEJJAR and Professor Abdelaziz BENSRHAIR. I truly appreciate your invaluable insights into my research.

Then, thanks to professor Abdelhamid RABHI, professor Nacer MSIRDI, professor Abdelaziz BENSRHAIR, and Dr. Malalatiana RANDRIAMASY for joining my defense.

Lastly, I am grateful to ESIGELEC and the China Scholarship Council (CSC) for providing me with the wonderful opportunity to accomplish my doctoral research.

List of abbreviations

Abbreviations	Description
5G	5th generation mobile network
6-DoF	Six degrees of freedom
AI	Artificial intelligence
A-SMGCS	Advanced-surface movement guidance and control system
ACKF	Adaptive cubature Kalman filter
CL	Cooperative localization
CIF	Covariance intersection filter
CMAD	Cross mean absolute difference
CKF	Cubature Kalman filter
DMR	Drivable moving search region
DOA	Direction-of-arrival
DR	Dead reckoning
EKF	Extended Kalman filter
FDE	Fault detection and exclusion
FRPDM	Free-resolution probability distributions map
GNSS	Global navigation satellite system
GPS	Global positioning system
GI	Guard interval
HD	High-definition
IMU	Inertial measurement unit
IoT	Internet of things
IoV	Internet of vehicle
ITS	Intelligent transportation system

ICP	Interval constraint propagation
ISCIF	Interval split covariance intersection filter
KF	Kalman filter
KLD	Kullback–Leibler divergence
LiDAR	Light detection and ranging
LCCH	left control channel
MCL	Monte Carlo localization
MSMV	Multi-sensor multi-vehicle
NCC	Normalized cross-correlation
NLOS	Non-line-of-sight
OBU	Onboard unit
PF	Particle filter
RAM	Random access memory
RCCH	Right control channel
RANSAC	Random sample consensus algorithm
RMSE	Root mean square error
RSSI	Received signal strength indication
RSUs	Roadside units
RMSE	Root mean square error
SBL	Sparse Bayesian learning
SLAM	Simultaneous localization and mapping
SCIF	Split covariance intersection filter
TDOA	Time difference of arrival
TDMA	time division multiple access
TPSM	Third party sparse maps
UAV	Unmanned aerial vehicle

UKF	Unscented Kalman filter
V2I	Vehicle-to-infrastructure
V2V	Vehicle-to-vehicle
V2X	Vehicle-to-everything
VANETs	Vehicular ad hoc networks
vSLAM	Vision SLAM

Contents

Acknowledgments i

List of abbreviations ii

Publications xi

Résumé xii

Chapter One: Introduction 2

1.1 Context of the thesis . . . 2

1.2 Objectives and contributions . . . 5

Chapter Two: Survey on vehicle localization techniques 7

2.1 Introduction . . . 7

2.2 Active sensor based self-localization Methods . . . 7

2.2.1 LiDAR-based Self-localization Methods . . . 7

2.2.2 Radar-based Self-localization Methods . . . 10

2.2.3 Ultrasonic-based Self-localization Methods . . . 11

2.2.4 Discussion . . . 12

2.3 Passive sensor based self-localization Methods . . . 13

2.3.1 IMU-based Self-localization Methods . . . 13

2.3.2 GPS-based Self-localization Methods . . . 14

2.3.3 Vision-based Self-localization Methods . . . 16

2.3.4 Discussion . . . 17

2.4 V2X Based Cooperative Localization Methods . . . 18

2.4.1 V2V-Based Localization Methods . . . 18

2.4.2 V2I-Based Localization Methods . . . 19

2.4.3 V2V and V2I-Based Localization Methods . . . 22

2.4.4 Discussion . . . 22
2.5 Multi-sensor Based Localization Methods . . . 23
2.5.1 Map-based Multi-sensor Localization Methods . . . 23
2.5.2 Data Fusion-based Multi-sensor Localization Methods . . . 24
2.5.3 Data Fusion-based Multi-sensor Cooperative Localization Methods . . . 27
2.5.4 Discussion . . . 28
2.6 Localization Methods Performance Analysis, Challenges and Research Questions 29
2.6.1 Methods Performance Analysis . . . 29
2.6.2 Challenges . . . 33
2.6.3 Research Questions . . . 40

Chapter Three: Proposed Multi-sensor Multi-vehicle cooperative localization 45

3.1 Introduction . . . 45
3.2 Intelligent transportation system (ITS) . . . 45
3.2.1 ITS architecture . . . 45
3.2.2 Communication techniques for ITS . . . 46
3.3 Related techniques for cooperative vehicle localization . . . 48
3.3.1 Interval analysis . . . 48
3.3.2 Interval constraints propagation (ICP) . . . 49
3.3.3 Split covariance intersection filter (SCIF) . . . 51
3.4 Proposed Interval split covariance intersection filter (ISCIF) and its consistency proof . . . 53
3.4.1 Proposed ISCIF . . . 53
3.4.2 Consistency proof of the ISCIF . . . 55
3.5 Cooperative Localization Method based on ISCIF . . . 62
3.5.1 System Model . . . 62
3.5.2 Prediction of the State Vector . . . 63
3.5.3 Absolute Positioning Stage . . . 65

3.5.4 Relative Positioning Stage 65
3.6 Fault Detection and Exclusion 69
3.7 Conclusion 75

Chapter Four: Simulation results **77**
4.1 Introduction 77
4.2 Algorithm Performance in Simulation Scenario 1 80
4.2.1 Results of Scenario 1.1: All Vehicles Have the Same Absolute Positioning Ability 81
4.2.2 Results of Scenario 1.2: One Vehicle Has an Excellent Absolute Positioning Ability 85
4.2.3 Results of Scenario 1.3: Cooperative Vehicle Localization with FDE . . 88
4.3 Algorithm Performance in Simulation Scenario 2 92
4.3.1 Results of Scenario 2.1: All Vehicles Have the Same Absolute Positioning Ability 93
4.3.2 Results of Scenario 2.2: One Vehicle Has an Excellent Absolute Positioning Ability 98
4.4 Computational burden analysis 103
4.5 Conclusion 104

Chapter Five: Conclusion and future work **106**

List of Figures

1.1 The process of the cooperative vehicle localization in MSMV system 2
2.1 Model based on RFID 20
2.2 The flow chart of AI. 31
2.3 Challenges for data collection. 33
2.4 Challenges for data processing method. 34
2.5 Challenges for cooperative localization 38
3.1 ITS architecture 46
3.2 An ITS scenario 47
3.3 The structure of TDMA frame 47
3.4 Intersection between two boxes 49
3.5 Contraction of one box by the contractor including two constraints 50
3.6 Decentralized cooperative localization architecture [1] 62
3.7 Relative observation between vehicles [1] 66
3.8 Date process of each vehicle [1] 70
3.9 The pdfs of the KLD values in the faulty and non-faulty cases. 73
4.1 Simulation scenario 77
4.2 Estimated trajectories for different methods in scenario 1.1 82
4.3 RMSE of vehicle 1 in scenario 1.1 83
4.4 RMSE of vehicle 2 in scenario 1.1 83
4.5 RMSE of vehicle 3 in scenario 1.1 84
4.6 Estimated trajectories for different methods in scenario 1.2 85
4.7 RMSEs based on different methods of vehicle 1 in scenario 1.2 86
4.8 RMSEs based on different methods of vehicle 2 in scenario 1.2 87
4.9 RMSEs based on different methods of vehicle 3 in scenario 1.2 87
4.10 RMSEs of vehicle 1 based on the time step in the absence of faults 88
4.11 KLD values of vehicle 1 based on the time step in the absence of faults 89

4.12 RMSE of vehicle 1 based on the time step in the presence of faults 90
4.13 KLD values of vehicle 1 based on the time step in the presence of faults 90
4.14 Trajectories of vehicle 2 using the FDE method and without using the FDE method 91
4.15 RMSEs of vehicle 2 with or without the FDE method 91
4.16 RMSE of vehicle 3 with or without the FDE method 92
4.17 Estimated trajectories for different methods in scenario 2.1 94
4.18 RMSEs of vehicle 1 for different methods in scenario 2.1 95
4.19 RMSEs of vehicle 2 for different methods in scenario 2.1 95
4.20 RMSEs of vehicle 2 for different methods in scenario 2.1 96
4.21 Average RMSEs of vehicle 1 for different methods in scenario 2.1 97
4.22 Average RMSEs of vehicle 2 for different methods in scenario 2.1 97
4.23 Average RMSEs of vehicle 3 for different methods in scenario 2.1 98
4.24 Estimated trajectories for different methods in scenario 2.2 99
4.25 Positioning error of vehicle 1 associated with different methods in scenario 2.2 99
4.26 Positioning error of vehicle 2 associated with different methods in scenario 2.2 100
4.27 Positioning error of vehicle 3 associated with different methods in scenario 2.2 100
4.28 Average RMSE of vehicle 1 associated with different methods in scenario 2.2 . 101
4.29 Average RMSE of vehicle 2 associated with different methods in scenario 2.2 . 102
4.30 Average RMSE of vehicle 3 associated with different methods in scenario 2.2 . 102
4.31 The execution time of SCIF and our method 104

List of Tables

2.1 The comparison of different sensor-based localization methods 30

2.2 Performances of different methods 30

2.3 Details of traditional algorithms 41

2.4 Details of cooperative algorithms 42

2.5 Details of multi-sensor based algorithms 43

4.1 Different variables on localization accuracy based on data from ten experiments 78

4.2 Details of the simulation parameters 81

4.3 Average RMSEs of different vehicles based on different methods in scenario 1.1 84

4.4 RMSEs of different vehicles based on different methods in scenario 1.2 86

4.5 Matrix operation complexity 103

Publications

1. Shan X, Cabani A, Chafouk H., "Cooperative Vehicle Localization in Multi-Sensor Multi-Vehicle Systems Based on an Interval Split Covariance Intersection Filter with Fault Detection and Exclusion", **Vehicles**, 2024, 6(1): 352-373. DOI: 10.3390/vehicles6010014 (Impact Factor: 2.2, CiteScore: 2.9)

2. Shan X, Cabani A, Chafouk H., "Interval Split Covariance Intersection Filter: Theory and its Application to Cooperative Localization in a Multi-sensor Multi-vehicle System", **Sensors**, 2024, 24(10):3124. DOI: 10.3390/s241031242024 (Impact Factor: 3.9, CiteScore: 6.8)

3. Shan X, Cabani A, Chafouk H. "A Survey of Vehicle Localization: Performance Analysis and Challenges", **IEEE Access**, 2023. DOI: 10.1109/ACCESS.2023.3318885 (Impact Factor: 3.9, CiteScore: 9)

4. Shan X, Cabani A, Chafouk H., "Cooperative localization based on GPS correction and EKF in urban environment", 2nd International Conference on Innovative Research in Applied Science, Engineering and Technology **(IEEE IRASET'22)**, March 03-04, 2022, Meknes, Morocco.

5. Shan X, Cabani A, Chafouk H., "Cooperative Localization Based on Interval Split Covariance Intersection Filter in MSMV System", The 16th IEEE TCCC International Conference on Cyber-Enabled Distributed Computing and Knowledge Discovery **(IEEE TCCC'24)**, October 24-26, 2024, Guangzhou, China (Submitted)

Résumé

La localisation joue un rôle important dans la conduite autonome et dans les systèmes de transport intelligents (ITS). Les méthodes traditionnelles de localisation de véhicules basées sur des capteurs (y compris les méthodes basées sur le GPS [2], les méthodes basées sur l'unité de mesure inertielle (IMU) [3], les méthodes basées sur des caméras [4], etc.) peuvent atteindre des niveaux de précision élevés dans certains scénarios. Cependant, les méthodes traditionnelles de localisation de véhicules présentent des inconvénients évidents. Par exemple, la précision des méthodes basées sur le GPS peut être facilement affectée par l'environnement. Les erreurs cumulatives peuvent sérieusement affecter la précision des méthodes basées sur les centrales inertielles pendant le processus de localisation à longue distance, et les méthodes basées sur les caméras nécessitent normalement des ressources supplémentaires pour la cartographie et le stockage des données. Avec le développement rapide des techniques de communication de véhicule à véhicule (V2V) et de véhicule à infrastructure (V2I), le partage de données est devenu possible entre les véhicules et les infrastructures du système. En utilisant les techniques de communication V2V [5] et V2I [6][7], la localisation coopérative de véhicules peut bénéficier du partage des données qui offre de meilleures performances que les méthodes de localisation traditionnelles. De nombreuses méthodes de fusion de données telles que le filtre de Kalman non parfumé (UKF) [8], le filtre de Kalman étendu (EKF) [9] et le filtre à particules (PF) [10] ont déjà été proposées pour réaliser une localisation coopérative de véhicules. Plus de détails sur la localisation des véhicules sont proposés dans [11][12].

Dans le domaine de la localisation coopérative, un défi important consiste à résoudre le problème de consanguinité des données ou data incest en anglais [13]. Cela est dû à l'utilisation multiple d'informations identiques, et ces informations sont considérées comme indépendantes les unes des autres [14]. De plus, la corrélation entre les estimations entre différentes sources d'estimation est causée par la consanguinité des données [15], qui produit des estimations incohérentes et un problème de convergence excessive [16]. Le problème de consanguinité des données se pose particulièrement dans les scénarios où les positions relatives entre les véhicules

sont utilisées. Plus précisément, lorsqu'il existe plusieurs mesures relatives, le problème de consanguinité des données devient plus grave en raison du flux de données complexe [1].

Le processus de localisation coopérative des véhicules dans le système multi-capteurs multi-véhicules est illustré dans Fig. 1.1. Après l'initialisation, à chaque étape d'itération, il y a quatre étapes pour chaque véhicule : collecte des données, positionnement absolu, fourniture de mesures relatives pour leurs voisins par partage de données, et positionnement relatif lorsque chaque véhicule reçoit ses mesures relatives. Lorsque trois véhicules communiquent et partagent des mesures relatives entre eux, chaque véhicule du système peut être confronté à un problème de consanguinité des données lors de l'étape de positionnement relatif à partir du deuxième processus d'itération, car les estimations relatives calculées par les mesures relatives fournies par les véhicules voisins peuvent avoir une corrélation avec son propre état. Le problème de consanguinité des données entraîne des résultats incohérents lors du processus de fusion des données en raison de la corrélation entre les estimations. Afin de résoudre ce problème, une méthode nommée filtre d'intersection de covariance (CI) est proposée dans [17]. Cependant, l'algorithme CI ne fait pas de distinction entre les parties indépendantes et corrélées dans les ressources d'estimation, ce qui fera perdre la précision du résultat de la fusion.

Afin d'augmenter encore la précision, une autre approche appelée filtre d'intersection de covariance divisée (SCIF) est rapportée dans [16]. Les parties indépendantes et corrélées des ressources de fusion sont toutes les deux prises en compte, ce qui peut donner lieu à une estimation cohérente. Cependant, dans le système multi-capteurs multi-véhicules (MSMV), il existe plusieurs mesures relatives lorsqu'un véhicule est observé par différents voisins. Le SCIF traditionnel ne convient donc pas, car le vecteur d'état est fréquemment mis à jour en utilisant plusieurs informations de position relative, et la qualité de ces informations de position relative ne peut être garantie, ce qui peut donner lieu à des estimations pessimistes. De plus, plusieurs itérations au cours de l'étape de positionnement relatif du véhicule entraînent une surcharge de calcul inutile.

De plus, la propagation des contraintes d'intervalle (ICP) est une méthode de fusion efficace

qui a été largement utilisée dans le domaine de la localisation de véhicules et de robots [18]. Elle utilise une technique de communication pour propager les contraintes possibles et réaliser une fusion de données basée sur des restrictions. Elle présente de bonnes performances de localisation, notamment face à des données redondantes. De plus, elle peut éviter le problème de convergence excessive en analysant les valeurs dans le domaine de confiance. Cependant, il est difficile de déterminer le poids de chaque contrainte dans une application réelle de localisation. En d'autres termes, lorsque différentes contraintes sont considérées comme ayant les mêmes poids, les résultats risquent de perdre en précision. Un filtre de Kalman à intervalle (IKF) est proposé pour augmenter la précision [19]. Cependant, l'inversion de la matrice de covariance d'intervalle ne peut être résolue qu'approximativement, et il s'agit d'un problème NP complexe [20].

En outre, la méthode de détection et d'exclusion de défauts (FDE) peut améliorer efficacement la robustesse du système de localisation des véhicules [21]. Cela peut améliorer la précision de la localisation, notamment en présence de défauts de capteurs. La divergence Kullback-Leibler (KLD), également connue sous le nom d'entropie relative, est un outil largement reconnu pour la détection et l'exclusion de défautes [22]. La méthode KLD quantifie la différence d'information entre deux fonctions de densité de probabilité (pdf). Elle peut également être considérée comme le logarithme anticipé du rapport de vraisemblance entre deux ensembles de distributions de données [23]. Un exemple de méthode FDE basée sur KLD est présenté dans [24]. Dans un premier temps, la localisation décentralisée des véhicules basée sur SCIF est proposée. Ensuite, une méthode de détection et d'isolement des défauts basée sur KLD est introduite et mise en œuvre pour améliorer la robustesse du système. Un autre travail FDE basé sur KLD est décrit dans [25], où il est implémenté dans des systèmes de positionnement basés sur des filtres d'informations étendus (EIF). La discussion des résultats tourne autour de l'utilisation d'un seuil déterminé par des critères conditionnels basés sur l'entropie et de l'utilisation de la courbe des caractéristiques de fonctionnement du récepteur (ROC). Ainsi, la méthode FDE basée sur KLD peut améliorer efficacement la robustesse du système coopératif

décentralisé de localisation de véhicules.

Notre objectif est de proposer un algorithme coopératif de localisation de véhicules cohérent, peu coûteux et robuste pour le système MSMV. Les contributions de cette thèse sont les suivantes :

- Motivé par la résolution du problème causé par la corrélation inter-estimations (consanguinité des données) et par l'évitement des problèmes causés par l'inverse de la matrice d'intervalle dans IKF. Une nouvelle méthode de fusion de données nommée ISCIF est proposée.

- La cohérence de l'ISCIF proposé est donnée.

- ISCIF intégrant le mécanisme ICP pour la localisation coopérative de véhicules à faible coût dans le système MSMV est présenté. La méthode ICP est utilisée pour prétraiter plusieurs estimations relatives et fournir des données d'entrée pour l'ISCIF.

- Une méthode FDE basée sur KLD est implémentée pour réduire le RMSE du résultat de localisation lorsque des défauts sont présents dans le système.

- Des simulations sont effectuées et les résultats montrent que notre méthode proposée peut atteindre de meilleures performances en termes de précision par rapport à plusieurs autres méthodes de fusion de données. De plus, la méthode FDE mise en œuvre permet d'obtenir de meilleures performances de précision lorsque des défauts sont présents dans le système.

Cette thèse est organisée comme suit : Une enquête sur les techniques de localisation de véhicules est proposée dans le chapitre II. La localisation coopérative multi-capteurs multi-véhicules proposée est détaillée dans le chapitre III. Les résultats de la simulation sont préntés dans le chapitre IV, suivi par la conclusion et les perspectives au chapitre V.

Cette thèse de doctorat aborde principalement le problème de consanguinité des données et vise à proposer une méthode de localisation coopérative précise, robuste et peu coûteuse dans

les systèmes coopératifs de localisation de véhicules multi-capteurs multi-véhicules (MSMV). Compte tenu de la structure du système de localisation coopératif de véhicules, étant donné que la structure centralisée traditionnelle présente des limites en termes de capacité informatique et de communication, nous adoptons une structure coopérative décentralisée. L'utilisation d'une structure coopérative décentralisée réduit non seulement la pression de calcul et de communication du réseau de véhicules, mais est également plus adaptée aux réseaux de véhicules dynamiques. Dans ce qui suit, une conclusion sur les principaux sujets abordés dans chaque chapitre de cette thèse est donnée.

Dans le chapitre 1, nous fournissons un aperçu de la localisation coopérative dans les MSMV et analysons les défis actuels non résolus. Comparé à l'algorithme d'auto-localisation traditionnel, l'algorithme coopératif de localisation de véhicules basé sur la technique de communication V2V présente une efficacité plus élevée. Cependant, dans le système de localisation coopératif MSMV, deux problèmes doivent être résolus : Le premier challenge est qu'il existe un problème de consanguinité des données lorsque les véhicules utilisent les estimations relatives fournies par les véhicules voisins pour le positionnement relatif, ce qui conduit à une fusion de données incohérente ; Le deuxième challenge est que l'algorithme SCIF (Split Covariance Intersection Filter) traditionnel présente une surcharge de calcul élevée dans l'étape de positionnement relatif, causée par des itérations complexes pour la mise à jour d'état.

Les principaux objectifs de notre thèse sont de proposer un nouvel algorithme de fusion de données, nommé filtre d'intersection de covariance fractionnée par intervalles (ISCIF), et de donner sa preuve de cohérence théorique. Ensuite, l'ISCIF intégrant la méthode de propagation par contrainte d'intervalle (ICP) est appliqué à la localisation coopérative du système MSMV. Enfin, afin d'améliorer la robustesse du système, la méthode de détection et d'exclusion de défauts est utilisée dans notre système.

Dans le chapitre 2, l'étude des techniques de localisation de véhicules de pointe est mise en évidence. Nous analysons les performances globales des techniques avancées de localisation de véhicules existantes et discutons de leurs défis. Dans un premier temps, nous analysons

les méthodes d'auto-localisations basées sur des capteurs actifs et passifs. Les résultats montrent que les techniques de détection et de télémétrie de la lumière (LiDAR) et de localisation basée sur la vision peuvent atteindre une grande précision. Cependant, ils présentent une grande complexité informatique. L'utilisation exclusive de l'unité de mesure inertielle (IMU), du système de positionnement global (GPS), du radar et des capteurs à ultrason peut ne pas permettre d'obtenir un résultat de localisation avec une grande précision. Ensuite, nous discutons des méthodes de localisation coopérative basées sur la communication V2X, analysons les techniques de localisation basées sur plusieurs capteurs et comparons leur performance. Bien que les techniques d'intelligence artificielle (IA) puissent améliorer l'efficacité des algorithmes de localisation basés sur la vision, leur grande complexité informatique doit néanmoins être prise en compte. De plus, étant donné que les capteurs IMU, GPS, radar et ultrasons ont de bonnes performances en termes de disponibilité, de fiabilité, d'évolutivité et de rentabilité, ils peuvent être utilisés comme capteurs auxiliaires pour obtenir de bonnes performances globales grâce à des techniques de fusion de données. Enfin, nous analysons les performances de différentes techniques de localisation de véhicules et discutons des enjeux de ces techniques.

Dans le chapitre 3, nous donnons tout d'abord un aperçu du système de transport intelligent (STI), y compris son architecture et ses techniques de communication. Ensuite, les techniques associées à la localisation coopérative de véhicules sont présentées dans la section 3.3. Afin de résoudre le problème de consanguinité des données dans le système de localisation MSMV, un nouvel algorithme de fusion de données nommé ISCIF est proposé, et la preuve de cohérence de l'ISCIF est fournie. De plus, l'ISCIF proposé est mis en œuvre dans les étapes de positionnement absolu et relatif dans un système de localisation MSMV décentralisé. Il convient de noter qu'au cours de l'étape de positionnement relatif, étant donné qu'il existe plusieurs estimations relatives, ce qui réduit la précision de la localisation et augmente la charge de calcul, la méthode ICP est utilisée pour atténuer l'impact provoqué par les multiples estimations de position relative et fournir des données d'entrée pour l'ISCIF. De plus, la méthode FDE basée sur KLD est implémentée pour augmenter la robustesse du système de localisation proposé.

De plus, les principales raisons pour lesquelles la méthode ICP peut produire des résultats précis incluent : une modélisation précise et une propagation des contraintes. En termes de modélisation précise, la méthode ICP peut déduire avec précision les plages possibles de variables en considérant les relations entre contraintes et variables. De plus, la propagation des contraintes est utilisée pour affiner les plages de variables, réduisant ainsi efficacement l'espace de solution et obtenant un positionnement précis du véhicule. Concernant l'algorithme ISCIF proposé, il aborde l'impact de l'estimation relative entre voisins en utilisant des techniques d'analyse d'intervalle, lui permettant de fournir des intervalles d'estimation d'état au lieu des estimations ponctuelles traditionnelles. Cela permet à l'algorithme de représenter de manière plus complète l'incertitude des variables d'état et d'atténuer l'impact de l'incertitude de l'estimation de l'état. De plus, les opérations arithmétiques par intervalles, par rapport aux calculs numériques traditionnels, peuvent réduire dans une certaine mesure les erreurs d'arrondi, produisant ainsi des résultats plus précis.

La méthode proposée est évaluée à travers des tests de simulation avec deux scénarios différents, et les résultats sont illustrés dans le chapitre 4. Tout d'abord, nous avons établi des coefficients corrélés dans les équations (3.52) et (3.55) sur la base de dix expériences. Dans la simulation 1, nous comparons notre méthode proposée avec le filtre de Kalman étendu (EKF), le filtre de Kalman de cubature (CKF), le filtre de Kalman de cubature adaptatif (ACKF) et le filtre d'intersection de covariance divisée (SCIF) en termes de précision de localisation. Lorsque tous les véhicules du système ont la même capacité de positionnement absolue, comme indiqué dans le paragraphe 4.2.1. Les résultats de simulation montrent que notre méthode améliore le RMSE de 8,9%, 12,8%, 40,6% et 18,7% par rapport aux méthodes SCIF, ACKF, EKF et CKF, respectivement. De plus, lorsque le véhicule possède une excellente capacité de positionnement absolu, comme le montre les résultats présentés dans le paragraphe 4.2.2, notre méthode améliore le RMSE de 15,5%, 41,1%, 58,2% et 45,0% par rapport au SCIF, ACKF. , EKF et CKF, respectivement. De plus, les résultats de simulation présentés dans le paragraphe 4.2.3 montrent des améliorations lorsque nous implémentons la méthode de détection et d'exclusion (FDE) de

pannes basée sur la divergence Kullback–Leibler (KLD). Lorsqu'une défaillance d'un capteur se produit dans le système, nous sommes en mesure de la détecter à temps et d'exécuter des mécanismes pertinents pour atténuer l'impact de la défaillance du capteur sur la précision de localisation du véhicule au sein du système.

De plus, afin d'étudier plus en détail la précision de localisation de notre méthode proposée, un autre scénario de simulation avec une trajectoire plus complexe est conçu dans la section 4.3. Dans ce chapitre, nous comparons notre méthode proposée avec la méthode de localisation unique (SL), la méthode de propagation par contrainte d'intervalle (ICP) et le filtre d'intersection de covariance divisée (SCIF) en termes de précision de localisation. Lorsque tous les véhicules ont la même capacité de positionnement absolue, comme indiqué dans le pargagraphe 4.3.1, notre méthode réduit le RMSE d'environ 65%, 11% et 43% par rapport aux méthodes ICP, SCIF et SL, respectivement. De plus, lorsque le véhicule possède une excellente capacité de positionnement absolu, comme indiqué dans le paragraphe 4.3.2, notre méthode réduit le RMSE d'environ 22%, 21% et 67% par rapport à l'ICP, SCIF et SL, respectivement. Par rapport aux méthodes de la littérature, notre approche réduit considérablement le RMSE dans les deux scénarios. De plus, la position réelle du véhicule peut être incluse presque tout le temps dans les intervalles générés par notre méthode, ce qui signifie que notre méthode peut être implémentée dans le système non linéaire à intervalles. De plus, sur la base de l'analyse de la charge de calcul, notre méthode proposée et implémentée dans la localisation coopérative de véhicules MSMV, présente des coûts de calcul inférieurs.

Enfin, dans nos futurs travaux, nous visons à proposer un algorithme adapté aux scénarios avec absence du signal GPS, car dans la pratique les signaux GPS peuvent facilement être affectés. De plus, nous avons l'intention de tester les performances de notre méthode proposée en utilisant des données réelles.

Chapter One

Introduction

1.1 Context of the thesis

Localization plays an important role in autonomous driving and intelligent transportation system (ITS). Traditional sensor-based vehicle localization methods (including GPS-based methods [2], inertial measurement unit (IMU)-based methods [3], camera-based methods [4], etc.) can reach high-performance localization in certain scenario. However, traditional vehicle localization methods have obvious drawbacks. For example, the accuracy of GPS-based methods can be affected easily by the environment, the cumulative errors can seriously affect the accuracy of IMU-based methods during long distance localization process, and the camera-based methods normally need additional overhead for map and data storage. With the rapid developing of the vehicle-to-vehicle (V2V) and vehicle-to-infrastructure (V2I) communication techniques, the data sharing is enabled among vehicles and infrastructures in the system. By using V2V [5] and V2I [6][7] communication techniques, the cooperative vehicle localization can benefit from the data sharing which has better performance than the traditional localization methods. Many data fusion methods like unscented Kalman filter (UKF) [8], extended Kalman filter (EKF) [9], and particle filter (PF) [10] have already been proposed to realize cooperative vehicle localization. More details about vehicle localization have been highlighted in [11][12].

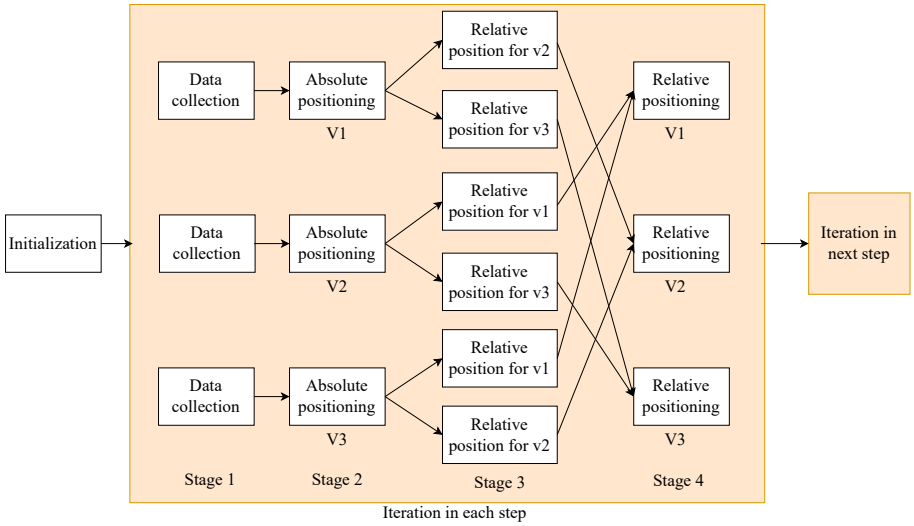

Figure 1.1: The process of the cooperative vehicle localization in MSMV system

In the cooperative localization domain, one significant challenge is to solve the data incest problem [13]. It is caused by the multiple usage of identical information, and these items of information are considered as independent with each other [14]. Furthermore, inter-estimate correlation among different estimate sources is caused by data incest [15], which yields inconsistent estimates and over-convergence problem [16]. The data incest problem especially arises in scenarios where the relative positions among vehicles are used. Specifically, when there are multiple relative measurements, the data incest problem becomes more serious due to the complex data flow [1]. The process of the cooperative vehicle localization in the MSMV system is shown in Fig. 1.1. After the initialization, in each iteration step, there are four stages for each vehicle: data collection, absolute positioning, providing relative measurements for their neighbors by data sharing, and relative positioning when each vehicle receives its relative measurements. When three vehicles communicate and share relative measurements with each other, each vehicle in the system may face data incest problem in the relative positioning stage from the second iteration process, because the relative estimates calculated by relative measurements provided by neighboring vehicles may have correlation with its own state. Data incest problem causes inconsistent result during data fusion process due to the inter-estimate correlation. In order to address the data incest problem, one method named covariance intersection filter (CI) is proposed in [17]. However, the CI algorithm does not distinguish between the independent and correlated parts in the estimate resources, which will lose the accuracy of the fusion result.

In order to further increase the accuracy, another approach named split covariance intersection filter (SCIF) is reported in [16]. The independent and correlated parts of fusion resources are both considered, which can yield consistent estimate. However, in the multi-sensor multi-vehicle (MSMV) system, there are multiple relative measurements when one vehicle is observed by different neighbors, the traditional SCIF is not suitable because the state vector is updated frequently by using multiple relative position information, and the quality of these relative position information can not be guaranteed, which may yield pessimistic estimates. Additionally, multiple iterations during the relative vehicle positioning stage causes unnecessary computa-

tional overhead.

Furthermore, the interval constraints propagation (ICP) is an effective fusion method which has been widely used in the vehicle and robot localization domain [18]. It uses communication technique to propagate the possible constraints and achieve data fusion based on these restrictions, it has good localization performance especially when faced with redundant data. Moreover, it can avoid the over-convergence problem by analysing the values within the confidence domain. However, it is difficult to decide the weight of each constraint in the real localization application. In other words, when different constraints are considered to have same weights, the results would have the problem of losing accuracy. In addition, interval Kalman Filter (IKF) is proposed to increase the accuracy [19]. However, the inversion of interval covariance matrix can only be solved approximately, and it is a NP-hardness problem [20].

In addition, the fault detection and exclusion (FDE) method can effectively enhance the robustness of the vehicle localization system [21]. It can improve the localization accuracy, particularly in the presence of sensor faults. Kullback-Leibler divergence (KLD), also known as relative entropy, is a widely recognized tool for FDE [22]. KLD quantifies the difference in information between two probability density functions (pdf). It also can be seen as the anticipated logarithm of the likelihood ratio between two sets of data distributions [23]. One example of FDE method based on KLD is presented in [24]. At first, the decentralized vehicle localization based on SCIF is proposed. Then, a KLD-based fault detection and isolation method is introduced and implemented to enhance the robustness of the system. Another FDE work based on KLD is outlined in [25], where it is implemented in extended information filter (EIF) based positioning systems. Additionally, the discussion of the results revolves utilizing threshold determined by conditional entropy-based criteria and employing the receiver operating characteristics (ROC) curve. So, the KLD-based FDE method can effectively enhance the robustness of decentralized cooperative vehicle localization system.

1.2 Objectives and contributions

We aim to propose a consistent, low-overhead, and robust cooperative vehicle localization algorithm for the multi-sensor multi-vehicle (MSMV) systems. The contributions of this thesis are as follows:

- Motivated by addressing the problem caused by the inter-estimate correlation (data incest). A new data fusion method named interval split covariance intersection filter (ISCIF) is proposed and the consistency of the proposed ISCIF is given.
- ISCIF incorporating the ICP mechanism for low-cost cooperative vehicle localization in the MSMV system is presented. ICP method is employed to preprocess multiple relative estimates and provide input data for ISCIF.
- A KLD-based FDE method is implemented to reduce the RMSE of the localization result when faults are present in the system.
- Simulations are carried out, and results show that our proposed method can achieve better accuracy performance compared to several data fusion methods. In addition, the implemented FDE method can achieve better accuracy performance when faults are present in the system.

This thesis is organized as follows: Survey on vehicle localization techniques is proposed in chapter II. Proposed multi-sensor multi-vehicle cooperative localization is detailed in chapter III. Simulation results are proposed in chapter IV, and the conclusion and future work are followed in chapter V.

Chapter Two

Survey on vehicle localization techniques

2.1 Introduction

In this section, we conduct an analysis and comparison of the comprehensive performances among state-of-the-art vehicle localization algorithms. Subsequently, we highlight the challenges associated with various methods and establish the research questions addressed in our thesis. The performances of vehicle localization includes accuracy, availability, scalability, real-time performance, and so on. The state-of-the-art methods for the vehicle localization methods are described in detail in the following subsections.

2.2 Active sensor based self-localization Methods

In this section, we analyze and compare the state-of-the-art vehicle self-localization methods which use the on-board active sensors in the data collection step. Active sensors, including LiDAR, radar, and ultrasonic sensors, they can emit energy to the environment and the data is collected by measuring the scattered or reflected signal. In the following sections, we illustrate the advantages and disadvantages of each data collection method. Additionally, we compare the economic cost of each sensor and analyze its latency, which affects the scalability and real-time performance during vehicle self-localization. Moreover, we discuss the advantages and disadvantages of each algorithm in detail in the following subsections.

2.2.1 LiDAR-based Self-localization Methods

Light detection and ranging (LiDAR) can collect emitted laser light and calculates the distance to the target based on the intensity and time of the received laser, which can provide accurate data for vehicle localization. By processing the data collected by LiDAR through the use of filters, mapping, artificial intelligence (AI), and multi-method techniques, it has excellent accuracy performance in the vehicle localization domain. For a LiDAR-based method, a map (including planar and point-cloud maps [26]) is generally required to match with the point cloud

data collected by LiDAR. If there is no prior map, the simultaneous localization and mapping (SLAM) method can be used to create a real-time map. The position of the vehicle can be determined by map matching.

To address the problem that the traditional map matching process is easily affected by the resolution, the authors of [27] proposed an algorithm based on a free-resolution probability distributions map (FRPDM) using 3D LiDAR. The FRPDM stores the probability distribution converted by the Gaussian mixture modeling (GMM) method, which effectively reduces space complexity. The size of the FRPDM is about 0.061 MB/km, which is smaller than the extended line map in [28] (0.134 MB/km), the binary grid map in [29] (0.901 MB/km), and the multi-resolution Gaussian mixture map in [30] (44.3 MB/km). The authors also proposed a data association method for the point-to-probability distribution scan matching method. The RMSE of the lateral and longitudinal directions is 0.057 m and 0.178 m, respectively. Although this method can reach an average map matching time of 37 ms, the extraction time is 146 ms, which results in a higher total data processing time (183 ms). Therefore, this method is not sufficient for applications that require high real-time performance. To increase the real-time performance, the authors of [31] proposed a localization method based on mapping and UKF techniques, using a distance-weight map (DWM) in an underground mine environment. The spatial localization error is 4 cm, and the processing time per frame is 60 ms. In order to further improve the availability of localization algorithms in mountainous rural environments, an algorithm exploiting multi-layer LiDAR was proposed in [32]. A 3D normal distribution map is built at first, and then the normal distribution transform (NDT) scan matching method and the EKF technique are employed to estimate the position. The average absolute error of longitudinal and lateral are 0.38 m and 0.08 m with the average velocity 45 km/h, respectively. However, it is not reliable enough for autonomous driving because it may cause the traffic accident during demonstrations. Additionally, another work which can reach high accuracy localization is proposed in [33]. This method includes the mapping and localization phase. In the mapping phase, the pole detector is designed, and the pole landmarks are extracted by the pole detector

from LiDAR scans. Then, the extracted pole landmarks are registered with a global map which is provided by the true trajectory. In the localization phase, the PF technique is implemented to realize position estimation by matching the pole landmarks provided by sensors with that in the map. The advantage of this algorithm is that the positioning RMSE is about 0.1 m, which can meet the accuracy requirement of AVs.

Furthermore, in recent years, the AI technique is employed in the localization domain to reach high real-time performance. The authors of [34] proposed an improved lightweight deep neural network to realize the deep local feature extraction in day-night changes environment. A prior map is built by using aligned dense LiDAR point clouds and imagery provided by a portable camera-LiDAR sensor. Meanwhile, the ground truth point cloud dataset with 5 cm accuracy is employed to evaluate the localization accuracy and robustness in vision-changed conditions. The extraction speed of the feature in this method is 92 frames per second, and this work is focus on the day-night changed environment, which also has high availability performance. Another work was proposed in [35], the authors proposed a siamese neural network-based algorithm by using a global prior map. The reduced dimension scan representations learned from neural networks are utilized to realize place recognition, and the global prior map is employed to determine the vehicle's position. The advantage of this algorithm is that the storage space for sensor data is reduced. Moreover, another work based on deep learning is proposed in [36]. In order to achieve fast and accurate information interaction during vehicle localization, only a few LiDAR points are used in the proposed framework. In addition, a clustering algorithm is employed to realize the non-semantic features extraction from the information collected by LiDAR and the data smoothing process occurs in the convolutional layers. In order to enhance the reliability of the algorithm, both the north campus long-term (NCLT) and Kitti dataset are used to evaluate the accuracy performance in the short and long term trajectory. Experimental results show that a reasonable accuracy (Mean positioning error is below 1 m) can be achieved.

In addition, a LiDAR-based road sign perception system using third-party sparse maps (TPSM) was proposed to improve the accuracy of traditional GNSS-based vehicle localization

algorithms [37]. This system uses LiDAR to detect road and lane sign features and employs the PF technique to estimate the position of vehicle. This algorithm increases the accuracy by using TPSM road features (0.31 m for the constrained update). However, the TPSM is not suitable for all sensors, limiting its scalability. To address the issue that the traditional normalized cross-correlation (NCC) algorithm requires sufficient feature points, a cross means absolute difference (CMAD) algorithm based on known map information using 3D LiDAR is proposed in [38]. This method includes offline and online parts. In the offline part, the map is built, calibrated, and segmented. The 3D map is then transformed into a 2D grid map and feature extraction is performed. In the online part, the same procedure is used for LiDAR scanning. The mean energy and feature registration method are used to initialize location and orientation of the vehicle, and the drivable moving search region (DMR) method is designed during feature registration during the process. The RMSE is about 0.1-0.3 m in outdoor environments and it has good real-time performance.

2.2.2 Radar-based Self-localization Methods

While the LiDAR-based and vision-based method can provide more precise data, radar-based methods cannot be easily replaced at the moment. This is because radar is the only sensor capable of accurately measuring the speed of objects under long distance conditions, as supported by Zhou et al. [39]. Moreover, radar-based methods can offer good real-time performance due to their low latency during data collection, as highlighted by Lu et al. [18]. Additionally, radar-based methods are capable of functioning effectively in adverse weather conditions, further enhancing their reliability. Some popular types of radar used in vehicle localization,including multiple-input multiple-output radar [40], millimeter wave automotive radar [41], and so on.

In order to enhance the availability of localization methods, the authors of [42] proposed an improved algorithm that uses a 76GHz omnidirectional millimeter-wave radar (MWR). They develop a novel error propagation model to calculate the unique noise characteristics of sensors operating in snowy environments. The process consists of four steps: image generation of

objects, template matching, probability updating, and offset updating. The lateral RMSE of 0.25 m can be achieved, regardless of the presence or absence of snowfall. Since the radar sensor has strong reliability and availability, especially in extreme weather conditions, the authors in [43] used ground penetrating radar to realize vehicle localization in inclement weathers. The positioning results show that the total mean positioning error (the sum of along-track and cross-track error) is 0.34 m, 0.39 m, and 0.77 m, in the clear, snow, and rain weather scenario, respectively. To improve the accuracy of radar based vehicle localization methods in urban environments, the accuracy is less than 0.5 m is achieved in [44].

In addition, the authors of [45] proposed a machine learning-based algorithm by using mmWave radars operating in the frequency range of 77 GHz-81 GHz. This algorithm consists of two steps: range estimation and angle estimation. For range estimation, unwanted clutter is removed based on the properties of mainlobe clutter and sidelobe clutter, followed by estimating the average range for a certain frame. To improve angle estimation accuracy, a polynomial regression model is proposed, achieving the RMSE of 2.56 degrees. Another work that utilizes artificial intelligence (AI) techniques was presented in [46]. The authors designe a deep radar object detection network (RODNet) which uses range-azimuth frequency heatmaps (RAMaps). RODNet increases the availability by incorporating three architectures, namely 3D convolution deconvolution, 3D stacked hourglass, and 3D stacked hourglass with temporal inception. Additionally, a new method for learning step is proposed by leveraging cross-model supervision. The latency is less than 100 ms for real-time performance.

2.2.3 Ultrasonic-based Self-localization Methods

Ultrasonic-based sensors are commonly used in low-cost curb detection and localization systems due to their affordability. Additionally, the ultrasonic sensor is widely used in indoor positioning algorithms [47]. Nevertheless, the limited detection range of ultrasonic sensors (approximately 3 m) makes them unsuitable for long distance measurement scenarios. In other words, the scalability performance is insufficient. To increase accuracy and real-time perfor-

mance of ultrasonic-based localization methods, the authors of [48] designed a low-cost curb detection and localization system utilizing multiple ultrasonic sensors. Initially, a ground reflection elimination filter is proposed to eliminate obvious reflections caused by ground reflections. Subsequently, the reliability of the measurement data is calculated, and a distance estimation algorithm is proposed by analyzing the obtained reliability. The complexity of this algorithm is $O(N^2)$, and when four ultrasonic sensors are implemented, the system achieves the accuracy with 13.5 cm on the RMSE.

Additionally, the execution time for processing raw sensor data (collected over 100 seconds) is 0.58 seconds, demonstrating good real-time performance. Another method with excellent real-time performance was reported in [49]. To further enhance the availability of ultrasonic-based methods in GPS-denied environments, a navigation estimation system is designed. The raw data from the ultrasonic sensors is preprocessed to reduce the effects of sensor noise, and during GPS blockage periods, The EKF technique is employed to estimate the vehicle's position. The result refresh rate is 92 Hz, achieving excellent real-time performance.

2.2.4 Discussion

Although LiDAR-based localization methods can provide high accuracy compared to other active sensor-based methods, they have higher computation requirements and economic expenses. In terms of 1D, 2D and 3D map matching method in LiDAR-based methods, the 3D map matching method can get the most accuracy and robustness localization result since the 3D maps have rich type of features, and it especially has good performance in complex scenarios. However, compared with 1D and 2D map-based methods, the storage requirement of map and the computation power increase dramatically compared with 1D and 2D map-based methods, which has bad influence on the performance of scalability. AI techniques can be employed to enhance the accuracy and real-time performance of 3D map matching methods [50], which could be beneficial for applications where accuracy and real-time performance are crucial, such as autonomous driving, in the future.

Furthermore, although radar-based localization methods may not always meet the accuracy requirements of autonomous driving or ITS, the radar still plays an irreplaceable role in the field of object detection [51]. On the one hand, the radar-based localization system has excellent performance in extreme weather scenarios. On the other hand, ultrasonic sensor-based methods offer excellent real-time performance, as reported in [49], which can serve as auxiliary sensors in certain scenarios.

2.3 Passive sensor based self-localization Methods

For passive sensors, such as IMU, GPS, and vision-based sensors, only the radiation or emission in the nature or from the target can be detected. In this section, we analyze the accuracy, real-time performance, and complexity performance of self-localization methods based on passive sensors that utilize popular data processing techniques, such as filters, AI, and mapping methods.

2.3.1 IMU-based Self-localization Methods

The IMU sensors are widely used for dead reckoning (DR) [52] and inertial navigation system (INS) [53]. However, a disadvantage of the IMU sensor is that when applied to long-distance positioning, the accumulated error can significantly decrease the accuracy of the final result. One approach which can mitigate this issue is to use multiple IMUs simultaneously to increase the accuracy of the localization system.

In [54], the authors proposed an algorithm based on multiple IMUs. They employ least-square and probabilistic marginalization methods to map measurements from all IMU sensors onto a virtual IMU, and the probabilistic estimators are used to estimate the location of the vehicle. This algorithm achieves real-time performance with localization refresh time of about 10 ms, based on sensor measurement rates of 200 Hz. However, the RMSE of this approach is 0.6 m. Another multi-IMU based system called real-time multi-IMU visual-inertial navigation

system (mi-VINS) was proposed in [55]. In this system, in order to enhance the real-time performance, a tightly-coupled EKF based estimation method is proposed to fuse asynchronous measurements from multiple sensors. The propagation method of the joint covariance and state estimation of each IMU is defined.

Furthermore, to ensure the consistency in the data fusion process, all the spatial and temporal calibration parameters are processed online for the calibration refinement of sensors, which can reduce the space complexity caused by offline steps. The RMSE of this approach is about 0.2 m with an average data processing time of 23 ms (43 Hz), and mi-VINS can increase the robustness in cases where one of the IMUs in the system does not work. To further increase the robustness of IMU-based methods, the authors of [52] proposed an algorithm based on KF and deep neural networks. The deep neural networks are utilized to optimize and provide noise estimates during the KF algorithm. The raw data of the IMU is refreshed at a rate of 100 Hz, and the translational error is about 1.1 percent. Additionally, in certain special environments, such as GPS-denied environments, IMU can play a crucial role in the localization system.Another work based on solely the commercial-of-the-shelf (COTS) IMU in GPS-denied environment is proposed in [56].A new developed Bayesian filter is proposed which can achieve the position error of less than 0.5 m.

2.3.2 GPS-based Self-localization Methods

GNSS, including GPS[2], Beidou [57], and Galileo[58], can provide convenient and low-cost global localization services by using four or more satellites. The accuracy of GPS is about from a few meters to twenty meters [26]. In order to increase the accuracy of GPS localization, various techniques such as real-time kinematic (RTK) [59], has been proposed. However, GPS accuracy is easily affected by factors such as obstacles, atmospheric conditions and signal blockage. So, the vehicle localization in GPS-denied environment is a popular research topic[60] [61].

In order to improve the accuracy of GPS-based localization by GNSS signal reception state

detection, the authors of [62] designed a multi-path detection system based on support vector machines (SVM). To enhance the effectiveness of the map-matching method, the authors of [63] proposed a spatio-temporal-based matching algorithm (STD matching) which considers the spatial features of roads (including road topology and detailed road information), vehicle speed constraints on different roads, and real-time vehicle movement during low-sampling rate GPS trajectories. Furthermore, the authors employ GPS clustering, GPS smoothing, and A^* algorithms to reduce the computational costs and improve the accuracy. The experimental result based on a road network containing 200,236 vertices and 90,709 road segments shows that the matching accuracy was over 80%, which is higher and more stable than the results obtained by the HMM-RCM algorithm proposed in [64]. However, the running time with 3-10 candidate points was about 11 seconds under low-sampling rate conditions.

Furthermore, to enhance the scalability of GPS-based localization methods, the authors of [65] designed a system which is intended for global-scale deployment. This system involves an offline map building step and an online query step. In the offline map building step, they design a structure-from-motion model and congas descriptors, and the structure and appearance compression methods are employed to reduce data storage space. Finally, the data is stored using a tiled model. In the online query step, congas extraction and projection, 2D-3D matching and voting, and pose recovery and refinement are included. The query latency of this system is about 200 ms, demonstrating excellent real-time performance. Additionally, this system is robust compared to previous methods, as it delivers significantly stable results. Unlike previous methods, aiming at improving the GPS localization accuracy in non-line of sight (NLOS) scenario, the authors of [66] employed 3D mapping techniques to improve the conventional ranging-based GNSS localization methods. Specifically, they utilize terrain height-aiding techniques to achieve additional virtual ranging measurements, and the NLOS reception is predicted by using 3D city models.

2.3.3 Vision-based Self-localization Methods

Vision-based data collection methods capture target images through vision devices such as monocular cameras [67], binocular cameras [68], or panoramic thermal cameras [69], and then the effective feature data can be extracted from the images. The SLAM algorithm [70] [71] [72] [73], which is a basic vehicle localization algorithm using vision sensors, is widely implemented in urban environment. SLAM algorithms include visual SLAM (vSLAM) [74], centralized collaborative monocular SLAM [75], and so on.

The vSLAM technique is widely used in vehicle localization and it mainly includes three modules: initialization, tracking, and mapping [76]. The initialization module is responsible for establishing the coordinate system, and the tracking and mapping modules have the function of building and updating the map. Meanwhile, the authors of [77] proposed a method which utilizes the LiDAR-based map, which can achieve the real-time performance on 0.06s and the RMSE is about 0.1 m. In order to further enhance the real-time performance, a topview system based on real-time capable image processing pipeline was designed in [78], and the estimation of position is realized by processing data collected by four fisheye cameras. The accuracy of this algorithm is about 0.33 m on the worst condition, and the result refresh time is 0.04 s. Furthermore, another work with high accuracy and real-time performance based on visual sensor is proposed in [79]. In the developed method, the back lane markings registry (BLMR) and data matching method with light-weigh is used. The visual lane marking is detected by sensors and matched with map, for the purpose of estimating the position of vehicle in the map reference. Additionally, the proposed algorithm has high reliability and availability, which can realize data processing and positioning even if the lane markings can not be observed by a short distance detection. The positioning mean error of this method is 0.06 m, for the real-time performance, the result refresh time is 7.66 ms.

Meanwhile, another work called high-speed pavement visual odometry (HSP-VO) method based on two cameras was proposed in [80]. The data collected by the lateral camera is used to match with the sparse visual map (noting that the sparse visual map is created in the offline step),

which includes GPS coordinates, visual features, and the 3D information. Another down-view high-speed camera is used to increase the efficiency of feature extraction during the vehicle's movement at high speed. Moreover, the KF technique is employed to fuse the data provided by the two cameras. The accuracy of this method is 0.19 m on mean error. In addition, the mean time consumption of the feature extraction and matching process by using raw images is about 14.1 ms, which is an excellent real-time performance.

2.3.4 Discussion

Although passive sensors can achieve low-cost localization, their accuracy, robustness, and availability may not meet the high-performance requirements of ITS applications. The accuracy of GPS positioning is easily affected by the NLOS and multi-path effect, and the GPS is completely ineffective in signal-denied environments. Nowadays, a more popular approach is to use GPS as an aid equipment, combining it with other sensors through data fusion methods to achieve higher-performance localization. For example, in low-cost sensor localization systems with excellent scalability performance, GPS receivers are important sensors. Additionally, only using an IMU sensor cannot achieve accurate result because the cumulative error grows rapidly over time. However, it can achieve localization with excellent real-time performance, as shown in [54]. Moreover, vision sensors play an irreplaceable role in the positioning domain, particularly in SLAM algorithms, and reasonable accuracy can be achieved. However, vision sensors depend on light intensity and weather conditions. In order to increase real-time performance, a graphics processing unit (GPU) with high-performance should be equipped, which increases economic expenses. Furthermore, vision sensor-based methods using maps require additional computation power to process and store the maps. With the development of AI techniques in the field of image processing, applying AI techniques to vision-based methods has great potential to enhance accuracy and real-time performance.

2.4 V2X Based Cooperative Localization Methods

Unlike the self-vehicle localization method, cooperative or collaborative vehicle localization methods use the V2X technique to share their state data (such as velocity, heading, location, and environment information) between vehicles or infrastructures, achieving the purpose of enhancing the efficiency through data sharing. V2X enables the data communication capability between vehicles and other objects (such as base stations) [81]. It includes V2V, V2I, vehicle-to-cloud (V2C), vehicle-to-road-signs (V2RS), vehicle-to-network (V2N), and vehicle-to-pedestrian (V2P). The V2X standards are DSRC (IEEE 802.11p) and C-V2X (3GPP LTE/5G NR) [82]. The 802.11p band is 5.9 GHz (5.85-5.925 GHz) [83]. The details of cellular-based V2X communications are in [84]. Combining main communication techniques such as UWB (802.15.4a) [85], Wi-Fi (IEEE 802.11) [86], RFID [87], and cellular-based (5G) [88] with AOA [89], TDOA [90], and RSS [91] [92] methods, the range estimation and cooperative vehicle localization can be achieved. In this section, we analyze the state-of-the-art vehicle localization based on V2V and V2I communication techniques.

2.4.1 V2V-Based Localization Methods

The V2V-based localization method refers to the vehicle localization method which utilizes the data shared between connected vehicles. By using the shared state of other vehicles, such as their distance, speed, position, and orientation angle data in V2V networks, a vehicle can achieve localization with reasonable accuracy [93]. The main protocol of V2V is IEEE 802.11p, and the communication data mainly includes three kinds of messages: cooperative awareness messages (CAMs), decentralized environmental notification messages (DENMs), and service announcement messages (SAMs) [26]. One work based on V2V communication technique named implicit cooperative positioning with data association (ICPDA) has been proposed in [94]. Two algorithms named ICP-DA-PF and ICP-DA-LC are proposed for vehicle localization in urban environment. Additionally, a new distributed Bayesian framework is designed and a

belief propagation algorithm is proposed to solve the data association problem over the framework in a distribute way. Considering the communication/processing overhead in the cooperative vehicle system, the distributed KF is employed to solve the trade-off between positioning accuracy and algorithm complexity. The experiment results shown that the RMSE of vehicle localization in real urban scenario is about 0.8 m.

Meanwhile, the authors of [95] proposed an algorithm which uses the chain branch leaf (CBL) clustering method in VAENTs, which can improve the adaptability to different data transfer rates during the V2V communication process. Additionally, they propose the multi-point relaying technique to reduce time delay and optimize network routing. Experimental results show that in real scenarios, the latency is less than 250 ms in all scenarios, and the average time delay is about 180 ms, which improves real-time performance. In the real world, radio-based cooperative vehicle localization methods are susceptible to the influence of multi-path signals provided by different types of objects in the process of information transmission, thereby reducing the accuracy of positioning.A work on mitigating the effects of multi-path signals on localization accuracy is proposed in [96]. Firstly, in order to make better use of the localization information provided by different objects, a radio map is established to store the number of objects, object type, and object state. Then, the probability hypothesis density filter and a map fusion routine are proposed to integrate the available information provided by multi-path signals to enhance the accuracy of vehicle localization. The RMSE of localization result is less than 0.3 m, which shows that this method can effectively utilize information generated from different types of objects and the high reliability. However, map matching based localization methods need to create and maintain a large-scale map which causes expensive calculation and data storage cost.

2.4.2 V2I-Based Localization Methods

The V2I technique can realize data sharing and communication between vehicles and roadside units (RSUs)/ base stations (BSs), and the protocol for V2I is IEEE 802.11p. Compared to

V2V-based methods, V2I-based methods have more effective information (such as the position of fixed RSUs and BSs). To make full use of the position of fixed BSs to increase the accuracy, the authors of [6][97] proposed the V2I-based method by using data-fusion technique to realize vehicle localization in the IoV system, and the GPS data correction technique is also employed. In the system model, the RSU is equipped with a GPS receiver that can provide the difference of received GPS data from the real position, which is utilized to correct the real-time position collected by on-board GPS receivers. In the data processing stage, a data fusion system consisting of KF and EKF techniques is designed to fuse the corrected GPS data and IMU data to obtain the position of the vehicle. The advantage of this algorithm is that only one single RSU is used to collect data from multiple vehicles, making the economic expense low. When the vehicle passes the toll gate ramp, the error is less than 0.1 m, which is accurate. However, if the GPS signal is not available or has high time delay during transmission, the real-time performance and accuracy will be seriously affected. To improve the accuracy when the GPS signal strength is insufficient, the authors of [98] proposed a direction of arrival (DOA) and V2I technique-based algorithm. The system model consists of three cooperating BSs, and the sparse Bayesian learning (SBL) robust technique is used to enhance the stability and effectiveness of DOA data. Finally, the vehicle position is estimated by processing the location data of BSs and DOA measurement data generated in different situations. The advantage of this algorithm is its high robustness, and it can be used in non-uniform noise scenes. The disadvantage is that it requires high hardware facilities (three BSs are required), and it is difficult to realize vehicle localization in an environment with insufficient BSs in the real world.

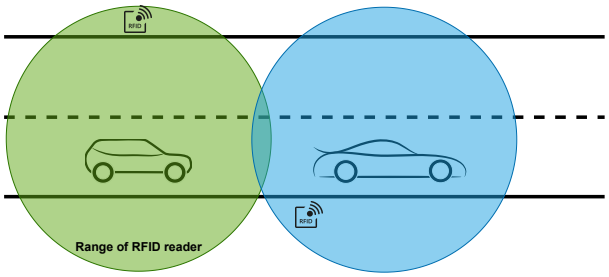

Figure 2.1: Model based on RFID

The radio frequency identification (RFID) technique is commonly used for indoor localization, where the tag reader reads data on the tag through radio signals to collect data. The communication diameter of the tag reader is shown in Fig. 2.1. Tags are deployed on the roadside, and the tag reader is equipped on the vehicle. When the distance between tags and the car is less than the communication range, the reader can get the information provided by the tags. The international standards organization (ISO) has three standards for RFID: ISO 14443, ISO 15693, and ISO 18000, and the tags include active tags and passive tags. The authors of [99] utilized ultrahigh frequency (UHF) RFID to achieve accurate localization in a GPS-less environment. They use the robust Chinese remainder theorem (CRT) and the levenberg-mlarquardt (LM) method to estimate the position of the vehicle. The frequency band of the reader is between 902.75 and 927.75 MHz, and the protocol is ISO/IEC 18000-6C Class1 Gen2. The error is less than 0.27 m with 90% probability. Since this method has excellent real-time performance, the error caused by the time delay is less than 0.1 m. However, this algorithm's complexity is made up of two parts: CRT ($O(nN^2)$) and LM ($O(Kk^3)$), where n and N are the number of tags and signal frequencies, respectively, and K and k are the number of iterations of the LM method and the dimensions of the matrix, respectively.

Furthermore, related work concerning unmanned aerial vehicle (UAV) accurate localization, a system which realizes six degrees of freedom (6-DoF) localization was proposed by [100]. Each UAV is equipped with three or more RFID tags, and the Bayesian filter method is implemented to estimate the location of the UAVs. The mean error and orientation estimation result is 0.04 m and 2.5 degrees, respectively. Meanwhile, for the purpose of enhancing the real-time performance, the authors of [101] designed a real-time localization system (RTLS) based on RFID and UWB technique. This system includes the real-time data acquisition layer, the data processing layer, the holographic workshop map layer, and the application service layer. The response time is less than 0.5 s and the average accuracy of RFID and UWB based localization method is 0.39 m and 0.18 m, respectively.

2.4.3 V2V and V2I-Based Localization Methods

For a localization method that takes advantage of both V2V and V2I communication techniques, the authors in [102] designed a generic stochastic localization framework which can process different type of data collected by sensors. A PF based algorithm is designed to fuse the relative positioning provided by neighbor vehicles, which can achieve a reasonable localization error with about 1 m. However, the data transmission delay and the relative data association is not considered, which may have a bad influence on the real-time performance.

Moreover, in order to realize vehicle localization in weak GPS signal environments, the authors of [103] designed an error-cognitive localization system that uses both the V2V and V2I technique. This system includes a tag-reading model, a tag deployment model, and a position correction model, etc. The roadside tag deployment method is obtained through matrix analysis, and data such as vehicle speed, tag distance, and correction parameters are used to increase the accuracy. This algorithm can realize vehicle localization in scenarios where there is no GPS signal or the GPS signal is weak, and the proposed tag deployment method reduces the number of tags utilized in the system, further reducing economic expenses. Additionally, the RMSE is less than 0.5 m. At the same time, the authors of [104] proposed a cooperative localization algorithm by using GPS pseudorange errors in the V2X network. V2V and V2I communication techniques are employed to share positions, pseudorange estimated errors, and DR data, while set inversion and constraint propagation (CP) techniques are used to design the distributed estimation algorithm. Highly reliable confidence domains can be calculated without the need for direct range measurements, and the latency is less than 0.1 s.

2.4.4 Discussion

The V2X-based vehicle localization method can enhance the cooperative interaction ability of the whole system by realizing information sharing, thereby further enhancing the information utilization effectiveness in the system. In addition, fault detection and exclusion methods can

also enhance the efficiency, which can also benefit from V2X communication techniques [105]. With the development of the 5G, the communication efficiency can be further enhanced, which can enhance the performance of V2X-based methods. Compared to V2I-based methods, the V2V-based method has better scalability performance since it does not require infrastructure deployment, such as base stations. However, the V2I-based localization can increase accuracy since the position of infrastructure is fixed, which can realize the correction of positioning errors. The disadvantages of V2X-based methods include the need of communication resources and time delay during communication process, especially in the large number vehicles scenarios. So, the time delay during data transmission should be considered in order to increase the accuracy. Additionally, the RFID-based method can provide excellent positioning performance in special application scenarios, such as highway toll gates or parking lots. In summary, V2X-based localization has excellent potential for high-precision vehicle positioning applications (such as autonomous driving).

2.5 Multi-sensor Based Localization Methods

From the above discussion, no single sensor can meet the availability, scalability, computational complexity, economic expenses, accuracy and real-time performances. So, taking advantages of multiple sensors has the substantial potential to achieve vehicle localization with more comprehensive performance. In this section, we will analyze the multi-sensor based localization methods.

2.5.1 Map-based Multi-sensor Localization Methods

The authors of [106] proposed a method based on an improved Monte Carlo localization (MCL) technique that utilizes both GNSS and LiDAR data to achieve robust localization in different environments. The GNSS data increases accuracy in feature-poor scenarios, and the LiDAR data can enhance accuracy in feature-rich scenarios. This method can achieve high accuracy in

complex environments (0.566 m position mean without GNSS and 0.3895 m on average position mean with GNSS). However, the sensor cost is high, which hinders large-scale implementation. Another algorithm that uses radar and camera was proposed in [107].

Meanwhile, to enhance the real-time performance of multi-sensor-based consistent localization methods using mapping, the authors of [108] proposed a global map based algorithm which achieves a result refresh rate of 25 Hz with an average error which is less than 0.1 m. To get the position of vehicle in underground parking lots, a method based on Wi-Fi and computer vision techniques was proposed in [109]. This algorithm uses dead-reckoning (DR), the random sample consensus (RANSAC) method, and complementary filter to realize data fusion and correct errors in offline maps, achieving the accuracy of less than 1 meter. The advantage of this algorithm is that it can achieve reasonable accuracy when GPS is unavailable, but the requirements for the various modules of the localization system can lead to high complexity. In addition, another map based multi-sensor data fusion vehicle localization method is proposed in [110]. The authors use images sequence and wheel-inertial ego-motion data to create a semantic local map at first. The position estimated by camera data is provided by matching the local map with the online map database. The map matching process is simplified by using the developed supervised neural network, which can reduce computational overhead. The mean absolute errors of positioning result are 0.04 m and 0.17 m in the lateral and longitudinal directions, respectively. However, the map matching process requires on line map, which may cause positioning time delay.

2.5.2 Data Fusion-based Multi-sensor Localization Methods

The authors of [111] proposed an algorithm named fuzzy adaptive Kalman filter, which can increase the performance of the conventional UKF by verifying and correcting the real-time noise of sensors. The proposed fuzzy adaptive Kalman filter can increase the accuracy by about 40 percent compared to the conventional UKF.

In order to increase the localization real-time performance and accuracy of AVs, the authors

in [112] proposed a real-time localization method based on UKF and PF. The main contribution of this thesis is that both the real-time performance and the accuracy is balanced by the proposed optimization method. The data collected by IMU, LiDAR, and GPS is fused to estimate the position. The result refresh time is about 8.2 ms and with the localization error which is less than 0.3 m. However, the computational complexity is not considered since the PF method has high complexity when the number of particles is large.

Furthermore, to further improve the accuracy, the authors of [113] proposed an IMM-UKF-GNN (grey neural network) algorithm, where the IMM method can achieve a soft switching among three different UKFs (noting that these UKFs have different noise). In this work, the GNN is employed to further increase the accuracy by training. Moreover, the bio-inspired technique has been implemented in data fusion methods. For example, the authors of [114] proposed an integrated robot localization method named particle swarm optimization enhanced particle filter (POF) based on PF and PSO techniques. The pose tracking of robots is realized by the particle set update, evolutionary search and normalization, and resampling steps. The mean error of the result is less than 0.05 m, and the position refresh rate is 96 ms. In addition, another work considering low-cost multiple sensors (gyroscopes, acceleration, magnetic, and mileage sensors) data fusion method was proposed in [115]. For the purpose of reducing the error of result outputted by the EKF, the authors propose an adaptive error correction EKF algorithm that uses the evolutionary iteration mechanism of genetic methods to optimize the noise covariances in the traditional EKF.

Focusing on the vehicle localization in GPS-denied environment, the authors of [116] propose an adaptive continuum shape constraint analysis (ACSCA) method. First of all, one novel identifiable specific target named icosahedron target is defined and detected by LiDAR sensor along the vehicle moving trajectories. The ACSCA algorithm can recognize the icosahedron target and get the relative position data for calculating the position of vehicle automatically. The RMSE of the localization result is less than 0.05 m. However, the time and economic requirements for preparation, data processing and data postprocessing is high. At the same

time, another work focusing on both real-time and accuracy performance is proposed in [117]. This method includes two parts, at the first part, the wheel odometry, IMU, and tightly coupled visual-inertial odometry are employed to collect data. And the data fusion of these different kinds of data is realized by EKF technique. At the second part is dense 3D point cloud mapping, which can process data in real-time based on a standard CPU. The average RMSE of the positioning based on six different experiment scenarios is less than 0.3 m. Moreover, these two algorithms have good performance in GPS-denied environments, which increases the reliability of the localization system. To increase real-time performance, a data fusion-based multi-sensor algorithm is proposed in [118], which has an excellent result refresh time (3 ms).

Additionally, another algorithm based on deep learning and PF was proposed in [107]. A deep learning-based scoring mechanism is designed to detect the position of the rear corner of the vehicle. Then, the authors use the PF to output the estimated vehicle position, and the output data is fused with the radar data to obtain the final position of vehicle, which can achieving an accuracy of 0.18 m. The advantage of this algorithm is that this system is robust. However, the requirements for the first-acquainted vehicle picture are strict because the picture needs to be applied to extract the rear corner location information, and the final result will be inaccurate if the radar data is inaccurate. At the same time, the authors in [119] utilized the graded KF technique to fuse the data collected by IMU and GPS. This algorithm satisfies the advanced-surface movement guidance and control system (A-SMGCS) standard, and it can achieve comprehensive utilization of sensor data. However, the performance of the result is not analyzed when the vehicle is moving in a non-linear motion, and the impact of changes in road conditions on the accuracy needs to be further considered.

In addition, another algorithm based on multi-sensor data fusion was proposed in [120]. The sensors in the data collection stage include GPS and camera, and the geographic information databases are employed to reduce the impact of accumulated errors on the accuracy due to time change. The error correction process depends on geography information database, if the data information in the database cannot be obtained or the information has big errors, it will affect

the accuracy performance. Another work was proposed in [121], which uses the data collected by camera, GPS, and inertial navigation system to achieve lane-level vehicle localization. The authors utilize the information collected by the camera to match the high-definition (HD) map. And they propose the method based on the iterative closest point (ICP) to deal with errors. The advantage of this algorithm is that it can achieve lane-level localization and does not employ expensive sensors (such as LiDAR), which is conducive to large-scale promotion.

2.5.3 Data Fusion-based Multi-sensor Cooperative Localization Methods

V2V communication technique can realize data sharing in the IoV, which can enhance the positioning performance through a cooperative or collaborative way. The authors of [122] propose a mathematical framework for cooperative vehicle localization by using GNSS, IMU, and UWB sensors. This framework can work in the centralized and distributed manner. The positioning error in both centralized distributed manner are less than 0.08 m. In addition, based on the conclusion of this thesis, we can conclude that compared with the centralized manner, the distributed manner has higher scalability and reliability. Because each vehicle in the system can realize data processing in an independent way. However, the accuracy is lower than that in the centralized manner, since the more precise computation of correlations among the states of vehicles can be processed in the data fusion center.

Moreover, the authors of [123] proposed a cooperative localization method based on GPS receiver and radar by using DSRC technique. The multiple pieces of information are fused by KF technique. When more than three neighbor vehicles communicate with the ego-vehicle, the RMSE is less than 0.5 m. Additionally, another work based on data fusion for cooperative vehicle localization is proposed in [8]. An adaptive ant colony optimization PF (AACOPF) method is proposed, which does not need any prior information. This method includes six steps: particles initialization, importance sampling, adaptive cooperative localization, update weights, ant colony optimization resampling, and output state estimation. Furthermore, the particle propagation model is designed and the weight updating method is developed by analysing range data

provided by UWB sensors. The positioning error is about 0.66 m.

For data fusion for non-linear systems with multiple sensors with correlated noise, the authors in [124] used the adaptive and robust UKF (ARUKF) to design a two-layer data fusion structure named ARUKF-MSIF (multi-sensor information filters). In the first layer, the redundant measurement noise covariance estimation (RMNCE) method is employed to process the unknown noise at each time at first. Then, the chi-square test and indicator calculation and the proposed Q-adaption algorithm are used to further reduce the error. Finally, the final estimation is determined in the fusion center in the second layer. In addition, the author of [17] proposed a data fusion method named covariance intersection (CI), which can solve the data fusion problem with unknown correlation between input data and yield consistent estimates. However, the CI method has pessimistic estimate results since the source data is treated as totally correlated, and the independent part is not considered. Therefore, the author of [125] proposed the split covariance intersection filter (SCIF), which can estimate the source data in both correlated and independent parts. Moreover, the authors of [126] use the SCIF to fuse the data from GNSS, camera, LiDAR, and HD maps, which achieved an accuracy with RMSE of 0.27 m.

2.5.4 Discussion

The analysis above shows that multi-sensor-based vehicle localization methods have a good performances since they combine the advantages of different sensors and communication methods. However, in order to obtain better algorithm performance, there are still many factors that need to be considered. The first factor is the independence of the data to be fused. When each input information source can be expressed as a random variable with a known mean, covariance, and cross-correlation with the other sources, rigorous estimate results can be achieved by traditional KF, EKF, UKF, and PF. However, the fusion result is not consistent when there is correlation between input estimates. Meanwhile, the CIF can yield consistent fusion results even when facing an unknown degree of source estimate correlation, but it neglects the independent information, which yields pessimistic estimate results. The SCIF can increase the accuracy of the

estimated result because both known independent information and unknown correlated information in source data are considered. The second factor is the redundancy of the input data, and the constraint propagation techniques on interval can realize a reliable result when facing redundant data. Moreover, the authenticity of the input data should also be considered. Since a large number of sensors are used in large-scale vehicle localization systems, fault detection and identification techniques need to be utilized to increase the robustness of the system. For an efficient data fusion structure, since the two-layer structure is easily affected by communication delay, high-efficiency data fusion algorithms for error correlation should be developed.

2.6 Localization Methods Performance Analysis, Challenges and Research Questions

2.6.1 Methods Performance Analysis

In this section, we analyze the comprehensive performance of state-of-the-art vehicle localization methods and identify the associated challenges. We present the characteristics of different data collection methods in Tab. 2.1, including their deployment strategy, the precision of collected data, ability to work without light, ability to capture color information, cost of the sensors, and ability to work in bad weather conditions. Additionally, we analyze and compare the comprehensive performance of different localization algorithms, as illustrated in Tab. 2.2. The data is based on the details of traditional active and passive sensors based methods, as shown in Tab. 2.3, the details of cooperative localization methods, as illustrated in Tab. 2.4, and the details of multi-sensor based algorithms, as shown in Tab. 2.5.

Table 2.1: The comparison of different sensor-based localization methods

CHARACTERISTICS	LIDAR-	RADAR-	ULTRASONIC-	GPS-	IMU-	VISION-	V2X-
DEPLOYMENT	Easy	Easy	Easy	Easy	Easy	Easy	Hard
DATA PRECISION	High	Middle	Low	Middle	Low	High	High
WITHOUT LIGHT	Yes	Yes	Yes	Yes	Yes	No	Yes
COLOR	No	No	No	No	No	Yes	No
PRICE	Expensive	Middle	Middle	Middle	Middle	Middle	Middle
WORK IN BAD WEATHER	No	Yes	Yes	Yes	Yes	No	Yes

Table 2.2: Performances of different methods

Performances	LOW	Middle	HIGH
Accuracy	Ultrasonic-, GPS-, IMU-	Radar-, V2V-, V2I-	LiDAR-, Vision-, Data Fusion-
Availability	Vision-, LiDAR-, V2I-	Data Fusion-, V2V-	GPS-, Ultrasonic-, Radar-, IMU-
Scalability	LiDAR-, Vision-, V2I-	V2V-, Data Fusion-	Ultrasonic-, Radar-, GPS-, IMU-
Reliability	IMU-, Ultrasonic-, GPS-	Radar-, V2V-, V2I-	Vision-, LiDAR-, Data Fusion-
Real-time	V2I-,V2V-, Data Fusion-	LiDAR-, Vision-, GPS-	Radar-, Ultrasonic-, IMU-

The LiDAR can provide the distance and angle data that between the vehicle and the object by receiving information such as the intensity and angle of the reflected light wave after the laser reaches the object. The data collected by LiDAR has high accuracy, strong stability, which is very suitable for applications with high localization accuracy requirements.The drawback is its susceptibility to interference from natural weather conditions, such as rain, snow, and fog, leading to a decrease in accuracy under severe weather conditions. Meanwhile, the vision sensors can provide precise data for localization by processing images and extracting feature points. However, the quality of collected data can be impacted by the light intensity. Based on the precise collected data, both the LiDAR-based and vision-based localization methods can achieve reasonable accuracy with high reliability. However, they have high computational complexity, the reason is that the picture and map generated by LiDAR (especially 3D maps) need large amount of computing and storage resources. One of the effective solution is that

applying AI technique to vehicle localization [127] [62], which has great potential since the AI technique has outstanding performance in the field of image processing. The flowchart of AI technique is shown in Fig. 2.2. It mainly includes the data collection, data preprocessing, data features selection, model training, optimization and analysis steps. In addition, the LiDAR-based and vision-based methods have low scalability, because their high economic expenses.

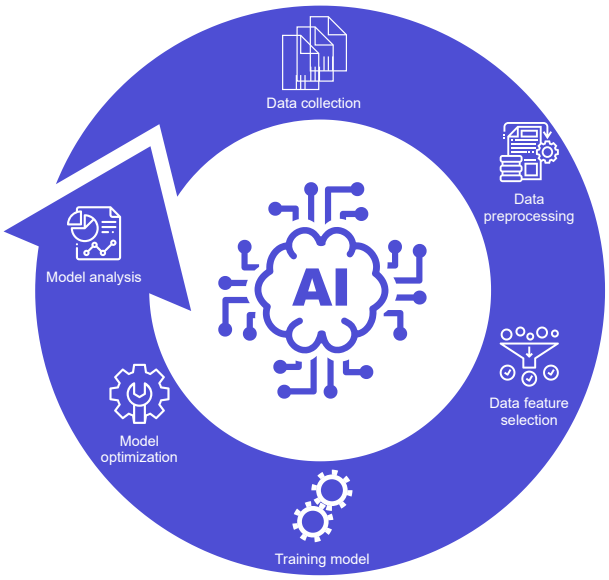

Figure 2.2: The flow chart of AI.

Although GPS-based, IMU-based, radar-based, and ultrasonic-based methods cannot meet the high accuracy requirement, these sensors play a key role in the data fusion system, especially in low-cost data fusion systems, because they have high scalability and availability. Moreover, these sensors can also effectively collect data in extreme weather while vision-based and LiDAR-based methods may not work well. For instance, compared to other data collection methods like LiDAR, the IMU sensor has better cost-saving performance and stronger anti-interference ability. Additionally, the data collected by the IMU is relatively stable and exhibits strong continuity across various weather and environmental conditions. However, the disadvantage is that the localization data error accumulates with time, affecting the accuracy of localization, and it is not suitable for scenes requiring high vehicle localization accuracy and localization applications with long time and distance requirements. As for GPS technique, its

advantages include low economic cost, easy deployment, and wide coverage of GPS signals. Therefore, as an auxiliary sensor, GPS is suitable for most localization scenarios since it is not easily affected by bad weather or light. Furthermore, data fusion-based methods can also achieve highly accurate localization results by making full use of resources collected by various sensors. By using certain optimization criteria, to obtain a reasonable fusion result [128] [129] [130]. Popular data fusion techniques include KF, EKF, UKF, PF, etc., can achieve high scalability, reliability, and computational efficiency in vehicle localization. Multiple sensors can provide more options for realizing vehicle localization, thereby increasing the robustness of localization system.

Moreover, the V2I and V2V based methods can reach a middle accuracy. And the V2X communication technique also plays an irreplaceable role in cooperative localization because it can realize data sharing in the IoV system. Compared with V2V-based methods, the V2I-based has a better performance on accuracy and reliability. The reason is that the position of infrastructure is fixed while the position of other vehicles has a certain error. For example, the RFID technique uses tags and readers to cooperate with each other to realize data transmission and collection. Generally speaking, in the process of vehicle localization, the reader is equipped on the vehicle, and the tags are equipped on the roadside or buildings with obvious signs to provide location information or other data. The advantages of this technique for data collection can realize fast data reading speed, which can efficiently collect data. Moreover, the RFID tag is small in size and its deployment is not easily restricted by environmental conditions. However, its communication distance is limited, and if the distance between the reader and the tag is too long, it will affect the efficiency and accuracy of data collection seriously. Compared with the V2I, the V2V has the better performance on the scalability and availability, since the deployment of the infrastructure will cause additional economic costs. However, the V2X-based methods have higher computational complexity than data fusion-based methods. Because the time delay during data transmission in both V2I and V2V can not be neglected. In addition, by utilizing the distance measurement methods (TOA, TDOA, RSSI), the location of vehicles can be calculated

by geometric method (The trilateration algorithm) [131] [132] [133] [134].

In addition, compared to non-cooperative vehicle localization methods, the cooperative vehicle localization algorithm has the advantage of utilizing information interaction and data sharing between vehicles and infrastructures. This enhances the utilization rates of data and resources, including data storage, computing, and communication resources. Moreover, most cooperative localization algorithms have distributed data processing capabilities, which greatly increases the parallelism of the localization process, reduces the centralized data processing burden on the server, and improves data processing efficiency. However, if there are a large number of vehicles in the ITS or the amount of collected sensor data is massive, the data transmission process may cause system channel congestion, resulting in additional time delays and affecting vehicle localization efficiency. Additionally, the computing power of the vehicle is limited, and if the data requires high computing power, the data processing efficiency may decrease.

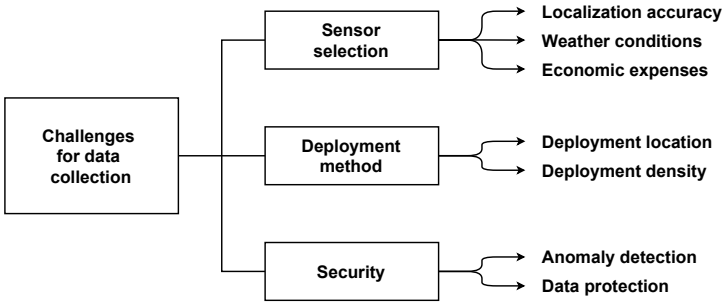

Figure 2.3: Challenges for data collection.

2.6.2 Challenges

We propose challenges for vehicle localization in the data collection and data processing steps. The challenges for data collection are illustrated in Fig. 2.3. The main challenges faced in the data collection stage of vehicle localization in ITS are three aspects: sensor selection, deployment method, and security. For the sensor selection problem, it is necessary to consider the comprehensive performance (analyzed in the last section) of different sensors. For example, the LiDAR collects data with the highest accuracy, the IMU is suitable for data collection in extreme

weather, and the LiDAR has high economic costs. Moreover, the environment should also be considered, such as GPS-denied environments [135]. For the deployment method, it is necessary to comprehensively consider the deployment method and density of the sensor. The IMU, LiDAR, GPS receiver, and some cameras belong to the onboard equipment, and their deployment method is simple. However, RFID requires the deployment of tags on the road or in the external environment, so it is necessary to make a decision on the deployment method based on economic costs and data collection efficiency factors. For the security of sensor data collection, it is necessary to consider two aspects: anomaly detection and data protection. Anomaly detection techniques can ensure the safety, effectively operate sensors and avoid malicious node intrusion. Data protection techniques can ensure data integrity and security and prevent data leakage.

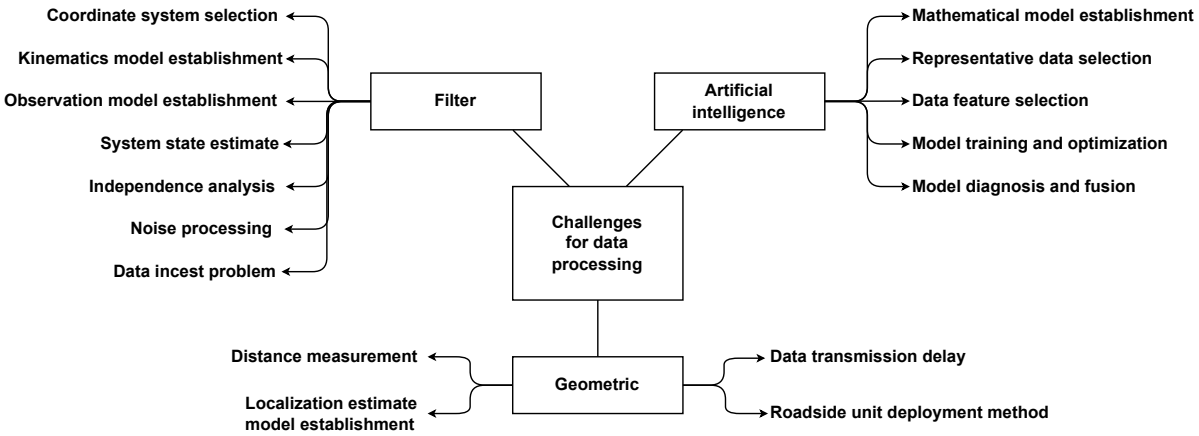

Figure 2.4: Challenges for data processing method.

The challenges at present of data processing method are shown in Fig. 2.4. For the data fusion technique, the challenges are seven aspects: coordinate system selection, kinematics model establishment, observation model establishment, system state estimate, independence analysis, noise processing, and data incest problem during data fusion. For coordinate system selection, especially in relative position estimation, the coordinate system transformation must be implemented. Moreover, the vehicle kinematics model should be determined. For example, the IMM filter technique can realize high accuracy localization since it considers the interaction among different models. And for the observation model establishment, we should consider the conver-

sion of partial observation. At the same time, the influence of noise on the observations should also be considered. And regarding the system state estimation, not only a priori estimate is required, but also a posteriori estimation should be calculated. So, reducing algorithm complexity brought by the matrix inversion calculation is also a challenge. And the process has a certain time delay, it is also necessary to consider the influence of the time delay on the subsequent system state estimate results to obtain the best estimation value. Furthermore, the independence analysis is a key step during data fusion, the CIF, SCIF has excellent performance when facing the uncertain independence between input data. For noise processing, the unbiased estimation and biased estimation technique should be selected reasonable. Finally, the data incest problem can not be ignored especially in multi-sensor multi-vehicle localization system, the constraint propagation on intervals technique can be implemented to solve this kind of problem.

Moreover, using AI techniques to achieve vehicle localization can improve the utilization rate of data during the localization process and enhance the accuracy of localization results, especially in applications that require high localization accuracy, such as autonomous driving. Exploiting AI techniques such as neural networks and deep learning can obtain precise localization results and improve the robustness of the system. For example, in a certain period when the data collected by sensors is lost or the data is inaccurate due to data transmission errors, the performance of traditional algorithms will inevitably be affected because their decision-making is very dependent on the accuracy of data collected by sensors. However, compared with traditional algorithms, AI techniques require a larger amount of different types of data, which increases the pressure in the data collection process. In terms of computational cost, the time and energy costs are greater than that in traditional algorithms, because it requires more time for data training, and regarding the neural network technique, its computational cost is affected by the depth of the neural network designed. Therefore, in the process of constructing a neural network, we not only need to consider its impact on the accuracy of the output result but also its complexity. For AI techniques, the challenges of applying them to vehicle localization are the establishment of mathematical model representative data selection, data feature selection,

model training and optimization, and model diagnosis and fusion.

First of all, for the mathematical model establishment, the problem and expected result should be divided and determined based on the existing data, and the field such as clustering or regression should be determined because it takes a lot of time to realize a certain function through AI techniques. Therefore, it is very important to determine the appropriate mathematical model. Then the representative data selection step is considered, because the amount of data that needs to be processed is huge. If all the data is processed, not only a lot of time and computing resources are wasted, but also the redundancy or wrong data in the data set will cause a bad influence on the results. So, it is necessary to select representative data for analysis and processing. And the possible solution to this type of problem is to evaluate the magnitude of the data in advance and use existing computing resources to estimate it. If the amount of data is too large and the existing computing resources cannot support its calculations, the dimensionality reduction method should be employed or the calculation method should be changed, such as using distributed computing instead of centralized computing or improving the complexity performance of the algorithm. Therefore, the representative data selection method can achieve the effect of enhancing the efficiency of the algorithm and reducing the computational burden.

For data feature selection, the main function of this step is to reduce the bad influence caused by erroneous or redundant data. This process requires feature preprocessing and validity analysis of the data. For data feature preprocessing, the effective methods are the removal of collinearity and normalization, etc. For feature validity analysis, the main methods includes the Chi-square test and correlation coefficient calculation. An effective data feature selection method can enhance the credibility of the results and reduce the waste of computing resources. For the model training and optimization stage, the main problem is that the parameter tuning problem. Excellent parameters are a necessary factor to enhance the efficiency of the algorithm, and therefore, it is necessary to have a deeper understanding of the algorithm and more attempts to discover the inherent laws. For model diagnosis and fusion, the first step is to perform the error analysis method on the output results, in order to obtain the reasons for the error such as

model selection or parameter selection error, and then using cross-validation or other methods to diagnose the model. In addition, if the model is overfitted, the eliminate overfitting techniques should be developed. The recent work for AI-based localization has been reported in [136].

In addition, the algorithm that takes advantage of geometric methods to achieve vehicle localization exploits data such as the position data, angle data, and communication time on a two-dimensional plane. The advantages of this type of algorithm are that the complexity is low. The disadvantage of this type of algorithm is that the accuracy of vehicle localization is lower than that of using AI technique and data fusion-based technique. And the time delay in the data transmission process, which is not conducive to real-time vehicle localization. The challenges of using geometric methods to process data are the distance measurement, the localization estimate model establishment, the data transmission delay, and the roadside unit deployment method. For distance measurement, such as wireless communication scenarios, using TOA, TDOA, and RSSI methods to calculate distance, the challenge is that the influence caused by time delay and noise interference on distance accuracy during data transmission. And the solution is to implement the noise reduction method on the signal and optimize the transmission time delay to obtain a more accurate distance measurement result. For localization estimate model establishment, it is necessary to comprehensively consider the influence of various data on location results, and establishing an effective mathematical model to operate on the data. Furthermore, its computational complexity and parameter optimization are also factors that must be considered. For data transmission delay, the solution is to increase the channel bandwidth and optimize the channel method used for data transmission. Finally, with regard to the roadside unit deployment method, it is necessary to comprehensively consider the impact of roadside deployment location and density on the localization results, and also to determine the optimal deployment method based on economic cost.

Furthermore, the challenges for vehicle cooperative localization mainly includes three aspects: network selection, algorithm design, and software design, as illustrated in Fig. 2.5. For network selection, the main communication methods are the V2V and V2I, and the challenges

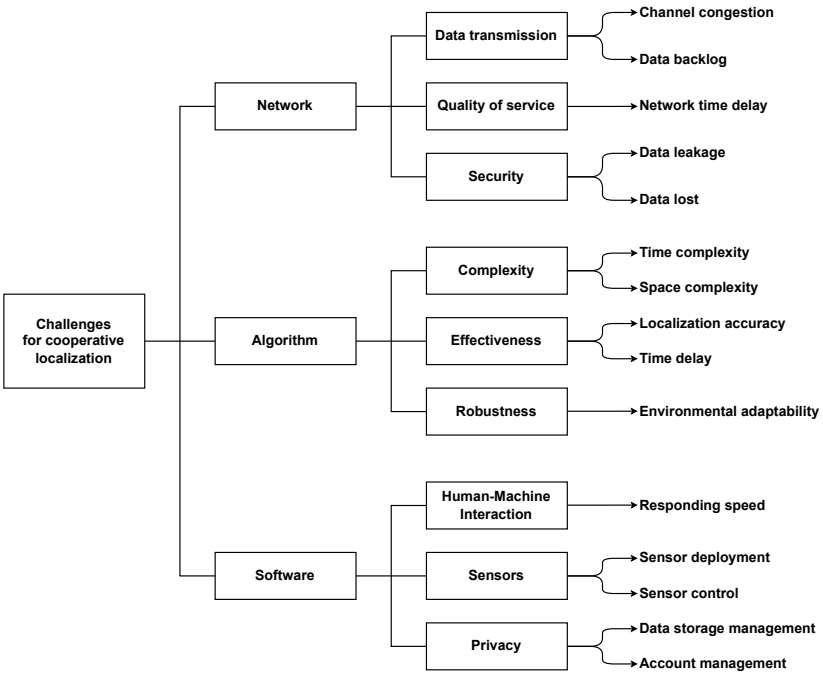

Figure 2.5: Challenges for cooperative localization

are similar, namely data transmission, quality of service, and security issues. For the data transmission process, if the number of vehicles and sensors in the communication range is large or the amount of data that needs to be exchanged is huge, it is easy to cause the channel congestion and data backlog, which can have a negative impact on the quality of service and network time delays. This issue can also affect the efficiency of data transmission and processing. Furthermore, network security issues can not be ignored too. Due to the openness of the network, when nodes or vehicles frequently exchange data by the network, they may give malicious programs the opportunity to implant and cause the data leakage. In addition, attacks on data storage databases are also an important reason for data leakage and loss. Possible solutions include improving and strengthening the identity authentication technique, effectively managing the nodes and vehicles that utilize the network, and reducing the possibility of malicious nodes joining the network. Recent encryption techniques can also be used to encrypt and save data in the database, and the key can be changed regularly to prevent the database from being used maliciously and to ensure the confidentiality, integrity, and authenticity of the data. Finally, the fault detection method [137] can be employed to increase the robustness of the multi-sensor

multi-vehicle cooperative localization system.

Moreover, the algorithm design mainly includes three aspects: algorithm complexity, algorithm efficiency, and robustness. Algorithm complexity mainly includes time complexity and space complexity, which together determine the efficiency of the algorithm. The time complexity of the algorithm mainly depends on the running time of the algorithm, and the space complexity is limited by the random access memory (RAM) requirements of the algorithm. When the localization algorithm is applied to a large-scale system, the data calculation time can be reduced and the algorithm efficiency can be enhanced by sacrificing the space complexity to reduce the algorithm time complexity, because the RAM and hardware in large-scale system are sufficient to meet the algorithm data processing requirements, and large-scale system has higher requirements for time performance and algorithm efficiency than small-scale system. For a small-scale system, the RAM and hardware in the system can be reduced by sacrificing the time complexity of the algorithm to achieve the purpose of reducing economic expenses. For algorithm efficiency, the main challenge in localization is accuracy and time delay performance. Additionally, the real-time performance mainly depends on the selection of the communication model and channel width, and the proper communication scheduling can also reduce the time delay. The recent work for real time performance analysis has been reported in [18]. For the robustness performance of the algorithm, since there will be sudden changes caused by the change of environment, such as weather and road conditions, the implementation of the localization algorithm should consider the response strategy for emergencies, to avoid the occurrence of invalid localization result due to external factors.

In addition, in terms of software design, the challenges facing the implementation of localization algorithms are human-machine interaction, sensor management, and software privacy protection. For the needs of human-computer interaction, the software augmented reality function should be considered. The user customization technique can be implemented since it bases on user needs which can minimize economic expenses. Moreover, the augmented reality function can better enhance the users' feeling of utilizing the software and enhance the

human-computer interaction. In addition, methods based on knowledge-driven and embedded computation to enhance computing power should be used to enhance the practicability of the software. For sensor management, it includes sensor deployment and sensor control methods. Sensor deployment methods include the selection of sensor deployment locations and the deployment density required by the system. Efficient sensor deployment methods can effectively provide the data required for localization and appropriately reduce economic costs. Sensor control methods include sensor data collection time and frequency control, and a reasonable sensor control method can enhance the interaction between sensors and vehicles, while can effectively collect data and increase the accuracy of localization while enhancing the robustness of the system. For software privacy protection, it mainly includes two aspects: data storage management and account management. For data management, the current challenges are database security and data access security, because if the database and data access process is maliciously invaded, it will affect the privacy of the software. In order to response to this problem, possible countermeasures include updating the software operating system in real-time, reducing software vulnerabilities, and making the system more secure can be employed. At the same time, implementing encrypted passwords method can reduce the possibility of malicious users damage the software security. In addition, real-time system backup method can be used to ensure the integrity of data when the software is unavailability. For account management, the system can employ a privacy database to protect the security of user accounts and passwords. Users should be vigilant about personal privacy, frequently changing account passwords, avoiding virus intrusion, and at the same time taking advantage of device lock and other device management software to manage the device to prevent malicious users from destroying the system.

2.6.3 Research Questions

Through the survey of state-of-the-art vehicle localization algorithms, the main research questions of this thesis includes the following three aspects:

Table 2.3: Details of traditional algorithms

REF	SENSOR(S)	DATA PROCESSING METHOD	ACCURACY	REAL-TIME PERFORMANCE	ADVANTAGES	SCENARIOS
[27]	3D LiDAR	Map matching	lat.=0.057 m long.=0.178 m	183 ms (Processing time)	FRPDM can reduce the space complexity significantly	Urban
[31]	3D LiDAR	DWM and UKF	4 cm	60 ms/frame	High accuracy	Underground mine
[32]	Multi-layer LiDAR	NDT and EKF	lat.=0.38 m, long.=0.08 m	NA	Can be implemented in mountainous rural environments	Public road
[34]	Camera-LiDAR sensor	Lightweight deep neural network	NA	92 frames/s	High reliability	Day-night changed
[38]	3D LiDAR	CMAD	0.1-0.3 m	NA	The traditional NCC method is improved	Real-world
[42]	76GHz MWR	Error propagation model	lat. 0.25 m on RMSE	NA	High availability	Snowfall weather
[45]	mmWave radars	polynomial regression model	2.56 degrees on RMSE	NA	Low complexity	Ground and aerial
[48]	Multiple ultrasonic sensors	Ground reflection elimination filter	13.5 cm on RMSE	Processing time is 0.58 s	Good real-time performance	Real-world
[77]	Vision sensor	Mapping	0.1 m on RMSE	Result refresh time 0.06 s	High accuracy	Urban
[80]	Vision sensor	Mapping	0.19 m on mean error	Mean time consumption is about 14.1 ms	High scalability	Campus road

Table 2.4: Details of cooperative algorithms

REF	COMM. TECHNIQUE	DATA PROCESSING METHOD	ACCURACY	REAL-TIME PERFORMANCE	ADVANTAGES	SCENARIOS
[138]	V2V	ICPDA	The RMSE is 0.8 m	NA	High scalability	Urban
[96]	V2V	PHD filter	RMSE is less than 0.3 m	NA	High Reliability	Real-world
[6]	V2I	KF and EKF	0.1 m on RMSE	NA	High accuracy	Highway
[100]	V2I	Bayesian filter	Mean error is 0.04 m	NA	High accuracy	Indoor
[101]	V2I	Map matching	Mean error is about 0.3 m	The response time is less than 0.5 s	Good real-time performance	Workshop
[101]	V2V and V2I	PF	Mean error is 1 m	NA	High reliability	Real-world
[103]	V2V and V2I	Error-cognitive	RMSE is less than 0.5 m	NA	High scalability	GPS weak
[104]	V2V and V2I	CP	NA	The latency is less than 0.1 s	High Robustness	Real-world

- For cooperative vehicle localization in MSMVs, we aim to address the data incest problem and propose a novel consistent multi-sensor data fusion algorithm.
- We implement the ISCIF algorithm to cooperative localization in MSMV systems. To address the high computational overhead during the relative positioning stage when using traditional SCIF method, the ICP algorithm is employed to preprocess multiple relative position estimates.
- In order to enhance the robustness of the cooperative vehicle localization in MSMV system, we implement the KLD-based FDE methods in our proposed model.

Table 2.5: Details of multi-sensor based algorithms

REF	SENSORS	DATA PROCESSING METHOD	ACCURACY	REAL-TIME PERFOR-MANCE	ADV.	SCENARIOS
[106]	GNSS and LiDAR	Mapping	Mean error is about 0.5 m	NA	High Robustness	Urban canyons
[108]	GNSS, LiDAR	Mapping	Mean error is less than 0.1 m	Result refresh rate of 25 Hz	High reliability	Real-world
[110]	Vision sensors	Mapping	Mean errors are 0.04 m and 0.17 m in the lat. and long. directions.	NA	Low complexity	Real-world
[112]	GPS, IMU, LiDAR	PF and UKF	Mean error is less than 0.3 m	Result refresh time is 8.2 ms	Good real-time performance	Real-world
[116]	IMU, LiDAR	ACSCA	RMSE is less than 0.05 m	NA	High accuracy	GPS-denied
[117]	IMU, vision sensor	EKF	RMSE is less than 0.3 m	NA	High reliability	GPS-denied
[122]	GNSS, UWB sensor	Math framework	Mean error is less than 0.08 m	NA	Low cost	Real-world
[123]	Radar, GPS	KF	RMSE is less than 0.5 m	NA	High scalability	Real-world
[126]	GNSS, camera, LiDAR	SCIF	RMSE is 0.27 m	NA	High accuracy and robustness	Real-world

Chapter Three

Proposed Multi-sensor Multi-vehicle cooperative localization

3.1 Introduction

In this section, we first introduce the ITS scenario in section 3.2. Then, the related techniques for cooperative vehicle localization are presented in section 3.3. After that, we propose the ISCIF algorithm and provide its consistency proof in section 3.4. Furthermore, the cooperative vehicle localization in the MSMV system based on ISCIF is detailed in 3.5. Finally, to enhance the robustness of the system, we implement the KLD-based FDE method to our system, which is shown in section 3.6.

3.2 Intelligent transportation system (ITS)

Intelligent transportation systems (ITS) utilize advanced data communication technique (V2V, V2I, and V2X), sensor technique, and automatic control technique to provide safer, more environmentally friendly, and more convenient transportation services and traffic management. Compared to traditional transportation systems, users and vehicles within ITS can promptly perceive road traffic conditions and incidents, enabling them to make effective transportation and mobility decisions, alleviate vehicle congestion, and enhance the efficiency of traffic networks.

3.2.1 ITS architecture

The architecture of ITS has been proposed in [139] [140], as shown in Fig .3.1, an ITS mainly comprises four components: the system center, vehicles, pedestrians, and the field. Through the use of communication technology, each component can communicate with one another, enabling information sharing. The functions of the system center mainly include traffic control, emergency management, data processing, service information provision, registration of vehicle and pedestrian information, safety monitoring, and target scheduling. In addition, The applications of ITS mainly include electronic toll collection system (ETC), driving behavior

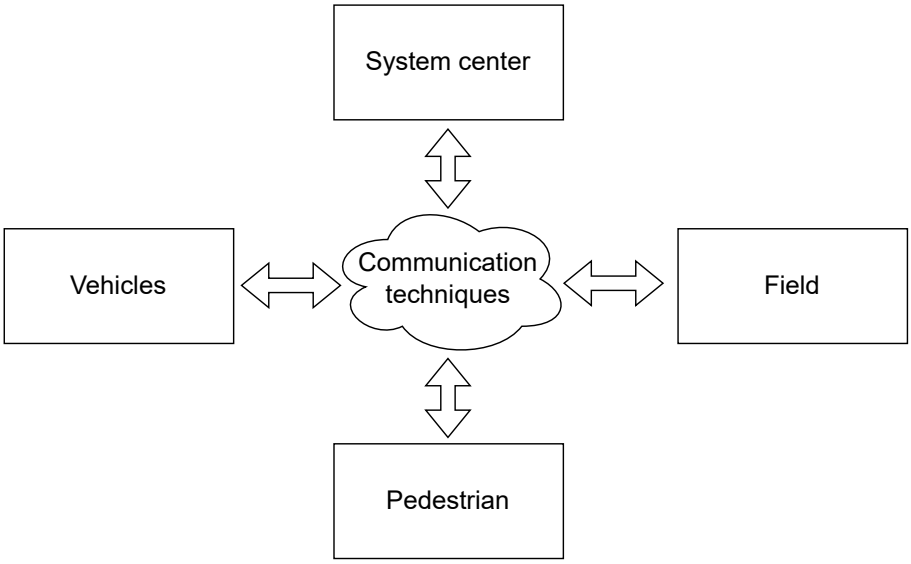

Figure 3.1: ITS architecture

monitoring, and advanced driver assistance systems (ADAS), etc.

3.2.2 Communication techniques for ITS

ITS achieves data sharing and communication among its components through wireless sensor networks. It includes four primary communication techniques: vehicle-to-vehicle (V2V), vehicle-to-infrastructure (V2I), vehicle-to-pedestrian (V2P), and vehicle-to-network (V2N).

An ITS scenario is illustrated in Fig. 3.2. V2V technique realize communication between vehicles, the communication between vehicle and infrastructure is realized by V2I technique, V2P and V2N techniques enable communication between vehicles and pedestrians, vehicles and networks, respectively.

In addition, the network frequency band for dedicated short range communication wireless access in vehicular environments is 5.9 GHz. To achieve safer and more effective information sharing between vehicles, we employ synchronous time division multiple access (TDMA) technique. We adopt the TDMA frame structure outlined in [141], as depicted in Fig. 3.3. Every frame spans 100 ms, during which the left control channel (LCCH) and right control channel (RCCH) are employed for secure data transmission, each enduring for 46 ms. Moreover, a 4 ms

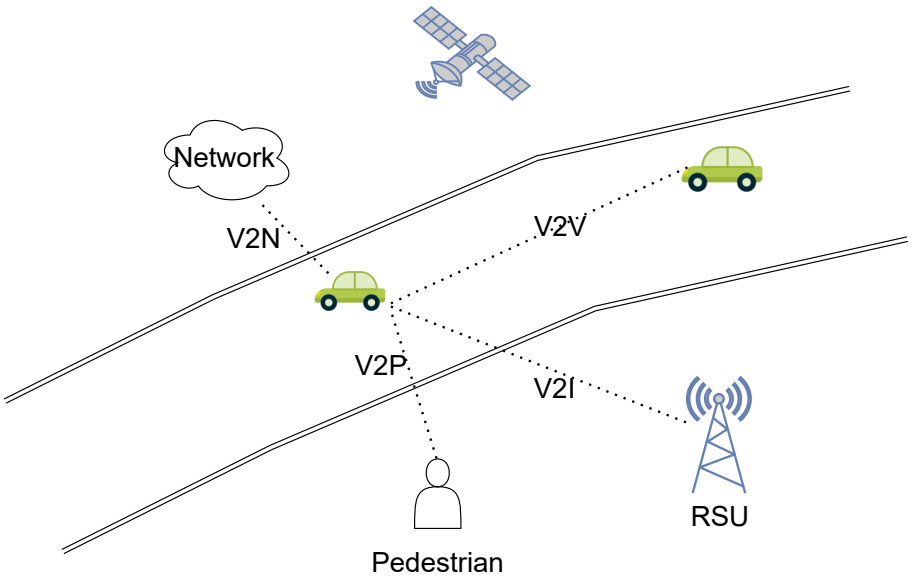

Figure 3.2: An ITS scenario

guard interval (GI) is included to assist in system synchronization.

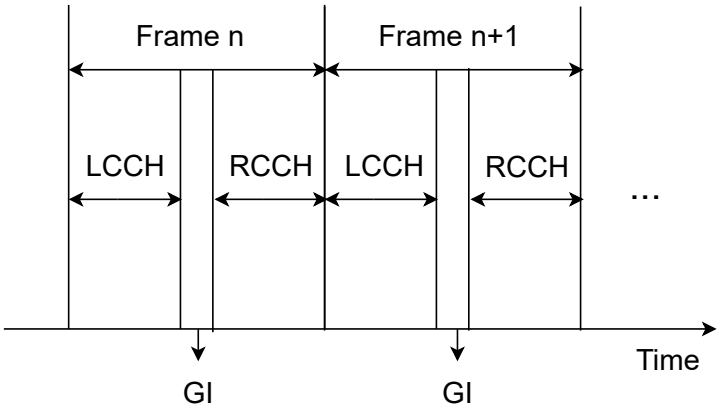

Figure 3.3: The structure of TDMA frame

3.3 Related techniques for cooperative vehicle localization

3.3.1 Interval analysis

Interval analysis is a numerical method that can provide guaranteed values by representing numbers as intervals. An interval is represented using the notation $[a]$, which includes the lower bound $\underline{a}$ and the upper bound $\overline{a}$:

$$[a] = [\underline{a}, \overline{a}] = \{a \in \mathbb{R}, \underline{a} \leq a \leq \overline{a}\} \tag{3.1}$$

The width of an interval can be calculated by the equation (3.2), and the midpoint of an interval can be denoted in equation (3.3).

$$width([a]) = \overline{a} - \underline{a} \tag{3.2}$$

$$mid([a]) = width([a])/2 + \underline{a} \tag{3.3}$$

An interval vector (A box) is the Cartesian product of n intervals, which can be denoted as:

$$[A] = [a_1] \times [a_2] \times \cdots \times [a_n] \tag{3.4}$$

Assuming there are two intervals $[a]$ and $[b]$, the addition and subtraction operations can be denoted as:

$$[a] + [b] = [\underline{a} + \underline{b}, \overline{a} + \overline{b}] \tag{3.5}$$

$$[a] - [b] = [\underline{a} - \overline{b}, \overline{a} - \underline{b}] \tag{3.6}$$

Moreover, the intersection operation can be defined in equation (3.7). The intersection operation of two boxes is shown in Fig. 3.4. Each component in two boxes is involved in the operation according to the defined rules.

$$\{c \in [A] \,\&\&\, c \in [B]\} = [A] \cap [B] \tag{3.7}$$

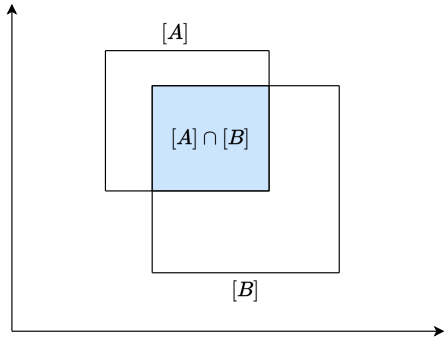

Figure 3.4: Intersection between two boxes

In addition, the inclusion function of $f : \mathbb{R}^a \to \mathbb{R}^b$ has been defined as $[f]$ to realize arithmetical operations and elementary functions in the function $f()$. Noting that the inclusion function is also suitable for the box $[A]$.

$$f([A]) \in [f]([A]), \forall [A] \in \mathbb{R}^a \tag{3.8}$$

In order to create an inclusion function, one popular method is to replace all the variables and operators in the original functions by their interval values [142]. For example, the inclusion function of the function $f(x) = x^3 + x^2 - x$ is $[f]([x]) = [x]^3 + [x]^2 - [x]$. Noting that the inclusion function can provide us equations denoted by interval variables (Also can be called constraints), which plays an important role in solving interval constraint satisfaction problems.

3.3.2 Interval constraints propagation (ICP)

The result of one interval constraints satisfaction problem (ICSP) should satisfy all the constraints at the same time. One ICSP $\mathbb{P}$, considering one box $[A]$ which includes n variables, and

m relations link these variables, can be denoted as:

$$\mathbb{P} : f_j(a_1, a_2, \cdots, a_n) = 0, j = 1, 2, \cdots, m \tag{3.9}$$

Each variable is an interval, which can be represented by $[a_i], i = 1, 2 \cdots n$. The interval constraint propagation (ICP) algorithm can solve the ICSP in a consistent way [143]. By developing a contractor, the domain of interval variables is reduced in the case that all constraints are satisfied, as shown in Fig. 3.5.

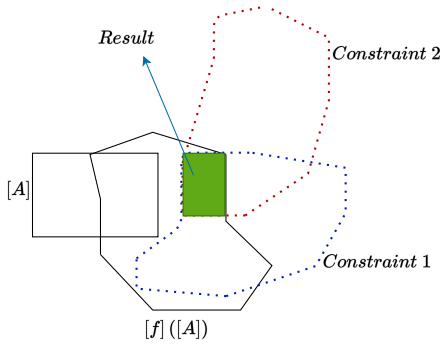

Figure 3.5: Contraction of one box by the contractor including two constraints

Specifically, in MSMV localization system, the ICSP solved by the ICP method can be denoted as:

$$\mathbb{P}1 : \left\{ \left[X_i^{pre}(t)\right] \cap \left[X_i^{abs}(t)\right] \cap \left[X_i^1\right] \cap \cdots \cap \left[X_i^m\right] \right\} \tag{3.10}$$

Where the $\left[X_i^{pre}(t)\right]$ is prediction box, the $\left[X_i^{abs}(t)\right]$ is absolute measurement box, and $\left[X_i^1(t)\right] \cdots, \left[X_i^m(t)\right]$ are m relative estimates box which are calculated based on relative measurements provided by m neighbors, $m \geq 2$. Since the complexity of the ICP algorithm depends on the dimension of the box, for the purpose of reducing the computation burden, the ICP method is used to calculate the position on both x and y coordinates by contracting multiple relative estimates for each vehicle in our thesis, which reduces the box dimension in [**?**] and [143]. The result $\left[x_i^R\right]$ obtained by the ICP method for all relative estimates can be denoted as

follows:

$$\left[x_i^R\right] = \left\{ \begin{bmatrix} [x_i^1(t)] \\ [y_i^1(t)] \end{bmatrix} \right\} \cap \cdots \cap \left\{ \begin{bmatrix} [x_i^m(t)] \\ [y_i^m(t)] \end{bmatrix} \right\} \tag{3.11}$$

Where the $x_i^m(t)$ and $y_i^m(t)$ are the relative position of vehicle i provided by vehicle m on the x and y coordinates, respectively.

3.3.3 Split covariance intersection filter (SCIF)

With two estimates to be fused $[X_1, P_1]$ and $[X_2, P_2]$, where the X_1 and P_1 are the state vector and covariance matrix of the first estimate, X_2 and P_2 are the state vector and covariance matrix of the second estimate. The fusion process by using traditional KF is denoted as:

$$\begin{aligned} P^{-1} &= P_1^{-1} + P_2^{-1} \\ X &= P(P_1^{-1}X_1 + P_2^{-1}X_2) \end{aligned} \tag{3.12}$$

Where the P and X are the covariance matrix and state vector of the fusion result. However, the KKF algorithm is indeed built upon several assumptions, one of which is that the estimates of inputs are mutually independent. This implies that the KF assumes there is no correlation or covariance between the input data. If there is correlation between the input data, meaning there is some form of association or dependency between them, the KF algorithm may produce inconsistent results, leading to over-convergence problem.

When there is correlation between input data, a simple weighted average may not be sufficient to produce accurate results. To address this issue, the covariance intersection filter (CIF) algorithm is proposed in [144]. In CIF, a convex combination method is applied to handle the updating process of the mean and covariance parts. The formulas for the CIF algorithm are as follows:

$$
\begin{aligned}
P^{-1} &= (P_1/w)^{-1} + (P_2/1-w)^{-1} \\
X &= P[(P_1/w)^{-1}X_1 + (P_2/1-w)^{-1}X_2]
\end{aligned}
\tag{3.13}
$$

Where w is the weighting coefficient, which can be determined by minimizing the determinant or trace of new covariance matrix P. However, the drawback of the CIF algorithm is that it assumes the input data to be completely dependent on each other. However, in practical applications, input data may have both independent and dependent components. Therefore, CIF disregards the information from the independent parts of the data, which leads to pessimistic estimates. So, in order to address this kind of problem, the split covariance intersection filter is proposed in [16]. Two input estimates: $\{X_1, P_{1d+1i}\}$ and $\{X_2, P_{2d+2i}\}$ to be fused, with the output result $\{X_1, P_d + P_i\}$ The formula for SCIF is as follows:

$$
\begin{aligned}
P_1 &= P_{1d}/w + P_{1i} \\
P_2 &= P_{2d}/1-w + P_{2i} \\
P^{-1} &= P_1^{-1} + P_2^{-1} \\
X &= P(P_1^{-1}X_1 + P_2^{-1}X_2) \\
P_i &= P(P_1^{-1}P_{1i}P_1^{-1} + P_2^{-1}P_{2i}P_2^{-1})P \\
P_d &= P - P_i
\end{aligned}
\tag{3.14}
$$

Where P_{1d} and P_{1i} are the correlated and independent covariance part of the first input estimate, respectively. P_{2d} and P_{2i} are the correlated and independent covariance part of the second input estimate, respectively. Noting that the covariance matrix is divided into independent and correlated parts, and they are calculated separately in SCIF. In addition, the coefficient satisfies $w \in [0,1]$, which can be determined by minimizing the trace or determinate of the covariance result P.

Additionally, in vehicle localization domain, when both X_1 and X_2 are two complete observations, they satisfy $X_1 = HX_{true}$ and $X_1 = HX_{true}$. The formula of SCIF can be denoted as:

$$
\begin{aligned}
P_1 &= P_{1d}/w + P_{1i} \\
P_2 &= P_{2d}/1-w + P_{2i} \\
K &= P_1 H^T (HP_1 H^T + P_2)^{-1} \\
X &= X_1 + K(X_2 - HX_1) \\
P &= (I - KH)P_1 \\
P_i &= (I - KH)P_{1i}(I - KH)^T + KP_{2i}K^T \\
P_d &= P - P_i
\end{aligned}
\tag{3.15}
$$

The equation (3.15) has the formula form of traditional KF, where K is the Kalman gain, and other symbols are the same as those in equation (3.14). When both P_{1d} and P_{2d} equal zero, the formula for SCIF is the same as traditional KF. So, SCIF is a general form of KF.

3.4 Proposed Interval split covariance intersection filter (ISCIF) and its consistency proof

3.4.1 Proposed ISCIF

In the MSMV cooperative localization system, when one vehicle utilizes relative measurements provided by neighboring vehicles for positioning, the estimated relative positions based on relative measurements may correlate with its own state. Consequently, the data to be fused are not independent of each other. Interval based multi-sensor data fusion methods can effectively address the problem of unknown correlation between data to be fused [145]. One popular interval based data fusion method is interval Kalman filter (IKF) [19] algorithm. It has the same

statistical assumptions on noise and recursive structure with the traditional KF algorithm, and the process of IKF is presented in the following:

The interval discrete-time controlled process is shown in equation (3.16), where the $[A]$, $[B]$, and $[H]$ are interval matrix, and the outputted results in each step are also intervals or boxes.

$$\begin{cases} [x_k] &= [A][x_{k-1}] + [B][U_{k-1}] + w_{k-1} \\ [Z_k] &= [H][x_k] + v_k \end{cases} \tag{3.16}$$

For the IKF method, the recursive structure is the same with that in the traditional KF, the prediction and correction steps can be represented by equation (3.17) and equation (3.18), respectively.

$$\begin{cases} \left[\widehat{x_k^-}\right] = [A]\left[\widehat{x_{k-1}}\right] + [B][U_{k-1}] \\ \left[P_k^-\right] = [A]\left[P_{k-1}\right][A]^T + Q \end{cases} \tag{3.17}$$

$$\begin{cases} [K_k] = \left[P_k^-\right][H]^T \left([H]\left[P_k^{-1}\right][H]^T + R\right)^{-1} \\ \left[\widehat{x_k}\right] = \left[\widehat{x_k^1}\right] + [K_k]\left([Z_k] - [H]\left[\widehat{x_k^-}\right]\right) \\ [P_k] = (I - [K_k][H])\left[P_k^-\right] \end{cases} \tag{3.18}$$

However, noting that the inversion of interval matrix in the IKF algorithm is an approximate solution, and it is NP-hardness [20], which may lose the possible result and increase the computational complexity during data fusion process. In order to solve these two problems, we propose a new algorithm named interval split covariance intersection filter (ISCIF) which based on the SCIF. In the ISCIF, the inversion of the interval covariance matrix is substituted with the ordinary matrix operation, thanks to the optimization process involving the split covariance matrix in SCIF.

In the proposed ISCIF, the input estimate to be fused can be denoted as $([X], P_I + P_D)$. Where the $[X]$ is the box state and it can be provided by interval analysis technique. Noting that the covariance matrix is always divided into independent and correlated parts (Which has the

same form with that in [146]), where the P_I is the degree of the independent part, and the P_D is the maximum degree of the possible correlated part with others. Giving two input estimates to be fused: $([A], P_{AI}+P_{AD})$ and $([B], P_{BI}+P_{BD})$, the formula of the ISCIF with the fusion result $([C], P_{CI}+P_{CD})$ can be represented by:

$$\begin{cases} P_1 = P_{AD}/w + P_{AI} \\ P_2 = P_{BD}/(1-w) + P_{BI} \\ P_C^{-1} = P_1^{-1} + P_2^{-1} \\ [C] = P_C\left(P_1^{-1}[A] + P_2^{-1}[B]\right) \\ P_{CI} = P_C\left(P_1^{-1}P_{AI}P_1^{-1} + P_2^{-1}P_{BI}P_2^{-1}\right)P_C \\ P_{CD} = I - P_{CI} \end{cases} \tag{3.19}$$

The weighting coefficient w belongs to the interval $[0,1]$ and it is determined by minimizing the trace or determinant of the output covariance matrix P_C. In our work, the w is calculated by minimizing the trace of the P_C. The proposed ISCIF has the same iterative structure with the traditional SCIF, and no additional assumptions are added. It can be used for interval discrete-time systems where the SCIF is not suitable. In addition, when the width of each variables equal to zero, the ISCIF will degenerate into SCIF, which increases the applicability of the proposed ISCIF.

3.4.2 Consistency proof of the ISCIF

To avoid the over-convergence problem of data fusion results caused by inter-estimate correlation, the data fusion method must be consistent, and the consistency of the SCIF with two input resources has been reported in [146]. However, it is not enough for data fusion process with multiple input resources [147]. So, we give the general proof for the consistency of our proposed ISCIF algorithm, which is also a complementary proof of the SCIF. Noting that in the following proof, the general form of the equation (3.19) which has n data fusion resources $\{[X_1], P_{1I}+P_{1D}\}, \{[X_2], P_{2I}+P_{2D}\}, \cdots, \{[X_n], P_{nI}+P_{nD}\}$ with the output result $\{[X], P_I+P_D\}$ is

used, as shown in equation (3.20).

$$\begin{cases} P_1 = \dfrac{P_{1D}}{w_1} + P_{1I} \\ P_2 = \dfrac{P_{2D}}{w_2} + P_{2I} \\ \vdots \\ P_n = \dfrac{P_{nD}}{w_n} + P_{nI} \\ P = (\sum_{k=1}^{n} {P_k}^{-1})^{-1} \\ [X] = P(\sum_{k=1}^{n} {P_k}^{-1}[X_k]) \\ P_I = P(\sum_{k=1}^{n} {P_k}^{-1}{P_{kI}}^{-1}{P_k}^{-1})P \\ P_D = I - P_I \end{cases} \tag{3.20}$$

Where the w_k satisfies $\sum_{k=1}^{n} w_k = 1$, and $w_k \in [0,1]$. In addition, the definition of the spilt form consistency has been reported in [146]. It always satisfies the consistency definition of the KF, and it includes A-split and B-split forms:

For the estimate in split form, it is A-split consistent if it satisfies:

$$\begin{aligned} P_D \geq P_D^* = E\left[\overline{X_D} * \overline{X_D}^T\right] \\ P_I \geq P_I^* = E\left[\overline{X_I} * \overline{X_I}^T\right] \end{aligned} \tag{3.21}$$

It is B-split consistent if it satisfies:

$$\begin{aligned} P_D \geq P_D^* = E\left[\overline{X_D} * \overline{X_D}^T\right] \\ P_I + P_D \geq P_I^* + P_D^* = E\left[\overline{X} * \overline{X}^T\right] \end{aligned} \tag{3.22}$$

Where the $\overline{X_D}$, $\overline{X_I}$, and $\overline{X}$ are the estimated error of the correlated, independent, and whole parts, respectively. In the ISCIF, the estimated error can be determined by calculating the difference between the midpoint of the estimated intervals and the true values.

Theorem 1: If the n source estimates are A-split consistent, for every $w_n \in [0,1]$, the data fusion result of ISCIF is consistent.

Proof of Theorem 1:

Since the n ($n \geq 2$) source estimates are A-split consistent, we can get:

$$\begin{aligned} P_{nD} \geq P_{nD}^{*} &= E\left[\overline{X_{nD}} * \overline{X_{nD}}^{T}\right] \\ P_{nI} \geq P_{nI}^{*} &= E\left[\overline{X_{nI}} * \overline{X_{nI}}^{T}\right] \end{aligned} \tag{3.23}$$

At first, the proof of the independent component of the fusion result can be given as follows:

$$P_I = P\left(P_1^{-1} P_{1I} P_1^{-1} + \cdots + P_n^{-1} P_{nI} P_n^{-1}\right) P \tag{3.24}$$

$$\overline{X_I} = P\left(P_1^{-1}\overline{X_{1I}} + \cdots + P_n^{-1}\overline{X_{nI}}\right) \tag{3.25}$$

$$\begin{aligned} P_I - P_I^{*} &= P_I - E\left[\overline{X_I} * \overline{X_I}^{T}\right] \\ &= \sum_{k=1}^{n} P\left(P_k^{-1} P_{kI} P_k^{-1}\right) P - \sum_{k=1}^{n} P P_k^{-1} E\left[\overline{X_{kI}} * \overline{X_{kI}}^{T}\right] P_k^{-1} P \\ &= \sum_{k=1}^{n} P P_k^{-1}\left(P_{kI}^{-1} - E\left[\overline{X_{kI}} * \overline{X_{kI}}^{T}\right]\right) P_k^{-1} P \\ &\geq 0 \end{aligned} \tag{3.26}$$

The proof of the independent component of the fusion result is finished. Then, the proof of the correlated component of the fusion result is shown as follows:

$$
\begin{aligned}
P_D &= P - P_I \\
&= P - \sum_{k=1}^{n} P P_k^{-1} P_{kI} P_k^{-1} P \\
&= P \left[P^{-1} - \sum_{k=1}^{n} \left(P_k^{-1} P_{kI} P_k^{-1} \right) \right] P \\
&= P \left[\sum_{k=1}^{n} P_k^{-1} \left(P_k - P_{kI} \right) P_k^{-1} \right] P \\
&= \sum_{k=1}^{n} P P_k^{-1} \frac{P_{kD}}{w_k} P_k^{-1} P \\
&\geq \sum_{k=1}^{n} P P_k^{-1} \frac{E\left[\overline{X_{kD}} * \overline{X_{kD}}^T \right]}{w_k} P_k^{-1} P
\end{aligned}
\tag{3.27}
$$

The correlated estimated error satisfies:

$$
\overline{X_D} = \sum_{k=1}^{n} P P_k^{-1} \overline{X_{kD}} \tag{3.28}
$$

So:

$$
\begin{aligned}
& P_D - E\left[\overline{X_D} * \overline{X_D}^T \right] \\
& \geq \sum_{k=1}^{n} P P_k^{-1} \frac{E\left[\overline{X_{kD}} * \overline{X_{kD}}^T \right]}{w_k} P_k^{-1} P \\
& - P \left\{ \sum_{k=1}^{n} \sum_{m=1}^{n} P_k^{-1} E\left[\overline{X_{kD}} * \overline{X_{mD}}^T \right] P_m^{-1} \right\} P \\
& = \sum_{k=1}^{n} P P_k^{-1} \frac{1 - w_k}{w_k} E\left[\overline{X_{kD}} * \overline{X_{kD}}^T \right] P_k^{-1} P \\
& - \sum_{k=1}^{n} \sum_{m=1, m \neq k}^{n} P P_k^{-1} E\left[\overline{X_{kD}} * \overline{X_{mD}}^T \right] P_m^{-1} P
\end{aligned}
\tag{3.29}
$$

Noting that:

$$
\sum_{m=1, m \neq k}^{n} w_m = 1 - w_k \tag{3.30}
$$

$$
\begin{aligned}
&P_D - E\left[\overline{X_D} * \overline{X_D}^T\right] \geq \\
&\sum_{k=1}^{n}\sum_{m=k+1}^{n} \frac{w_m}{w_k} P P_k^{-1} E\left[\overline{X_{kD}} * \overline{X_{kD}}^T\right] P_k^{-1} P \\
&+ \sum_{k=1}^{n}\sum_{m=k+1}^{n} \frac{w_k}{w_m} P P_m^{-1} E\left[\overline{X_{mD}} * \overline{X_{mD}}^T\right] P_m^{-1} P \\
&- \sum_{k=1}^{n}\sum_{m=k+1}^{n} P P_k^{-1} E\left[\overline{X_{kD}} * \overline{X_{mD}}^T\right] P_m^{-1} P \\
&- \sum_{k=1}^{n}\sum_{m=k+1}^{n} P P_m^{-1} E\left[\overline{X_{mD}} * \overline{X_{kD}}^T\right] P_k^{-1} P \\
&= \sum_{k=1}^{n}\sum_{m=k+1}^{n} \frac{w_m^2}{w_k w_m} P P_k^{-1} E\left[\overline{X_{kD}} * \overline{X_{kD}}^T\right] P_k^{-1} P \\
&+ \sum_{k=1}^{n}\sum_{m=k+1}^{n} \frac{w_k^2}{w_k w_m} P P_m^{-1} E\left[\overline{X_{mD}} * \overline{X_{mD}}^T\right] P_m^{-1} P \\
&- \sum_{k=1}^{n}\sum_{m=k+1}^{n} \frac{w_k w_m}{w_k w_m} P P_k^{-1} E\left[\overline{X_{kD}} * \overline{X_{mD}}^T\right] P_m^{-1} P \\
&- \sum_{k=1}^{n}\sum_{m=k+1}^{n} \frac{w_k w_m}{w_m w_k} P P_m^{-1} E\left[\overline{X_{mD}} * \overline{X_{kD}}^T\right] P_k^{-1} P \\
&= P\left\{\sum_{k=1}^{n}\sum_{m=k+1}^{n} \frac{1}{w_k w_m} E\left[A * A^T\right]\right\} P
\end{aligned}
\tag{3.31}
$$

Where $A = \left(w_m P_k^{-1}\overline{X_{kD}} - w_k P_m^{-1}\overline{X_{mD}}\right)$. Since the w_k and w_m both belong to the interval $[0,1]$, so:

$$
P_D - E\left[\overline{X_D} * \overline{X_D}^T\right] \geq 0 \tag{3.32}
$$

The proof of the theorem 1 is finished.

Theorem 2: If the n source estimates are B-split consistent, for each $w_n \in [0,1]$, the data fusion result of ISCIF is consistent.

Proof of Theorem 2:

Based on the definition of the B-split consistency, we can get:

$$
\begin{aligned}
P_{nD} &\geq E\left[\overline{X_{nD}} * \overline{X_{nD}}^{T}\right] \\
P_{nD} + P_{nI} &\geq E\left[\overline{X_{n}} * \overline{X_{n}}^{T}\right]
\end{aligned}
\tag{3.33}
$$

Noting that the B-split consistency of the correlated part P_D can be proved identically in theorem 1. And the proof of entire covariance P is shown as follows:

$$
\begin{aligned}
P &= P_D + P_I \\
&= P\left\{\sum_{k=1}^{n} P_k^{-1} P_k P_k^{-1}\right\} P \\
&= P\left\{\sum_{k=1}^{n} P_k^{-1}\left(\frac{P_{kD}}{w_k} + P_{kI}\right) P_k^{-1}\right\} P \\
&= \sum_{k=1}^{n} P P_k^{-1} P_{kI} P_k^{-1} P \\
&+ \sum_{k=1}^{n} P P_k^{-1}\left(\frac{P_{kD} - E\left[\overline{X_{kD}} * \overline{X_{kD}}^{T}\right]}{w_k}\right) P_k^{-1} P \\
&+ \sum_{k=1}^{n} P P_k^{-1}\left(\frac{E\left[\overline{X_{kD}} * \overline{X_{kD}}^{T}\right]}{w_k}\right) P_k^{-1} P \\
&\geq \sum_{k=1}^{n} P P_k^{-1} E\left[\overline{X_{kI}} * \overline{X_{kI}}^{T}\right] P_k^{-1} P \\
&+ \sum_{k=1}^{n} P P_k^{-1} \frac{E\left[\overline{X_{kD}} * \overline{X_{kD}}^{T}\right]}{w_k} P_k^{-1} P
\end{aligned}
\tag{3.34}
$$

$$
\begin{aligned}
\overline{X}_I &= \sum_{k=1}^{n} P\left(P_k^{-1}\overline{X_{kI}}\right) \\
\overline{X}_D &= \sum_{k=1}^{n} P\left(P_k^{-1}\overline{X_{kD}}\right) \\
E\left[\overline{X} * \overline{X}^T\right] &= E\left[\overline{X_I} * \overline{X_I}^T\right] + E\left[\overline{X_D} * \overline{X_D}^T\right]
\end{aligned}
\tag{3.35}
$$

$$
\begin{aligned}
& P - E\left[\overline{X} * \overline{X}^T\right] \\
& = P_I + P_D - E\left[\overline{X} * \overline{X}^T\right] \\
& \geq \sum_{k=1}^{n} P P_k^{-1} E\left[\overline{X_{kI}} * \overline{X_{kI}}^T\right] P_k^{-1} P \\
& + \sum_{k=1}^{n} P P_k^{-1} \frac{E\left[\overline{X_{kD}} * \overline{X_{kD}}^T\right]}{w_k} P_k^{-1} P \\
& - \sum_{k=1}^{n} P P_k^{-1} E\left[\overline{X_{kI}} * \overline{X_{kI}}^T\right] P_k^{-1} P \\
& - \sum_{k=1}^{n} \sum_{m=1}^{n} P P_k^{-1} E\left[\overline{X_{kD}} * \overline{X_{mD}}^T\right] P_m^{-1} P \\
& = \sum_{k=1}^{n} P P_k^{-1} \frac{1 - w_k}{w_k} E\left[\overline{X_{kD}} * \overline{X_{kD}}^T\right] P_k^{-1} P \\
& - \sum_{k=1}^{n} \sum_{m=1, m\neq k}^{n} P P_k^{-1} E\left[\overline{X_{kD}} * \overline{X_{mD}}^T\right] P_m^{-1} P
\end{aligned}
\tag{3.36}
$$

Noting that the result of equation (3.36) is the same with that in equation (3.29). Since $\sum_{m=1,m\neq k}^{n} w_m = 1 - w_k$, combing with equation (3.31), the entire covariance P satisfies:

$$
P - E\left[\overline{X} * \overline{X}^T\right] \geq 0 \tag{3.37}
$$

Meanwhile, the proof of theorem 2 is finished. Noting that when the number of data fusion

resources satisfies $n = 2$, the general proof of the ISCIF is the same with that in [146]. Given the general proofs of both A-split and B-split consistency above, either the A-split or B-split consistency can guarantee the consistency of the data fusion result, which means that it is not necessary to always distinguish or give the explicit definition before using the proposed algorithm. Furthermore, no additional confidence is incorporated into the data fusion process, thus mitigating the issue of over-convergence stemming from correlated data.

3.5 Cooperative Localization Method based on ISCIF

3.5.1 System Model

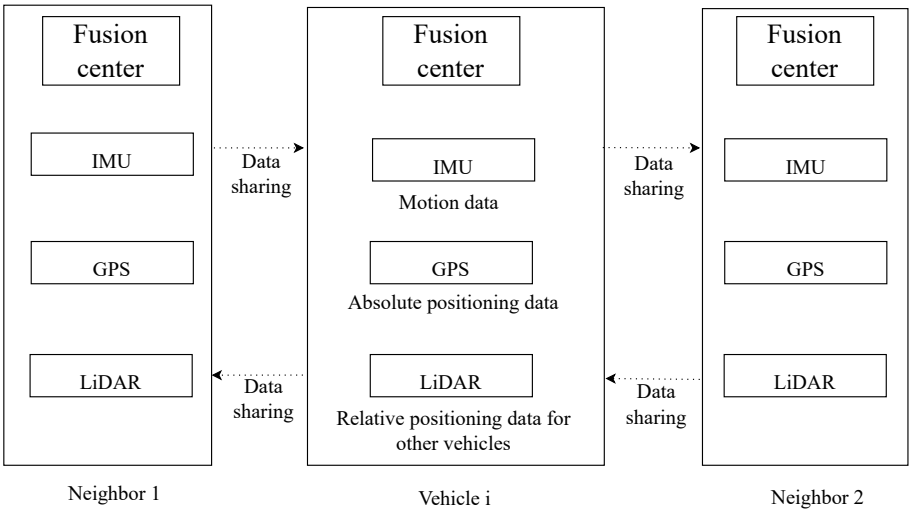

Figure 3.6: Decentralized cooperative localization architecture [1]

We consider the general system model which consists multi-sensors and multi-vehicles, where the number of vehicles, N, is unknown, as presented in [148]. The following assumptions are met by our system model:

(1). Each vehicle is equipped with an IMU, GPS, and LiDAR, which respectively provide motion data, absolute positioning data, and relative positioning data.

(2). When vehicles are within communication range, data sharing is realized by V2V communication technique.

(3). The designed cooperative vehicle localization system works in a decentralized manner, which is shown in Fig. 3.6. In addition, each vehicle can timestamp their data by a global system time, which can increase the real-time performance of the localization system.

3.5.2 Prediction of the State Vector

In our model, the state vector or box of each vehicle includes the position in both the x and y coordinates, as well as the orientation of the vehicles. The state vector of vehicle i at time t is represented as:

$$X_i(t) = [x_i(t), y_i(t), \theta_i(t)]^T \tag{3.38}$$

The $x_i(t)$ and $y_i(t)$ are the coordinate of the vehicle on the x-axis and y-axis, respectively. And the $\theta_i(t)$ is the direction of the vehicle.

Using the kinematic bicycle model, the propagation model is defined as:

$$\begin{cases} x_i(t) = x_i(t-1) + \Delta d_i(t) cos\left(\theta_i(t-1) + \frac{\Delta\theta_i(t)}{2}\right) \\ y_i(t) = y_i(t-1) + \Delta d_i(t) sin\left(\theta_i(t-1) + \frac{\Delta\theta_i(t)}{2}\right) \\ \theta_i(t) = \theta_i(t-1) + \Delta\theta_i(t) \end{cases} \tag{3.39}$$

Where the $\Delta d_i(t)$ is the traveled distance of the vehicle from time $t-1$ to time t, the $\Delta\theta_i(t)$ is the difference of the directional angle of the vehicle from time $t-1$ to time t.

Adding the process noise, the propagation model can be expressed in the function form:

$$\begin{bmatrix} x_i(t) \\ y_i(t) \\ \theta_i(t) \end{bmatrix} = f\left(\begin{bmatrix} x_i(t-1) \\ y_i(t-1) \\ \theta_i(t-1) \end{bmatrix}, \begin{bmatrix} \Delta d_i(t) \\ \Delta\theta_i(t) \end{bmatrix}\right) + Q_i(t) \tag{3.40}$$

Where the $Q_i(t)$ is the Gaussian white noise of process state. We assume that the noise of the motion measurements follows a Gaussian distribution with zero mean, and the covariance matrix is $Q_i^U(t)$. So, the $Q_i^U(t)$ can be defined as:

$$Q_i^U(t) = \begin{bmatrix} \sigma^2_{\Delta d_i(t)} & 0 \\ 0 & \sigma^2_{\Delta\theta_i(t)} \end{bmatrix} \tag{3.41}$$

The covariance of vehicle i at time t can be updated by:

$$\begin{aligned} P_i(t) &= F_i(t)P_i(t-1)F_i(t)^T \\ &+ B_i(t)Q_i^U(t)B_i(t)^T + Q_i(t) \end{aligned} \tag{3.42}$$

Where the $F_i(t)$ and $B_i(t)$ are Jacobian matrices which are calculated by the follow equations:

$$F_i(t) = \begin{bmatrix} 1 & 0 & -\Delta d_i(t) sin\left\{\theta_i(t-1) + \frac{\Delta\theta_i(t)}{2}\right\} \\ 0 & 1 & \Delta d_i(t) cos\left\{\theta_i(t-1) + \frac{\Delta\theta_i(t)}{2}\right\} \\ 0 & 0 & 1 \end{bmatrix} \tag{3.43}$$

$$B_i(t) = \begin{bmatrix} cos\left\{\theta_i(t-1) + \frac{\Delta\theta_i(t)}{2}\right\} & -\frac{1}{2}\Delta d_i(t) sin\left\{\theta_i(t-1) + \frac{\Delta\theta_i(t)}{2}\right\} \\ sin\left\{\theta_i(t-1) + \frac{\Delta\theta_i(t)}{2}\right\} & \frac{1}{2} cos\left\{\theta_i(t-1) + \frac{\Delta\theta_i(t)}{2}\right\} \\ 0 & 1 \end{bmatrix} \tag{3.44}$$

Since both the total state covariance $P_i(t)$ and the independent part $P_{iI}(t)$ can be determined at each time, the independent part is calculated by:

$$\begin{aligned} P_{iI}(t) &= F_i(t)P_{iI}(t-1)F_i(t)^T \\ &+ B_i(t)Q_i^U(t)B_i(t)^T + Q_{iI}(t) \end{aligned} \tag{3.45}$$

Where the $Q_{iI}(t)$ is the independent component of the $Q_i(t)$.

3.5.3 Absolute Positioning Stage

Since the absolute localization measurement provided by the GPS at each time is completely independent of any existing estimates or measurements. So, there is no data incest problem in the absolute positioning stage. The state update with the absolute localization measurement by using ISCIF can be degenerated and transferred to the update strategy proposed in [16]. For each vehicle i, the absolute measurement provided by GPS can be denoted as $Z_i(t) = \left(x_i^G, y_i^G\right)$. The observation model of the absolute measurement at time t can be represented by:

$$Z_i(t) = H_i(t)X_i(t) + R_i(t) \tag{3.46}$$

Where:

$$H_i(t) = \begin{bmatrix} 1 & 0 & 0 \\ 0 & 1 & 0 \end{bmatrix} \tag{3.47}$$

The $R_i(t)$ is the Gaussian white noise which follows $N\left(0, \sigma_i(t)^2\right)$. So, the state updates by using absolute localization measurement (GPS data in our model) is represented in the following equations:

$$\begin{aligned} K &= P_i(t)H_i^T\left(H_iP_i(t)H_i^T + \sigma_i(t)^2\right)^{-1} \\ X_i(t) &= X_i(t) + K(Z_i(t) - H_iX_i(t)) \\ P_i(t) &= (I - KH_i)P_i(t) \\ P_{iI}(t) &= (I - KH_i)P_{iI}(t)(I - KH_i)^T + K\sigma_i(t)^2K^T \\ P_{iD}(t) &= P_i(t) - P_{iI}(t) \end{aligned} \tag{3.48}$$

3.5.4 Relative Positioning Stage

After absolute positioning stage, we use interval analysis technique to generate interval (or box) form of the data in the system. The relative observation between two vehicles is shown in

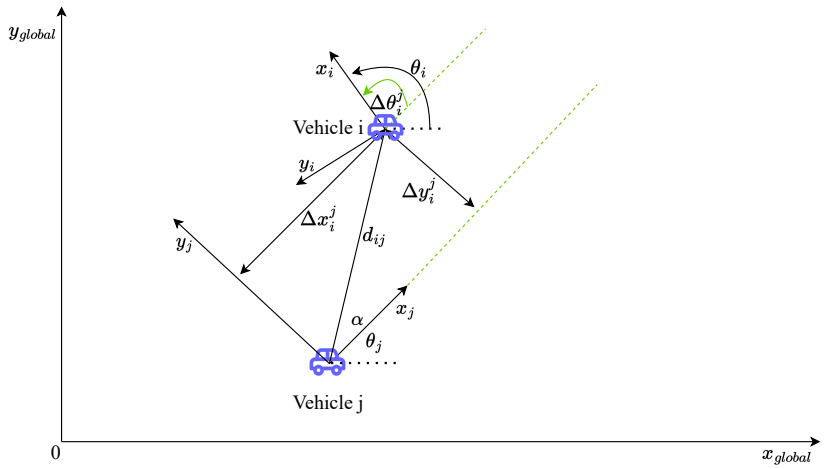

Figure 3.7: Relative observation between vehicles [1]

Fig. 3.7. When vehicle i is observed by vehicle j, the relative estimate of vehicle i provided by vehicle j can be denoted as:

$$[X_i^j(t)] = \begin{bmatrix} [cos]([\theta_j(t)]) & -[sin]([\theta_j(t)]) & 0 \\ [sin]([\theta_j(t)]) & [cos]([\theta_j(t)]) & 0 \\ 0 & 0 & 1 \end{bmatrix} [\Delta X_i^j(t)] + [X_j(t)] \tag{3.49}$$

Where the $\left[X_i^j(t)\right]$ represents the box relative estimate of vehicle i when it is observed by vehicle j. The $[\Delta X_i^j(t)] = \left\{[\Delta x_i^j(t)], [\Delta y_i^j(t)], [\Delta\theta_i^j(t)]\right\}^T$ is the relative measurements in the box form. The $[X_j(t)] = \left\{[x_j(t)], [y_j(t)], [\theta_j(t)]\right\}^T$ is the box state of the vehicle j in the global coordinate system.

Based on the $\alpha(t)$ and $d_{ij}(t)$, which are provided by sensors, the interval relative distance $[d_{ij}(t)]$ and the interval relative bearing $[\alpha(t)]$ can be calculated by:

$$\begin{aligned} [\alpha(t)] &= [\alpha(t) - 3\sigma_\alpha, \alpha(t) + 3\sigma_\alpha] \\ \left[d_{ij}(t)\right] &= \left[d_{ij}(t) - 3\sigma_d, d_{ij}(t) + 3\sigma_d\right] \end{aligned} \tag{3.50}$$

Where the σ_α and σ_d are the standard deviation of sensors. So, the $[\Delta x_i^j(t)]$ and $[\Delta y_i^j(t)]$ can be calculated by:

$$\begin{aligned}\left[\Delta x_i^j(t)\right] &= [cos]\left([\alpha(t)]\right) * \left[d_{ij}(t)\right] \\ \left[\Delta y_i^j(t)\right] &= [sin]\left([\alpha(t)]\right) * \left[d_{ij}(t)\right]\end{aligned} \tag{3.51}$$

Where $[cos]$ and $[sin]$ represent the inclusion function. In addition, the $[X_j(t)]$ in equation (3.49) is optimized by adding tolerance variables (α_{xj}, α_{yj}, and $\alpha_{\theta j}$) by interval analysis:

$$\begin{aligned}\left[x_j(t)\right] &= \left[x_j(t) - \alpha_{xj}, x_j(t) + \alpha_{xj}\right] \\ \left[y_j(t)\right] &= \left[y_j(t) - \alpha_{yj}, y_j(t) + \alpha_{yj}\right] \\ \left[\theta_j(t)\right] &= \left[\theta_j(t) - \alpha_{\theta j}, \theta_j(t) + \alpha_{\theta j}\right]\end{aligned} \tag{3.52}$$

Where the $x_j(t)$, $y_j(t)$, and $\theta_j(t)$ is the result of the equation (3.48). Meanwhile, regarding the covariance part, we can calculate the covariance matrix of the relative estimate of vehicle i, which is provided by vehicle j, using the following equations:

$$\begin{aligned}P_{X_i^j}(t) &= J_1 P_j(t) J_1^T + J_2 Q_j J_2^T \\ P_{X_{iI}^j}(t) &= J_1 P_{jI}(t) J_1^T + J_2 Q_{jI} J_2^T\end{aligned} \tag{3.53}$$

Where the $P_{X_i^j}(t)$ and $P_{X_{iI}^j}(t)$ are the total covariance of the relative estimate and the independent part of covariance at time t, respectively. The $P_j(t)$ and $P_{jI}(t)$ are the total covariance of the state of vehicle j in the global coordinate system and the independent part of $P_j(t)$, respectively. In addition, the J_1 and J_2 are Jacobian matrices with respect to the $X_j(t)$ and the relative measurements $\Delta X_i^j(t)$, respectively. They can be denoted as:

$$J_1 = \frac{\partial X_i^j}{\partial X_j(t)} = \begin{bmatrix} 1 & 0 & -\Delta x_i^j sin\theta_j - \Delta y_i^j cos\theta_j \\ 0 & 1 & \Delta x_i^j cos\theta_j - \Delta y_i^j sin\theta_j \\ 0 & 0 & 1 \end{bmatrix}$$
$$J_2 = \frac{\partial X_i^j}{\partial \Delta X_i^j(t)} = \begin{bmatrix} cos\theta_j & -sin\theta_j & 0 \\ sin\theta_j & cos\theta_j & 0 \\ 0 & 0 & 1 \end{bmatrix} \tag{3.54}$$

Before state update using ISCIF, we use ICP method to preprocess multiple relative estimates. The relative estimate result $\left[X_i^{R(t)}\right]$ which fuses all relative estimates can be provided by solving the ICSP by using ICP method in equation (3.11). Moreover, in order to increase the localization accuracy, we use the same method of equation (3.52) by using parameters β_{xi}, β_{yi}, and $\beta_{\theta i}$ to process the result in absolute positioning stage (equation (3.48)):

$$\begin{aligned} [x_i(t)] &= [x_i(t) - \beta_{xi}, x_i(t) + \beta_{xi}] \\ [y_i(t)] &= [y_i(t) - \beta_{yi}, y_i(t) + \beta_{yi}] \\ [\theta_i(t)] &= [\theta_i(t) - \beta_{\theta i}, \theta_i(t) + \beta_{\theta i}] \end{aligned} \tag{3.55}$$

The box state of vehicle i with relative information can be represented as:

$$\left\{[X_i(t)], P_{iI}(t) + P_{iD}(t), [X_i^R(t)]\right\} \tag{3.56}$$

Where the $[X_i(t)]$ is the state box of vehicle i at time t, the $P_{iI}(t)$ and $P_{iD}(t)$ are the independent component and correlated component of the covariance matrix, respectively. The $[X_i^R(t)]$ is the result of all relative estimates based on ICP method, which is also the input data of ISCIF.

Regarding the covariance part, since all the relative estimates have been optimized by ICP technique with the result $\left[X_i^R\right]$, we can assume that the related covariance of $\left[X_i^R\right]$ is equal to

the matrix with the minimal trace among all $P_{X_i^j}(t)$:

$$\begin{aligned} P_{X_{iI}^R} &= P_{X_{iI}^k} \\ P_{X_{iD}^R} &= P_{X_{iD}^k} \end{aligned} \tag{3.57}$$

Where the $P_{X_{iI}^R}$ and $P_{X_{iD}^R}$ are independent component and correlated component of the related covariance of $\left[X_i^R\right]$. Moreover, vehicle k has the smallest trace.

So, the formula of ISCIF for localization using relative estimates can be defined as follows:

$$\begin{aligned} P_1 &= \frac{P_{iD(t)}}{w} + P_{iI}(t) \\ P_2 &= \frac{P_{X_{iD}^R(t)}}{1-w} + P_{X_{iI}^R}(t) \\ K &= P_1(P_1+P_2)^{-1} \\ [X_i(t)] &= [X_i(t)] + K\left\{\left[X_i^R(t)\right] - [X_i(t)]\right\} \\ P_i(t) &= (I-K)P_1 \\ P_{iI}(t) &= (I-K)P_{iI}(I-K)^T + KP_{X_{iI}^R}(t)K^T \\ P_{iD}(t) &= P_i(t) - P_{iI}(t) \end{aligned} \tag{3.58}$$

In order to form a loop with localization process of state prediction and absolute positioning stages, the input variables in the state vector $X_i(t)$ (Equation (3.39)) are determined by calculating the midpoint of the variables in state box $[X_i(t)]$ (Result in equation (3.58)). Additionally, the localization procedures of each vehicle are illustrated in Fig. 3.8.

3.6 Fault Detection and Exclusion

In order to enhance the robustness of the system, we implement a fault detection and exclusion (FDE) method based on Kullback–Leibler divergence (KLD). Our method mainly includes three

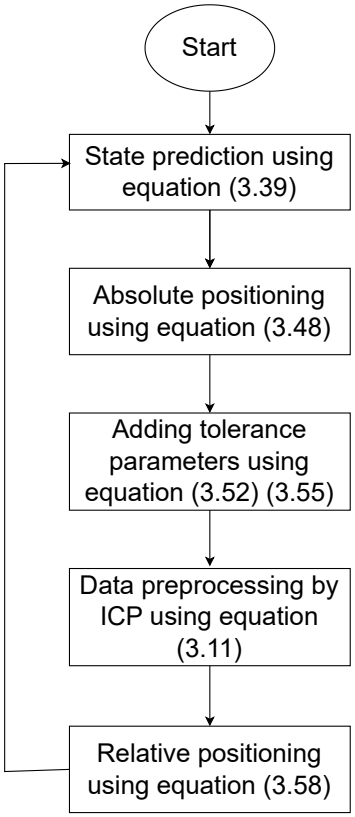

Figure 3.8: Date process of each vehicle [1]

steps: fault detection, threshold optimization, and fault isolation. Each vehicle in the system uses the proposed FDE method after the absolute positioning stage.

Considering two probability density functions (pdfs) (f_1 and f_2), the KLD from f_1 to f_2 can be denoted as

$$KLD(f_1||f_2) = \sum_x log\frac{f_1(x)}{f_2(x)}f_1(x) \tag{3.59}$$

The KLD for vehicle i is computed based on the state vector and covariance matrix both before and after absolute positioning. The calculation formula for the KLD is as follows:

$$\begin{aligned} KLD^i = &\frac{1}{2}trace(P_{t/t}P_{t/t-1}^{-1}) + \frac{1}{2}log\frac{det(P_{t/t-1})}{det(P_{t/t})} - \frac{1}{2}M \\ &+ \frac{1}{2}(X_{t/t} - X_{t/t-1})^T(X_{t/t} - X_{t/t-1}) \end{aligned} \tag{3.60}$$

where $P_{t/t-1}$ and P_t denote the total covariance of vehicle i before and after data fusion in the absolute positioning stage, respectively. $X_{t/t-1}$ and X_t denote the state vector of vehicle i before and after data fusion in the absolute positioning stage, respectively. M is the dimension of the state vector. $trace()$ and $det()$ represent matrix operations for the calculation of the trace and determinant, respectively.

Equation (3.60) is a generalized residual test that considers both the Mahalanobis distance and mean differences between predicted and corrected distributions. Moreover, in the fault-free case, the distribution of the KLD is related to the F and Chi-square distributions, which are denoted in the following equation [25]:

$$\begin{aligned} KLD \sim &\frac{M(n-1)}{2n(n-M)}F_{M,n-M} + \frac{1}{2n-2} \\ &* \frac{1}{1 - \frac{1}{6(n-1)-1}(2M+1-\frac{2}{M+1})}\chi^2_{\frac{1}{2}M(M+1)} \end{aligned} \tag{3.61}$$

where n is the number of samples and M is the dimension.

After obtaining the KLD residual, a threshold should be determined to evaluate whether there is a fault in the system. The decision includes the detection probability p_D and the false

alarm probability p_F, which can be denoted as

$$\begin{aligned} p_D &= p(s_1|H_1) \\ p_F &= p(s_1|H_0) \end{aligned} \tag{3.62}$$

where H_1 is the hypothesis that there is no fault in the system, H_0 is the hypothesis that there is a fault in the system, s_1 is the action of selecting hypothesis H_1, and s_0 is the action of selecting hypothesis H_0. We can assume that H_0 and H_1 are known:

$$\begin{aligned} p(H_0) &= p_0 \\ p(H_1) &= 1 - p_0 \end{aligned} \tag{3.63}$$

We define the pdfs of KLDs $f(KLD|H_0)$ and $f(KLD|H_1)$ as being under the H_0 and H_1 cases, respectively. They satisfy

$$\begin{aligned} H_0 &: KLD \sim f(KLD|H_0) \\ H_1 &: KLD \sim f(KLD|H_1) \end{aligned} \tag{3.64}$$

One example of these distributions is shown in Fig. 3.9. So, the detection probability and the false alarm probability in Equation (3.62) can be calculated as follows:

$$\begin{aligned} P_D &= \int_{\lambda}^{\infty} f(KLD|H_1) d(KLD) \\ P_F &= \int_{\lambda}^{\infty} f(KLD|H_0) d(KLD) \end{aligned} \tag{3.65}$$

Threshold λ can be optimized by minimizing the conditional entropy [105]. The formulation is shown in Equation (3.66).

$$\begin{aligned} h(H|s) &= E[log \frac{1}{p(H|s)}] \\ &= -\sum_{i \in [0,1]} (v_i log \frac{v_i}{v_i + k_i} + k_i log \frac{k_i}{v_i + k_i}) \end{aligned} \tag{3.66}$$

So, combining Equations (3.62) and (3.66), when the conditional entropy is minimized,

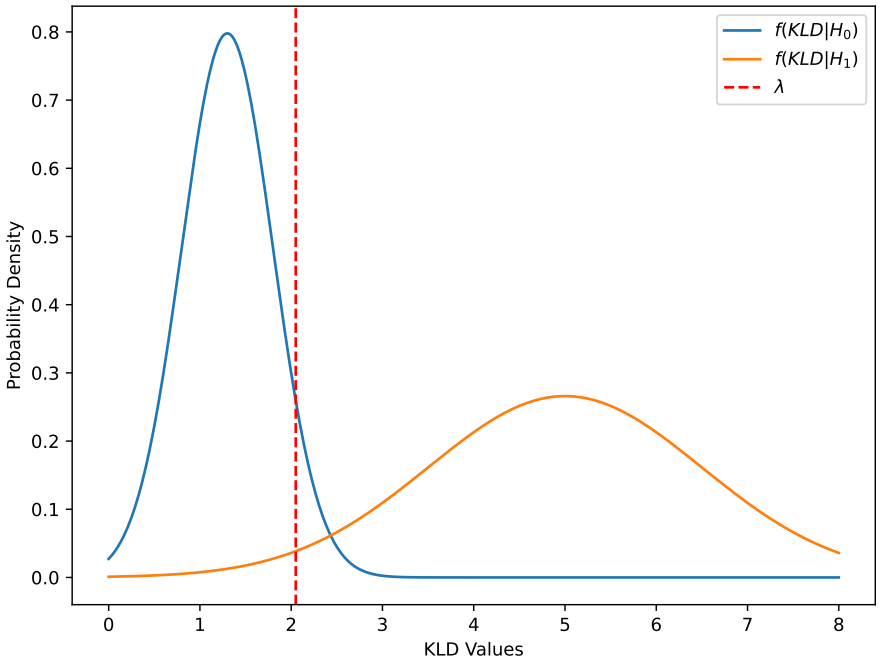

Figure 3.9: The pdfs of the KLD values in the faulty and non-faulty cases.

threshold λ can be determined. The decision criterion based on the KLD and threshold can be expressed as

$$\begin{aligned} s_0 &: KLD < \lambda \\ s_1 &: KLD \geq \lambda \end{aligned} \tag{3.67}$$

When a fault is detected, an isolation method should be implemented to mitigate the impact of faulty data on the positioning accuracy. The strategy that we propose is that if a fault is detected after the absolute positioning stage of a vehicle, it should immediately cease cooperation with other vehicles to avoid affecting their positioning performance. In addition, given that we use the ICP method in the relative positioning stage, when a fault occurs in a relative position measurement sensor, the fault can be automatically detected during the execution of the ICP method.

For example, considering a system with three vehicles, if a fault is detected in the absolute positioning stage of vehicle 1, it withholds the provision of relative position measurements for vehicle 2 and vehicle 3 until the KLD is lower than the threshold. In addition, when no vehicles

detect any faults in the absolute positioning stage and vehicle 1 detects no intersections between the relative position intervals provided by its neighboring vehicles during the execution of the ICP algorithm, this means that there is a fault in the relative position measurement of vehicle 2 or vehicle 3. In such cases, vehicle 1 should halt its relative positioning until the relative measurement data are deemed free of faults.

3.7 Conclusion

In this section, we first provide a general proof of consistency for our proposed ISCIF, which can serve as a supplementary proof to traditional SCIF. Additionally, since each vehicle in the MSMV system has multiple relative position estimates, we preprocess them using the ICP method. Then, we utilize the proposed ISCIF method to fuse the preprocessed data.

By using V2V technique, the data sharing can be realized after the absolute positioning stage of each vehicle. Additionally, after the relative positioning stage, the output is in the form of a box. In the prediction stage for the next time step, the input data can be generated using the midpoint of each component within the output box from the last time step. This process provides the iteration for the algorithm.

As mentioned previously, our proposed ISCIF algorithm can be effectively applied to cooperative vehicle localization system using both absolute and multi-relative measurements. This approach enhances localization accuracy and addresses the issues (data incest) arising from multiple relative estimates. The KLD based FDE method is implemented, which enhances the robustness of the MSMV cooperative localization system. Additionally, the parameters for determining the interval width in equation (3.52) should be adjusted according to the specific requirements of different applications.

Furthermore, considering the communication time delay in V2V communication, the error caused by the time delay can be mitigated by adjusting the noise component in the prediction and update steps [16].

Chapter Four

Simulation results

4.1 Introduction

A comparison of the positioning performance of different techniques is performed based on the scenario illustrated in Fig. 4.1. There are three vehicles that could observe each other, and the data sharing was performed by using the V2V communication technique. The reason for our selection of this scenario is that we focused on solving the data incest problem with high-redundancy data. The more mutual observation between vehicles, the more data redundancy there is. In addition, this scenario is a basic scenario with highly redundant data, and this is also common in real traffic transportation systems.

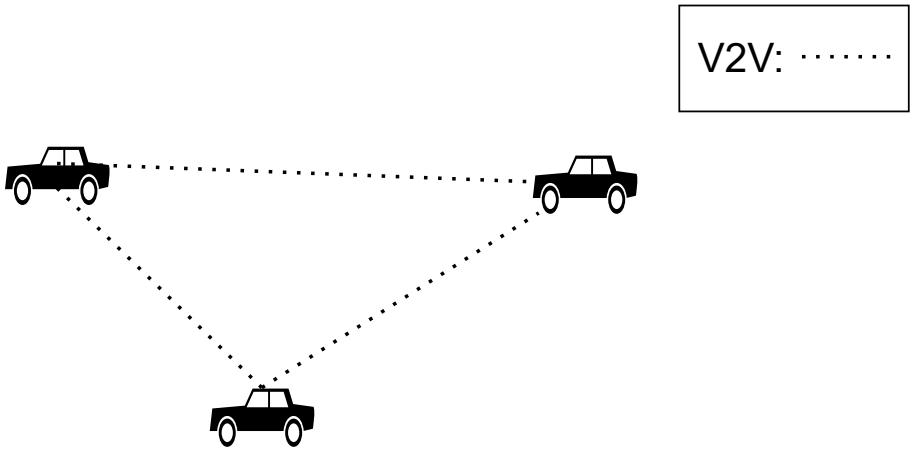

Figure 4.1: Simulation scenario

Without loss of generality, in order to thoroughly test the positioning performance with different absolute positioning abilities, for each scenario, we set up two simulation situations in [16]: The absolute positioning ability of all vehicles in the system is the same, and one vehicle in the system has an excellent absolute localization ability.

Table 4.1: Different variables on localization accuracy based on data from ten experiments

Para.	RMSEs	R1	R2	R3	R4	R5	R6	R7	R8	R9	R10
$\alpha_{xj,yj}=3$	V1	1.43	1.39	1.36	1.33	1.37	1.34	1.42	1.38	1.33	1.44
$\beta_{xi,yi}=0.1$	V2	1.41	1.41	1.44	1.4	1.43	1.35	1.44	1.49	1.36	1.44
$\alpha_{\theta j},\beta_{\theta i}=0$	V3	1.47	1.48	1.46	1.48	1.48	1.43	1.51	1.54	1.4	1.5
$\alpha_{xj,yj}=3$	V1	1.44	1.32	1.38	1.38	1.39	1.43	1.44	1.42	1.34	1.36
$\beta_{xi,yi}=0.2$	V2	1.51	1.4	1.42	1.46	1.44	1.44	1.46	1.43	1.4	1.42
$\alpha_{\theta j},\beta_{\theta i}=0$	V3	1.54	1.46	1.47	1.52	1.52	1.49	1.51	1.49	1.46	1.47
$\alpha_{xj,yj}=3$	V1	1.41	1.33	1.35	1.33	1.3	1.35	1.3	1.46	1.36	1.35
$\beta_{xi,yi}=0.3$	V2	1.57	1.43	1.42	1.47	1.36	1.46	1.45	1.46	1.54	1.4
$\alpha_{\theta j},\beta_{\theta i}=0$	V3	1.61	1.42	1.41	1.45	1.36	1.44	1.42	1.48	1.5	1.4
$\alpha_{xj,yj}=3.5$	V1	1.41	1.37	1.4	1.38	1.33	1.36	1.37	1.38	1.38	1.32
$\beta_{xi,yi}=0.1$	V2	1.46	1.46	1.41	1.44	1.39	1.43	1.48	1.41	1.37	1.39
$\alpha_{\theta j},\beta_{\theta i}=0$	V3	1.54	1.53	1.45	1.49	1.43	1.45	1.49	1.48	1.46	1.48
$\alpha_{xj,yj}=3.5$	V1	1.37	1.36	1.36	1.31	1.36	1.38	1.36	1.3	1.36	1.39
$\beta_{xi,yi}=0.2$	V2	1.38	1.45	1.37	1.36	1.48	1.42	1.43	1.34	1.38	1.39
$\alpha_{\theta j},\beta_{\theta i}=0$	V3	1.46	1.5	1.42	1.42	1.54	1.48	1.5	1.39	1.46	1.44
$\alpha_{xj,yj}=3.5$	V1	1.45	1.33	1.38	1.53	1.43	1.47	1.32	1.36	1.34	1.6
$\beta_{xi,yi}=0.3$	V2	1.52	1.41	1.43	1.55	1.42	1.49	1.39	1.46	1.47	1.52
$\alpha_{\theta j},\beta_{\theta i}=0$	V3	1.57	1.47	1.49	1.58	1.45	1.54	1.44	1.52	1.53	1.59
$\alpha_{xj,yj}=4$	V1	1.4	1.35	1.36	1.39	1.46	1.35	1.33	1.45	1.4	1.43
$\beta_{xi,yi}=0.1$	V2	1.41	1.49	1.49	1.35	1.51	1.37	1.41	1.49	1.49	1.45
$\alpha_{\theta j},\beta_{\theta i}=0$	V3	1.46	1.57	1.55	1.44	1.57	1.44	1.47	1.53	1.54	1.46
$\alpha_{xj,yj}=4$	V1	1.34	1.41	1.38	1.35	1.38	1.4	1.51	1.41	1.45	1.35
$\beta_{xi,yi}=0.2$	V2	1.41	1.48	1.41	1.59	1.46	1.38	1.47	1.48	1.47	1.39
$\alpha_{\theta j},\beta_{\theta i}=0$	V3	1.48	1.53	1.44	1.65	1.48	1.42	1.53	1.5	1.53	1.45
$\alpha_{xj,yj}=4$	V1	1.48	1.38	1.41	1.45	1.39	1.36	1.39	1.31	1.42	1.35
$\beta_{xi,yi}=0.3$	V2	1.49	1.46	1.48	1.45	1.44	1.41	1.45	1.4	1.5	1.47
$\alpha_{\theta j},\beta_{\theta i}=0$	V3	1.54	1.52	1.54	1.5	1.51	1.47	1.5	1.48	1.56	1.51

Details of impact on correlated coefficients in equation (3.52) and (3.55) on localization accuracy based on ten experiments are illustrated in Tab. 4.1. Based on the result, we can conclude that different interval width values have a certain impact on localization accuracy, and our algorithm achieves higher accuracy when all interval width values satisfy $\alpha_{xj} = 3.5$, $\alpha_{yj} = 3.5$, $\alpha_{\theta j} = 0$, $\beta_{xi} = 0.2$, $\beta_{yi} = 0.2$, and $\beta_{\theta i} = 0$, respectively.

In addition, the network frequency band for dedicated short range communication wireless access in vehicular environments is 5.9 GHz. To achieve safer and more effective information sharing between vehicles, we employ synchronous time division multiple access (TDMA) technique. We adopt the TDMA frame structure outlined in [141], as depicted in Fig. 3.3. Every frame spans 100 ms, during which the left control channel (LCCH) and right control channel (RCCH) are employed for secure data transmission, each enduring for 46 ms. Moreover, a 4 ms guard interval (GI) is included to assist in system synchronization.

4.2 Algorithm Performance in Simulation Scenario 1

In this section, the proposed localization method, along with several other methods, are implemented using identical data, followed by a comparison of their respective performances. The methods being tested included the following:

- Extended Kalman filter (EKF) [149];
- Cubature Kalman filter (CKF) [150];
- Adaptive cubature Kalman filter (ACKF) [151];
- Split covariance intersection Kalman filter (SCIF) [16].

Furthermore, the parameters in our simulation scenario 1 are shown in Tab. 4.2.

The simulation experiment for scenario 1 is divided into two parts: scenario 1.1 (As shown in section 4.2.1), where all vehicles have the same absolute positioning capability, and Scenario 1.2 (As shown in section 4.2.2), where vehicle 1 has excellent positioning capability, evaluating the accuracy of vehicle positioning. In addition, scenario 1.3 (As shown in section 4.2.3) demonstrates the advantages of the implemented FDE method.

Table 4.2: Details of the simulation parameters

Parameter	Value
Discrete time step	0.1 (s)
Simulation duration	60 (s)
Velocity of vehicles	15 (m/s)
Standard error of velocity	0.2 (m/s)
Standard error of direction	0.3 (degree)
Standard error of relative distance	0.2 (m)
Standard error of relative orientation r	0.1 (degree)
Standard error of absolute positioning on x-axis	5 (m)
Standard error of absolute positioning on y-axis	5 (m)
Standard error of excellent absolute positioning on x-axis	0.5 (m)
Standard error of excellent absolute positioning on y-axis	0.5 (m)
α_{xj}, α_{yj}	3.5 (m)
β_{xj}, β_{yj}	0.2 (m)
$\alpha_{\theta j}$, $\beta_{\theta i}$	0
TDMA frequency band	5.9 (GHz)
TDMA frame period	100 (ms)

4.2.1 Results of Scenario 1.1: All Vehicles Have the Same Absolute Positioning Ability

Fig. 4.2 displays the true trajectory and the estimated trajectories of vehicle 1 using different methods over a span of 1 min. It should be noted that our method can provide a real-time interval that includes the true position of the vehicle almost all the time.

In addition, Fig. 4.3–4.5 illustrate the root mean square errors (RMSEs) of vehicle 1, vehicle

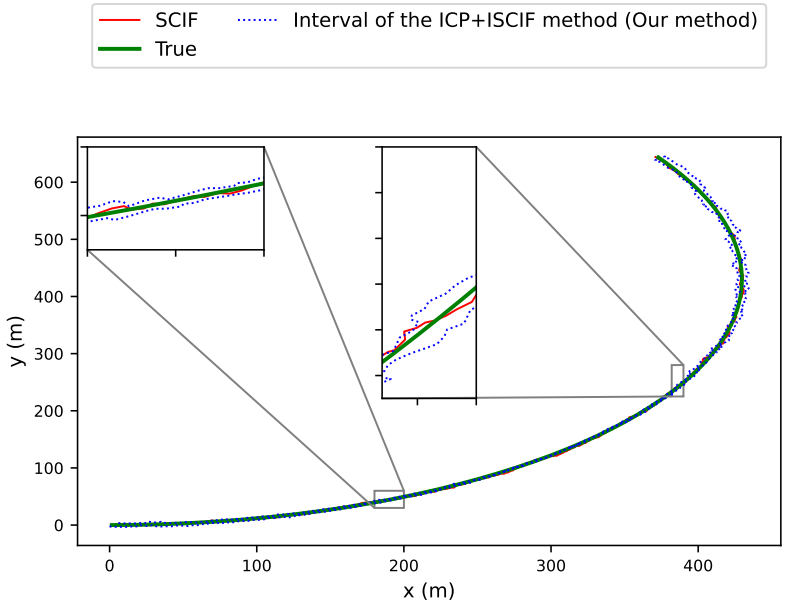

Figure 4.2: Estimated trajectories for different methods in scenario 1.1

2, and vehicle 3 in 30 rounds of simulations, respectively. The x coordinate indicates the test index, and the RMSE is indicated by the y coordinate. Moreover, average RMSEs of the different vehicles based on the different methods in scenario 1.1 are demonstrated in Tab. 4.3. Based on our proposed method, each vehicle was able to achieve the most accurate localization result. In 30 tests, the average RMSEs for the three vehicles when utilizing the SCIF, ACKF, EKF, CKF, and our method were 1.597 m, 1.668 m, 2.450 m, 1.790 m, and 1.455 m, respectively. When all vehicles possessed similar absolute positioning capabilities, our method demonstrated an approximate reduction in the RMSE by 8.9%, 12.8%, 40.6%, and 18.7% compared to the SCIF, ACKF, EKF, and CKF methods, respectively.

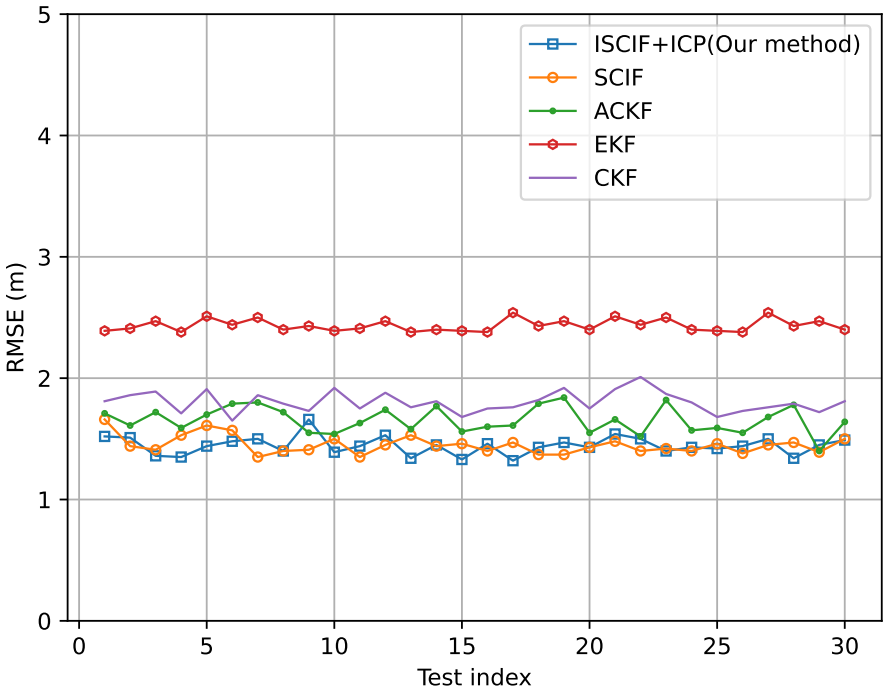

Figure 4.3: RMSE of vehicle 1 in scenario 1.1

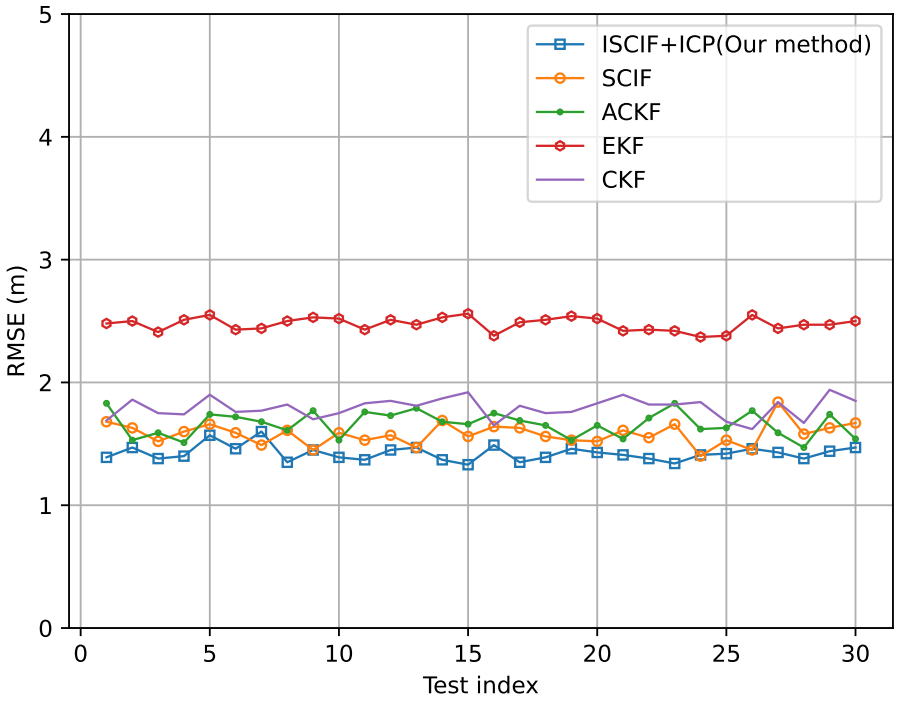

Figure 4.4: RMSE of vehicle 2 in scenario 1.1

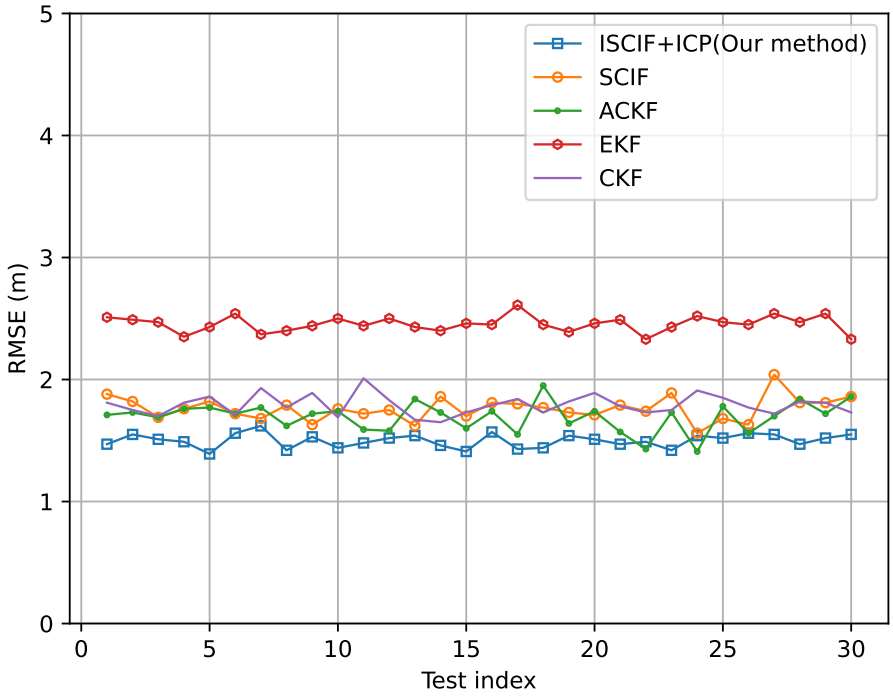

Figure 4.5: RMSE of vehicle 3 in scenario 1.1

Table 4.3: Average RMSEs of different vehicles based on different methods in scenario 1.1

Methods	**RMSE of V1**	**RMSE of V2**	**RMSE of V3**	**Average RMSE**
Our method	1.498 m	1.424 m	1.444 m	1.455 m
SCIF	1.761 m	1.581 m	1.450 m	1.597 m
ACKF	1.693 m	1.661 m	1.650 m	1.668 m
CKF	1.791 m	1.793 m	1.800 m	1.790 m
EKF	2.455 m	2.475 m	2.430 m	2.450 m

4.2.2 Results of Scenario 1.2: One Vehicle Has an Excellent Absolute Positioning Ability

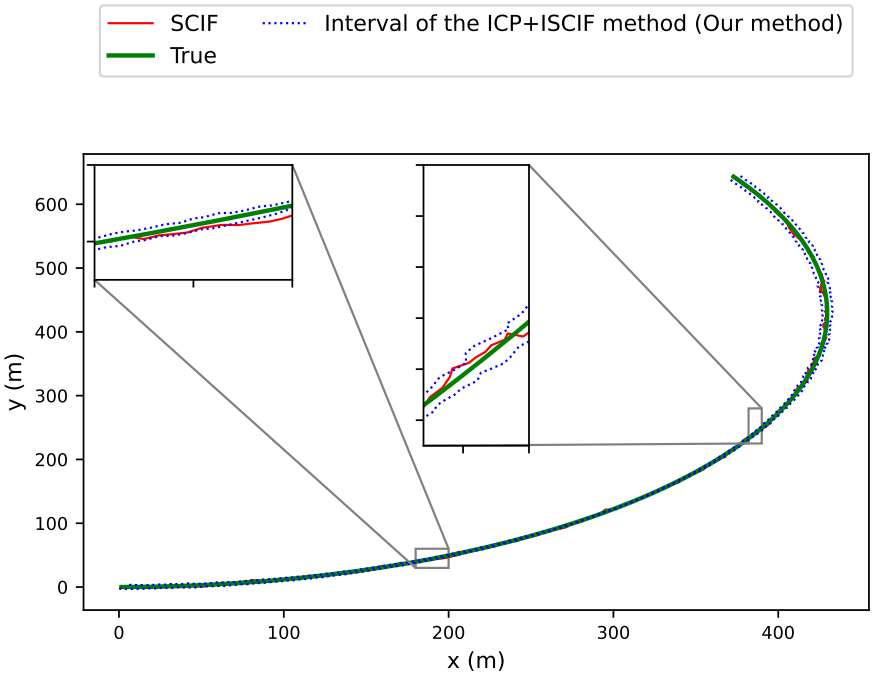

Figure 4.6: Estimated trajectories for different methods in scenario 1.2

Fig. 4.6 illustrates the true trajectory and the estimated trajectories of vehicle 1 when using different methods over a span of 1 min. Compared with the results in scenario 1.1, more closed trajectories were obtained by using the SCIF and our method. The reason is that the vehicle had an excellent absolute positioning ability, and it could obtain a more accurate absolute positioning result. In addition, the RMSEs of vehicle 1, vehicle 2, and vehicle 3 based on 30 rounds of simulations are shown in Fig. 4.7–4.9, respectively. Furthermore, the average RMSEs of the different vehicles based on different methods in scenario 1.2 are listed in Tab. 4.4. The average RMSEs across all vehicles when using the SCIF, ACKF, EKF, CKF, and our method were 0.888 m, 1.274 m, 1.796 m, 1.363 m, and 0.750 m, respectively. Our method showcased reductions in the RMSE of 15.5%, 41.1%, 58.2%, and 45.0% compared to the SCIF, ACKF, EKF, and CKF methods, respectively. This effectively emphasizes the advantages of our proposed method for vehicle localization in MSMVs scenarios involving redundant data.

Table 4.4: RMSEs of different vehicles based on different methods in scenario 1.2

Methods	RMSE of V1	RMSE of V2	RMSE of V3	Average RMSE
Our method	0.450 m	0.788 m	1.010 m	0.750 m
SCIF	0.440 m	1.033 m	1.190 m	0.888 m
ACKF	0.510 m	1.643 m	1.670 m	1.274 m
CKF	0.520 m	1.800 m	1.770 m	1.363 m
EKF	0.460 m	2.497 m	2.431 m	1.796 m

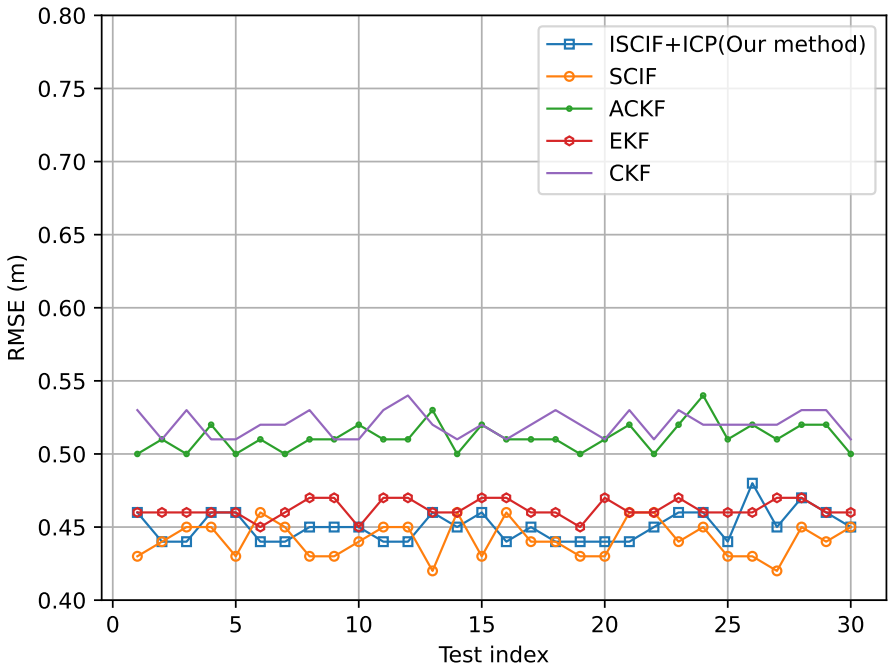

Figure 4.7: RMSEs based on different methods of vehicle 1 in scenario 1.2

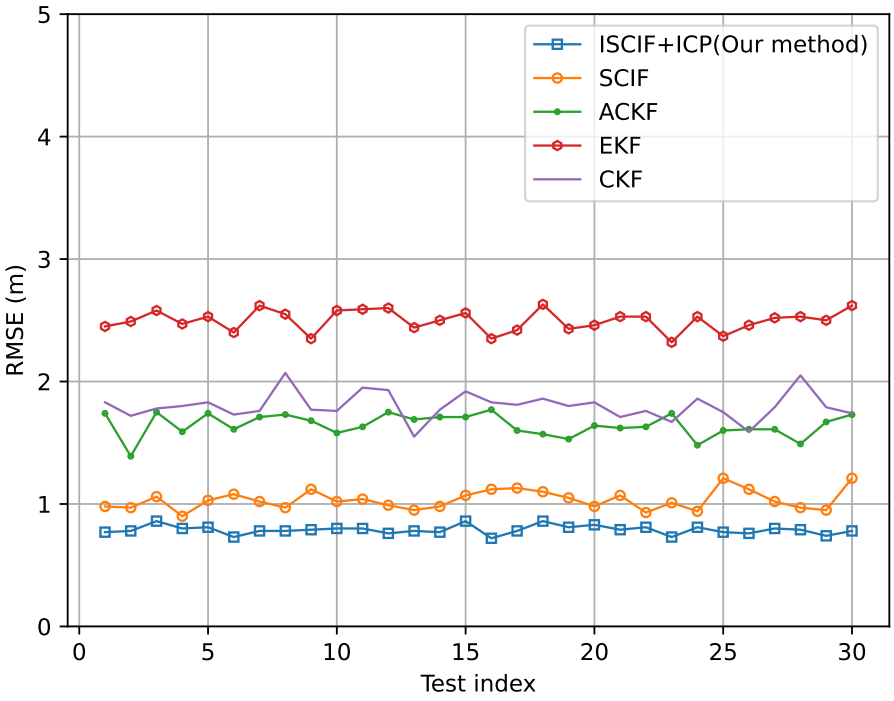

Figure 4.8: RMSEs based on different methods of vehicle 2 in scenario 1.2

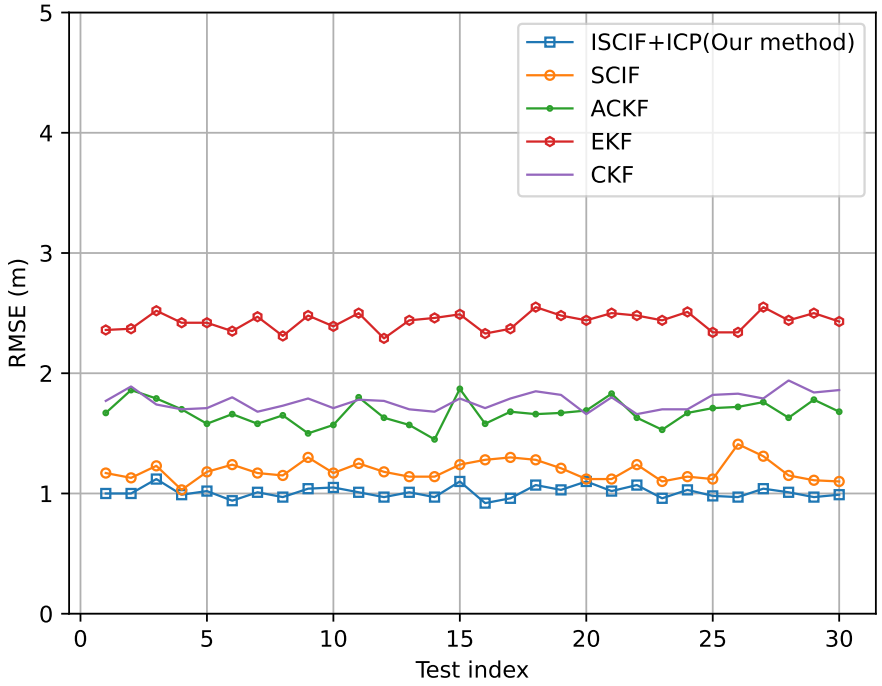

Figure 4.9: RMSEs based on different methods of vehicle 3 in scenario 1.2

4.2.3 Results of Scenario 1.3: Cooperative Vehicle Localization with FDE

The values of the probability density function (pdf) of Kullback–Leibler divergence (KLD) in the both presence and absence of faults in the system were calculated based on empirical data [25]. Threshold λ is approximately 2.137 when the conditional entropy is about 0.1267. In the absence of faults, the RMSE of vehicle 1 over the time steps is depicted in Fig. 4.10. The KLD values based on the time steps are illustrated in Fig. 4.11. We can notice that all of the KLD values are less than the threshold, which indicates the accuracy of the relationship between the threshold and KLD values.

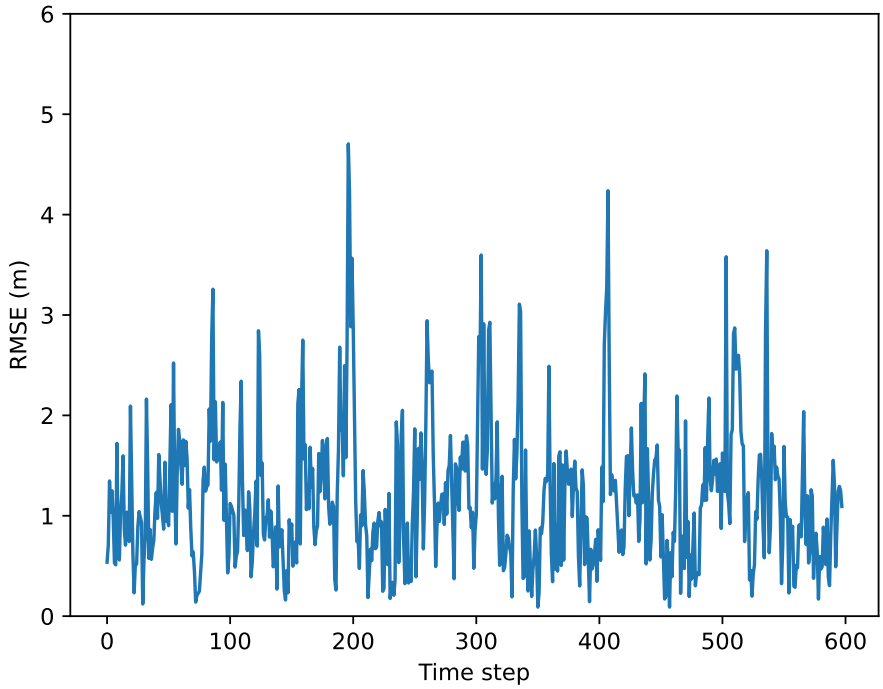

Figure 4.10: RMSEs of vehicle 1 based on the time step in the absence of faults

In order to evaluate the effectiveness of our proposed FDE method, we add impulse noise to the sensor for achieving the absolute positioning of vehicle 1 from 51 s to 54 s [24]. The results of the RMSE based on the time step are shown in Fig. 4.12. We can notice that the RMSE increased dramatically when there is a fault in the system. At the same time, the KLD value based on the time step is illustrated in Fig. 4.13. At time 51 s (time step 510), the KLD value is immediately higher than the threshold, which showes the good real-time performance and

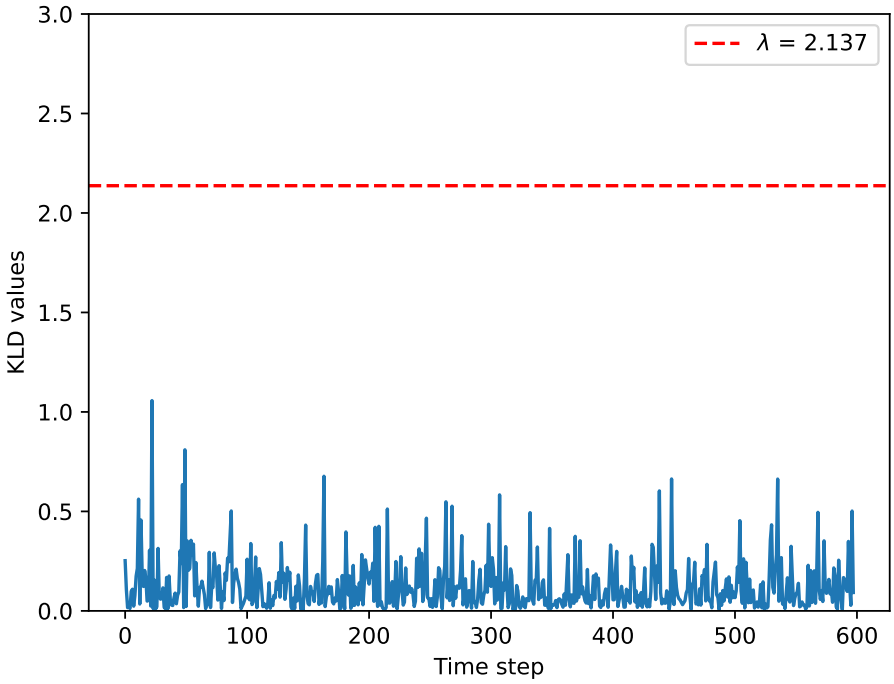

Figure 4.11: KLD values of vehicle 1 based on the time step in the absence of faults

sensitivity of our proposed FDE method. In addition, the KLD value is lower than the threshold value when there are no faults in the system.

After the fault detection, we implement fault exclusion based on our proposed isolation strategy. The estimated trajectories of vehicle 2 using the FDE method and without using the FDE method when the sensor of vehicle 1 had a fault are shown in Fig. 4.14. We can notice that our FDE method could provide a more accurately estimated position when there was a fault in the system. The RMSEs of vehicle 2 and vehicle 3 when their neighbor (vehicle 1) had a fault are illustrated in Fig. 4.15 and Fig. 4.16, respectively. By employing our proposed FDE method, there is about an average 55 percent reduction in the RMSE for vehicles 2 and 3, which indicates the effectiveness of the proposed FDE method.

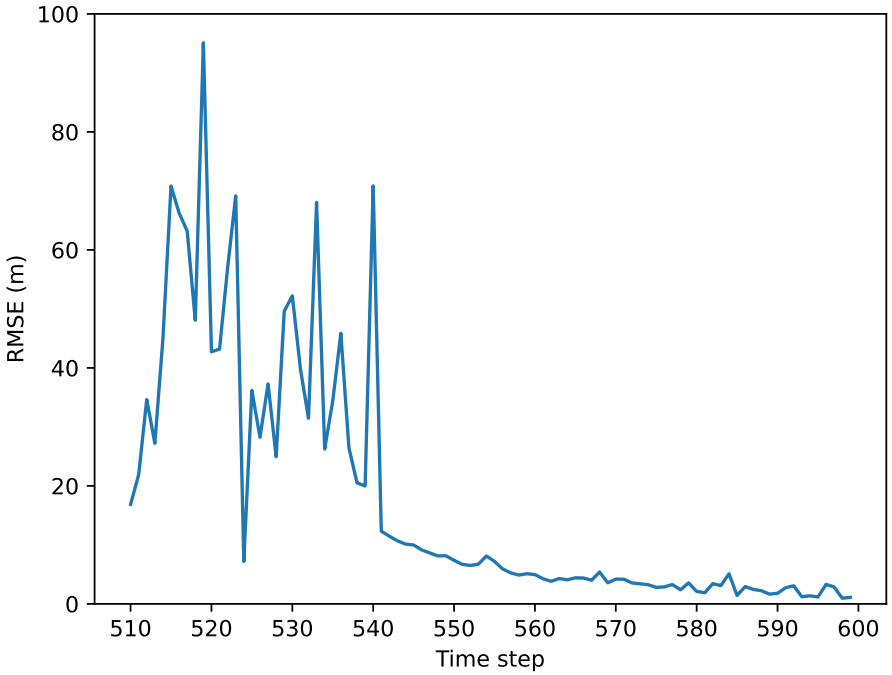

Figure 4.12: RMSE of vehicle 1 based on the time step in the presence of faults

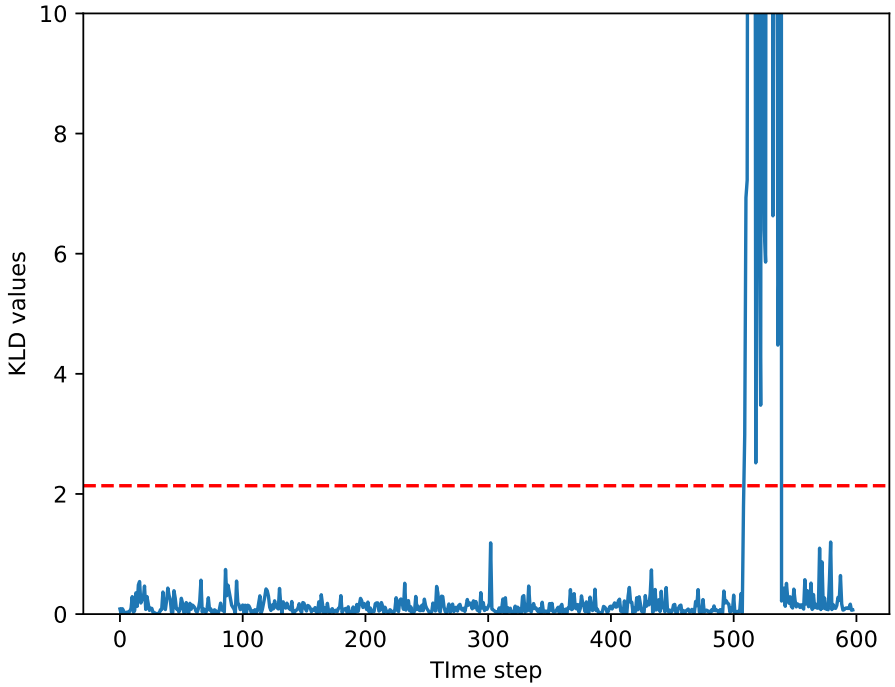

Figure 4.13: KLD values of vehicle 1 based on the time step in the presence of faults

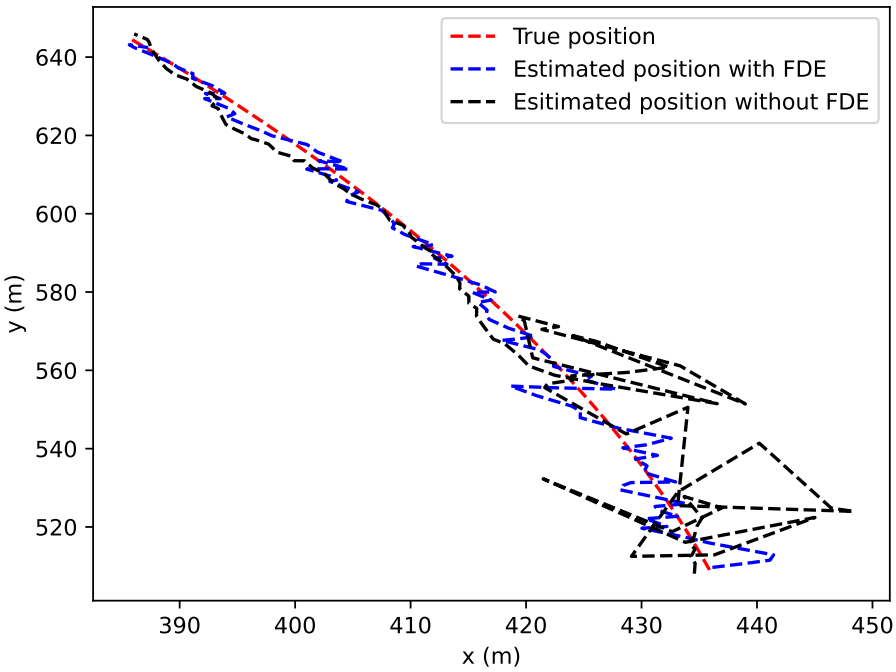

Figure 4.14: Trajectories of vehicle 2 using the FDE method and without using the FDE method

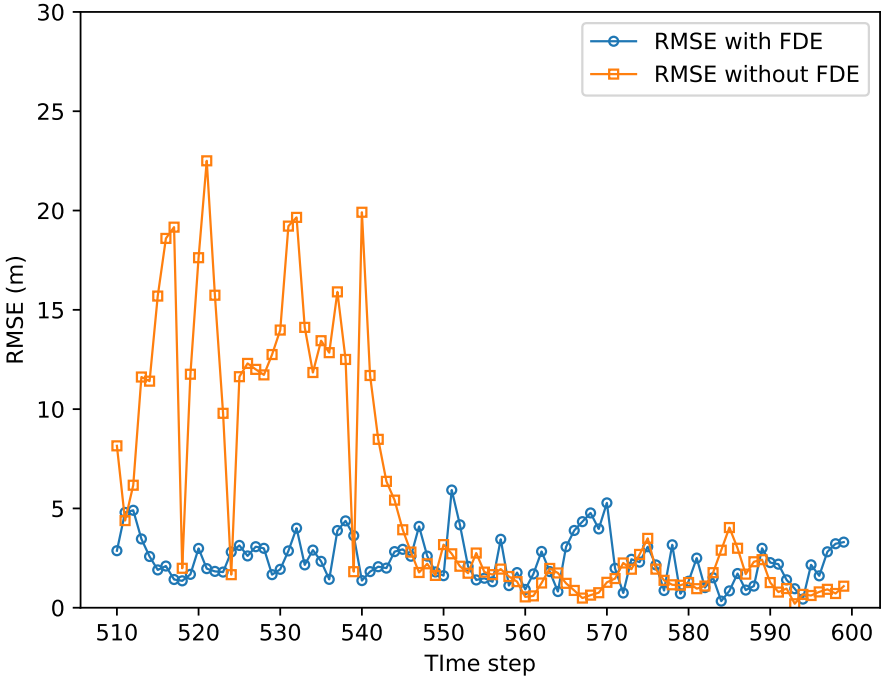

Figure 4.15: RMSEs of vehicle 2 with or without the FDE method

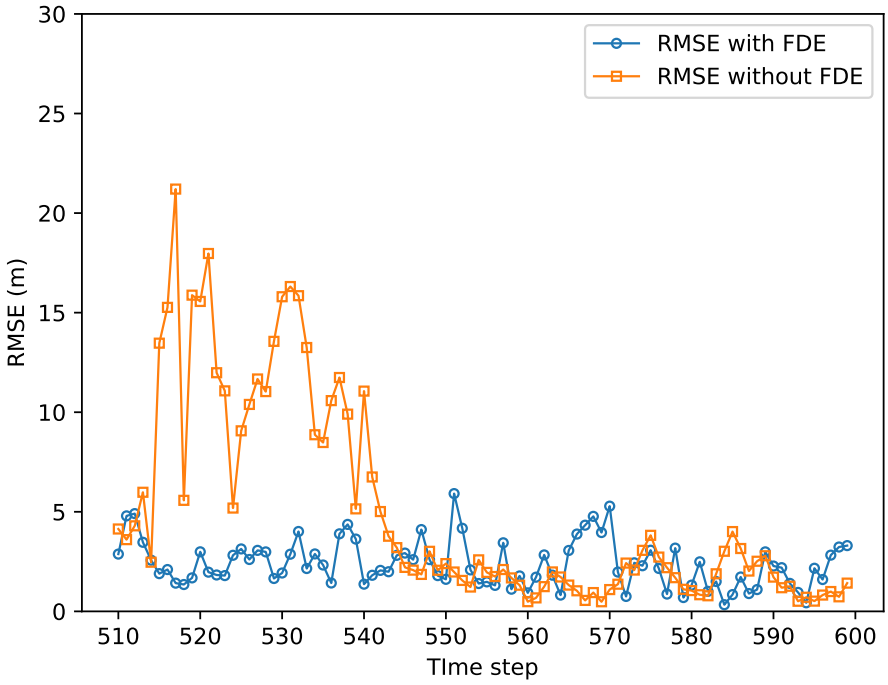

Figure 4.16: RMSE of vehicle 3 with or without the FDE method

4.3 Algorithm Performance in Simulation Scenario 2

To further investigate the accuracy performance of our algorithm proposed, simulation experiments based on scenario 2 are presented in this section. In scenario 2, we also present two separate scenarios: Scenario 2.1 (As shown in section 4.3.1), where all vehicles have the same absolute positioning capability; scenario 2.2 (As shown in section 4.3.2), where vehicle 1 has excellent positioning capability, evaluating the accuracy performance of vehicle positioning. Compared to scenario 1, the vehicle trajectories in scenario 2 are more complex, and the duration of vehicle operation is increased. Noting that the parameters of scenario 2 are the same as those in scenario 1, except for the simulation duration (from 1 minute to 2 minutes). Additionally, the CSP algorithm is included as a comparative algorithm. The compared methods are introduced as follows:

1. Single vehicle localization method (SL)

   Each vehicle in the system achieves vehicle localization through the collected motion and

GPS data by its own onboard sensors. No cooperation between vehicles is required, and the data fusion method is shown in equation (3.48).

2. The ICP method proposed in [143]

   ICP method is used to contract the prediction result, absolute position measurement, and relative position estimations to achieve vehicle localization, as shown in equation (3.10).

3. The SCIF method proposed in [16]

   SCIF algorithm is employed in both absolute and relative positioning stages. During the absolute positioning stage, each vehicle updates its own position based on absolute measurements. In the relative positioning stage, when each vehicle receives relative position measurements from neighboring vehicles via V2V technique, the state vector of each vehicle is updated.

4. Cooperative localization by using ISCIF incorporating ICP (ICP+ISCIF)

   Details have been described previously.

4.3.1 Results of Scenario 2.1: All Vehicles Have the Same Absolute Positioning Ability

. The simulation in scenario 2.1 is conducted with each vehicle has the same absolute positioning ability, the proposed method and several other methods are executed simultaneously using the same synthetic data.

Fig. 4.17 displays the trajectories of vehicle 1 using different methods over a span of 2 minutes. Noting that both our method and the ICP method can consistently provide an interval that includes the true position of the vehicle almost all the time.

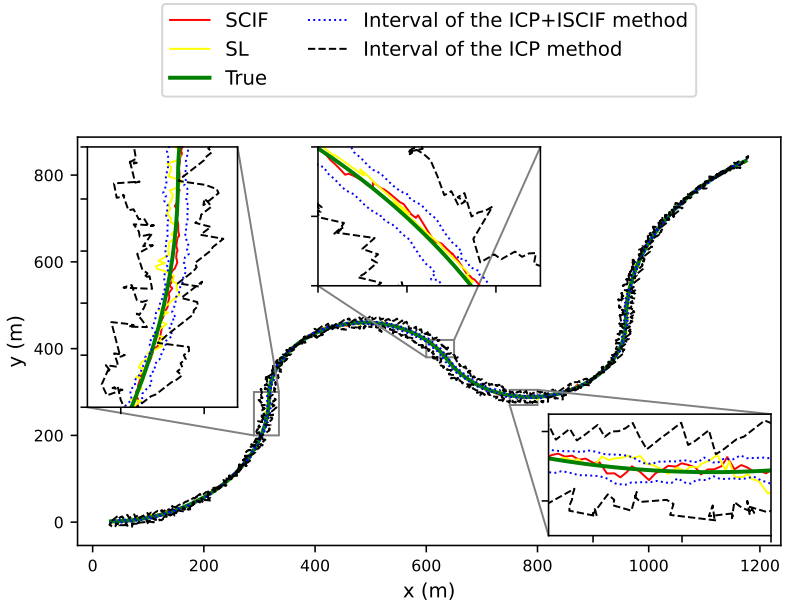

Figure 4.17: Estimated trajectories for different methods in scenario 2.1

The accuracy performance of vehicle 1, 2, and 3 based on one round of simulation is shown in Fig. 4.18, Fig. 4.19, and Fig. 4.20, respectively. The x-axis represents the time sequence and the positioning error is indicated by y-axis. It is noteworthy that our method achieves the most accurate results compared to the other three methods, demonstrating its effectiveness in solving the data incest problem when facing multiple relative estimates in MSMVs. Furthermore, the SCIF method exhibits better accuracy performance than the SL method, owing to the cooperation between vehicles.

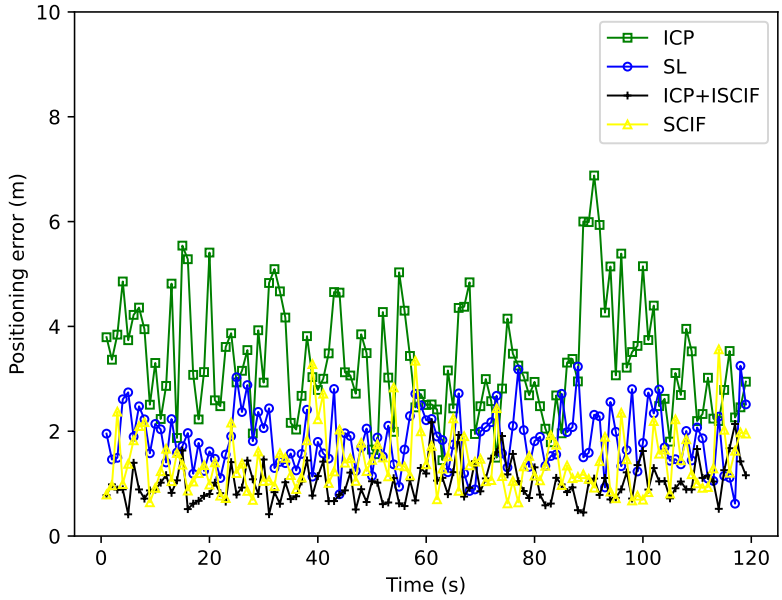

Figure 4.18: RMSEs of vehicle 1 for different methods in scenario 2.1

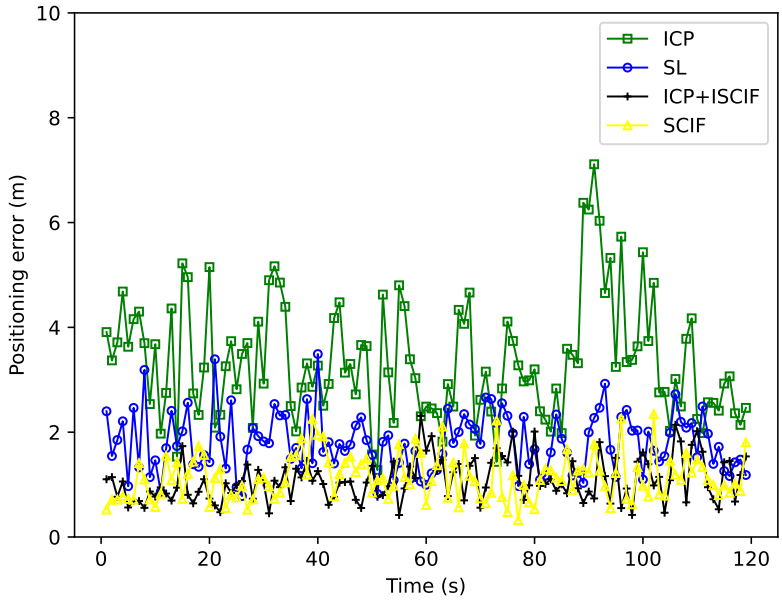

Figure 4.19: RMSEs of vehicle 2 for different methods in scenario 2.1

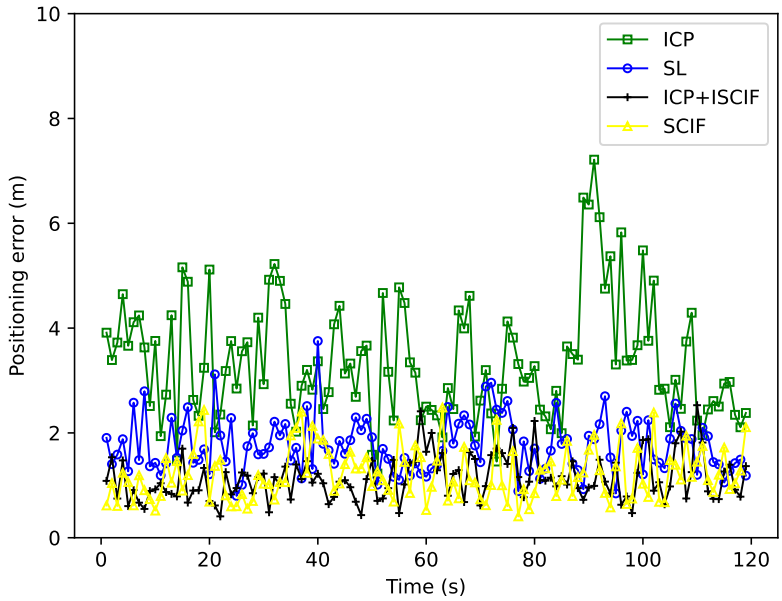

Figure 4.20: RMSEs of vehicle 2 for different methods in scenario 2.1

Additionally, Fig. 4.21, Fig. 4.22, and Fig. 4.23 illustrate the average RMSE of fifty rounds of simulations of vehicle 1, vehicle 2, and vehicle 3, respectively. The x-axis denotes the test index and the average RMSE is indicated by y-axis. The average RMSE of three vehicles in fifty tests using the ICP, SL, SCIF, and our method is 4.01 m, 2.46 m, 1.57 m, and 1.40 m, respectively. Our method reduces the RMSE by about 11 percent compared to the SCIF method.

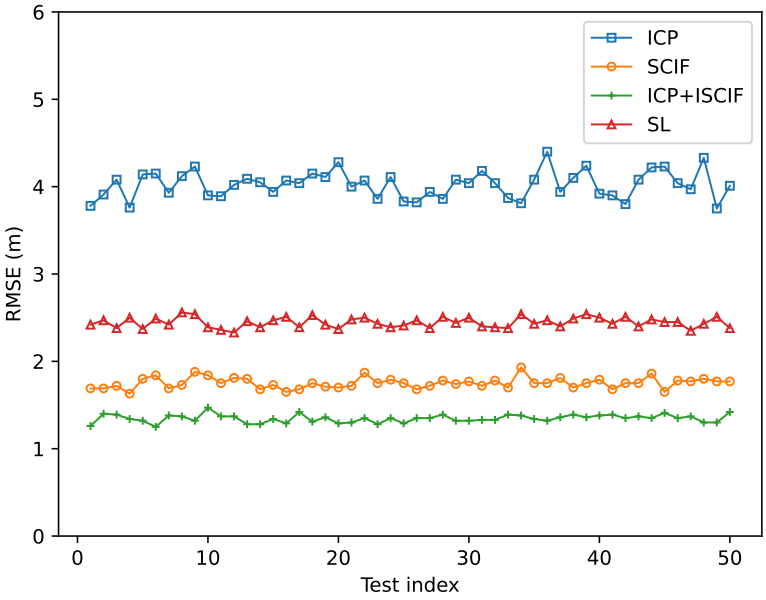

Figure 4.21: Average RMSEs of vehicle 1 for different methods in scenario 2.1

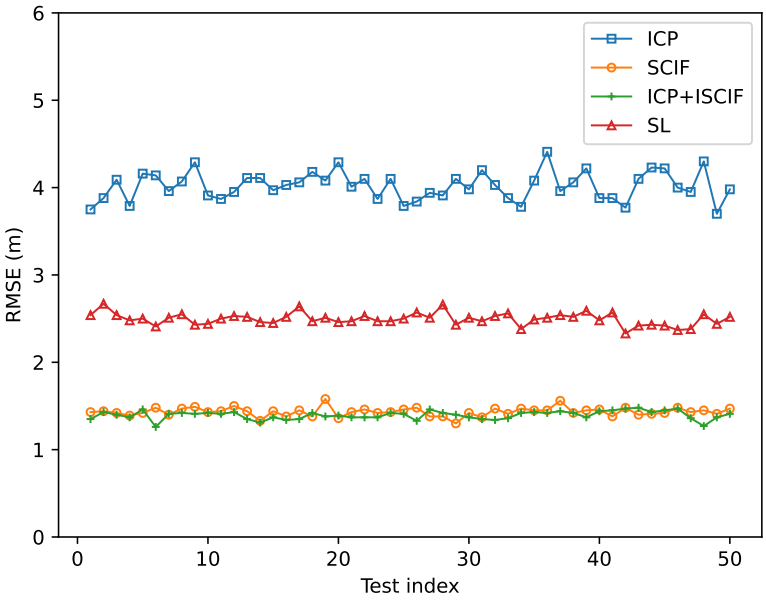

Figure 4.22: Average RMSEs of vehicle 2 for different methods in scenario 2.1

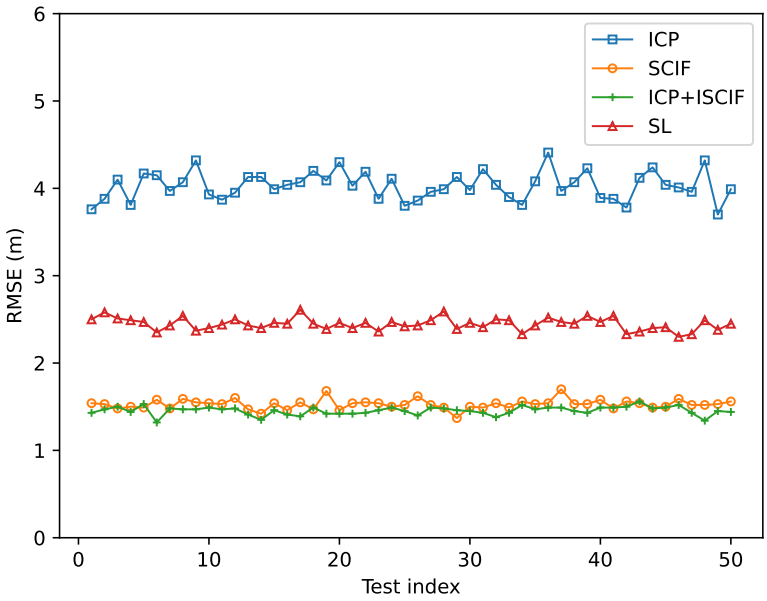

Figure 4.23: Average RMSEs of vehicle 3 for different methods in scenario 2.1

4.3.2 Results of Scenario 2.2: One Vehicle Has an Excellent Absolute Positioning Ability

In scenario 2.2, the absolute positioning standard errors of vehicle 1 on both x and y coordinates are 0.5 m, while the absolute positioning capability of other vehicles remains unchanged. The trajectories of vehicle 1 using different methods based on one round of simulation are shown in Fig. 4.24. Noting that the true position may not be included in the intervals provided by the ICP method. In other words, the ICP method may lose the possible solution.

The Fig. 4.25, Fig. 4.26, and Fig. 4.27 illustrate the comparison results of four methods based on one round of simulation. The x-axis in these figures represents the time sequence, and the y-axis indicates the positioning error. We can notice that for all the vehicles, the positioning error provided by the ICP method decrease significantly compared with the results in scenario 2.1. Additionally, for vehicle 1, the positioning errors based on the SL, SCIF, and the ICP+ISCIF methods are similar, as the data fusion method utilizing GPS sensor with excellent absolute positioning capability can achieve a reasonable accuracy. Furthermore, for vehicle 2

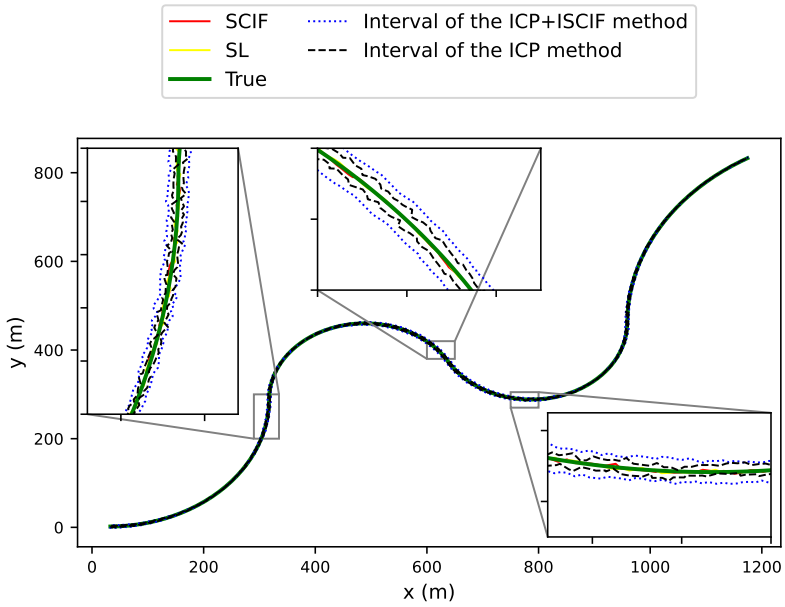

Figure 4.24: Estimated trajectories for different methods in scenario 2.2

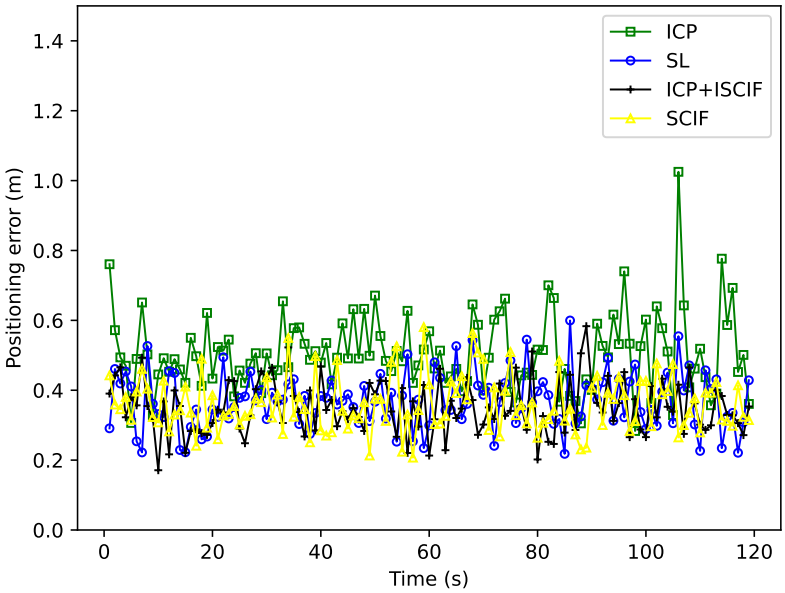

Figure 4.25: Positioning error of vehicle 1 associated with different methods in scenario 2.2

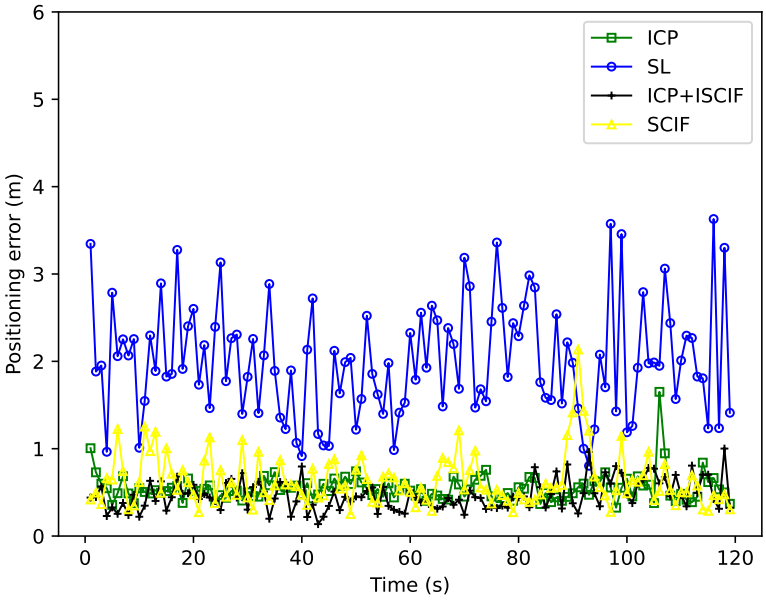

Figure 4.26: Positioning error of vehicle 2 associated with different methods in scenario 2.2

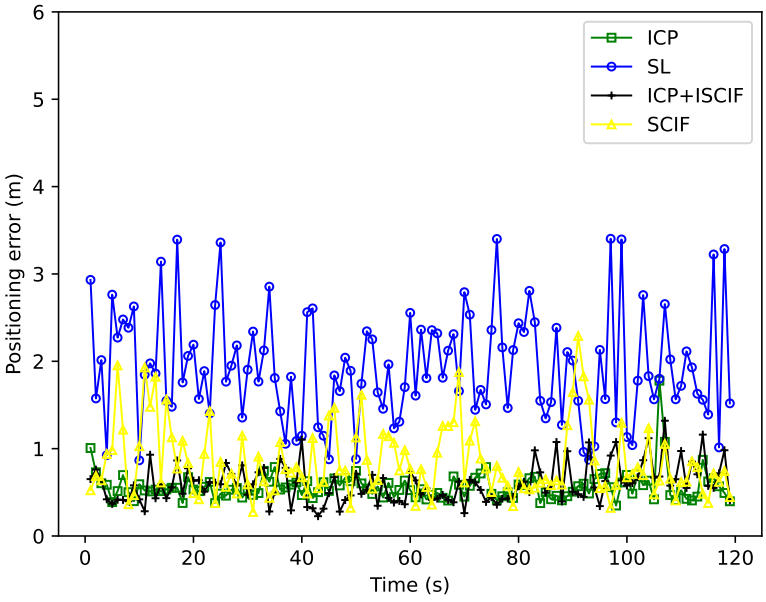

Figure 4.27: Positioning error of vehicle 3 associated with different methods in scenario 2.2

and 3, the positioning accuracy based on the ICP, SCIF, and the ICP+ISCIF methods can also be improved compared to that in scenario 1, benefiting from the mutual cooperation between vehicles. In other words, cooperative localization method can effectively enhance the accuracy performance compared to the SL method.

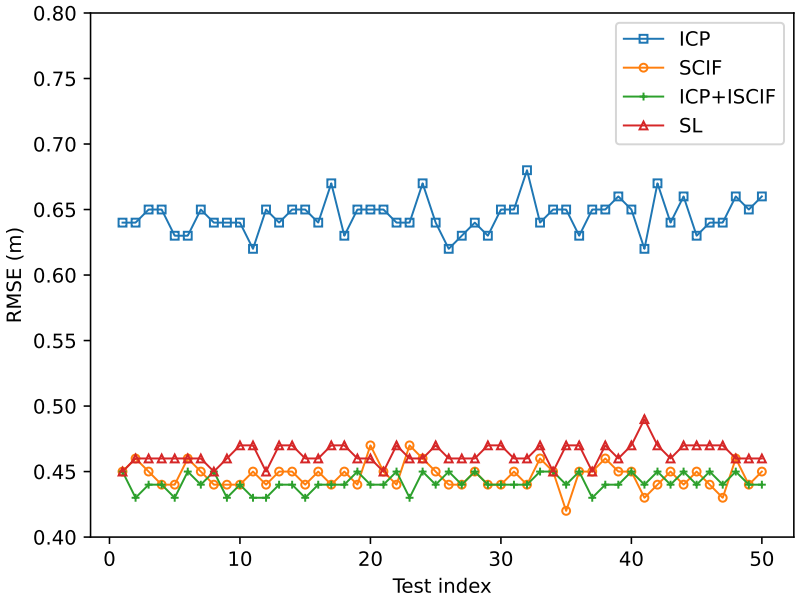

Figure 4.28: Average RMSE of vehicle 1 associated with different methods in scenario 2.2

In addition, the statistical RMSE results based on 50 times of vehicle 1, vehicle 2, and vehicle 3 are shown in Fig. 4.28, Fig. 4.29, and Fig. 4.30, respectively. The average RMSE of the ICP method for all vehicles is 0.77 m, which benefits the most compared with the result in scenario 2.1. However, at certain steps, the true position may not included in the estimated interval. The average RMSEs of the SL, SCIF, and ICP+ISCIF methods are 1.8 m, 0.76 m, and 0.6 m, respectively. Thus, compared to the SCIF method, our proposed method (ICP+ISCIF) can reduce the RMSE by about 21 percent in scenario 2.2.

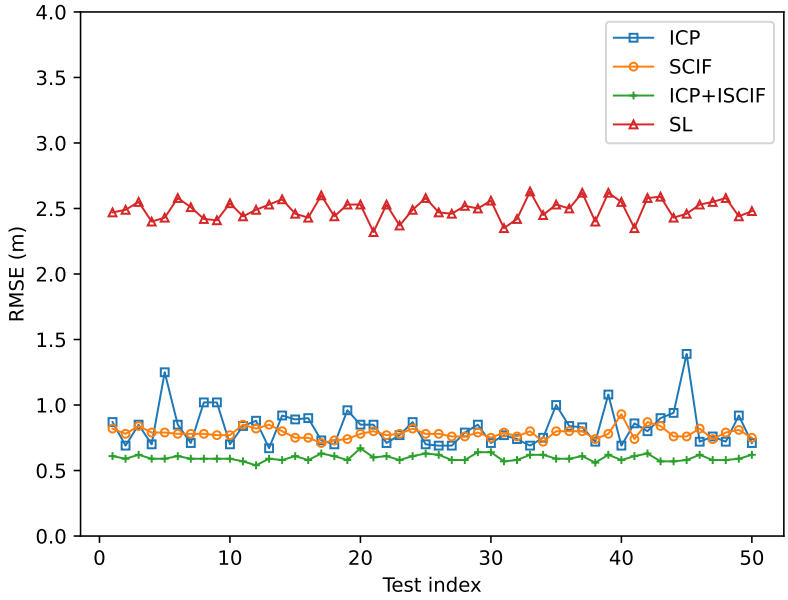

Figure 4.29: Average RMSE of vehicle 2 associated with different methods in scenario 2.2

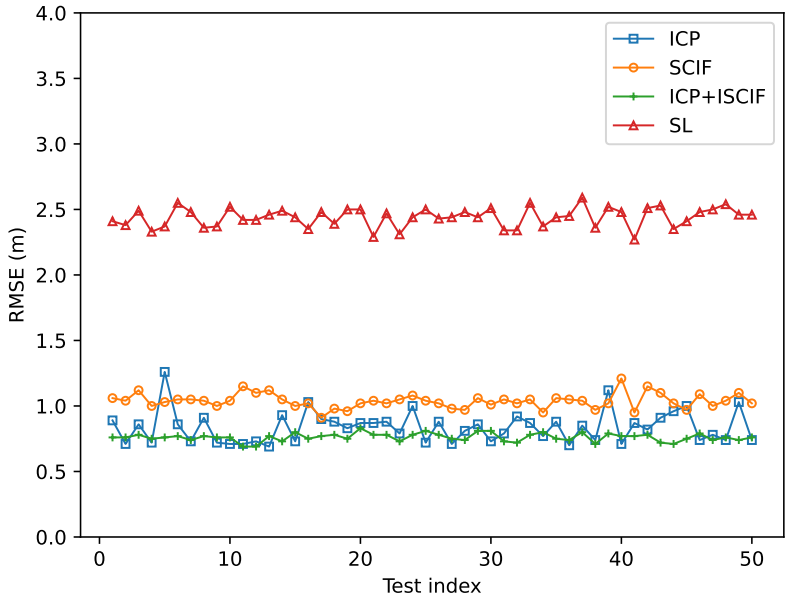

Figure 4.30: Average RMSE of vehicle 3 associated with different methods in scenario 2.2

4.4 Computational burden analysis

Table 4.5: Matrix operation complexity

Matrix operation	Matrix dimension	Complexity
$X+Y$	$[a*b]$+$[a*b]$	$O(ab)$
$X.Y$	$[a*b].[b*c]$	$O(abc)$
X^{-1}	$[a*a]$	$O(a^3)$

The matrix operation complexity is shown in Tab. 4.5, noting that performing addition, multiplication, inverse operations with interval matrix incurs the same level of complexity as with regular matrices. So, by using big O notation, the complexity of both ISCIF and SCIF algorithms are $O(n^3)$ (where n is the dimension of the covariance matrix), which depends on the inverse operation of the matrix.

Moreover, in order to further investigate the computational overhead of our proposed algorithm, experiments based on execution time are conducted. The result is shown in Fig. 4.31, the average execution time per time step of SCIF and our method based on 30 times of experiments are 10.70 ms and 8.29 ms, respectively. Compare to SCIF method, our method achieves a reduction in execution time of approximately 23%.

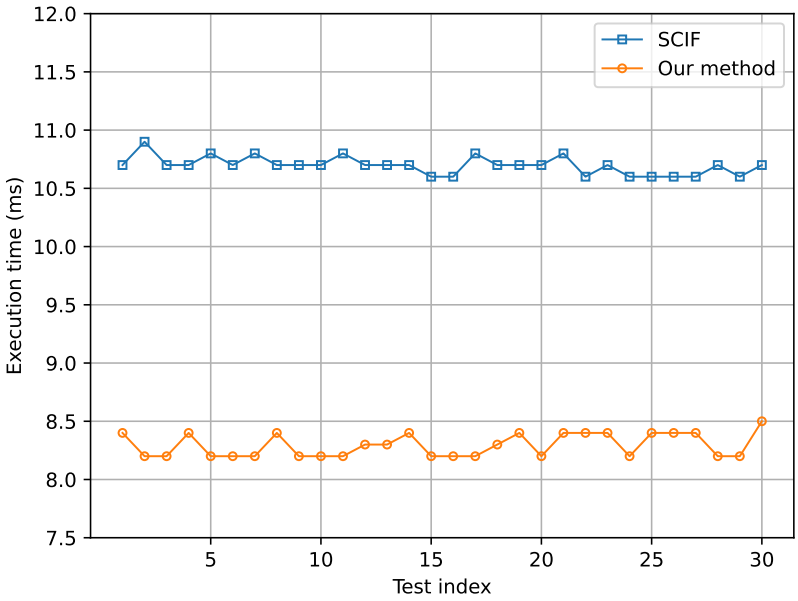

Figure 4.31: The execution time of SCIF and our method

4.5 Conclusion

In this section, we design two different simulation scenarios to validate the accuracy of our algorithm. Simulation experiments demonstrate that, compared to state of the art methods such as SCIF, CSP, and CKF, our proposed approach shows a significant improvement in accuracy. Additionally, we apply the KLD-based FDE method to the designed MSMV localization system, significantly enhancing its robustness. Finally, the computational overhead results show that our approach has lower computational costs compared to SCIF method in [16].

Chapter Five

Conclusion and future work

This Ph.D thesis mainly addresses the data incest problem, aims to propose an accurate, robust, and low-cost cooperative localization method in the multi-sensor multi-vehicle (MSMV) cooperative vehicle localization systems. Considering the structure of the vehicle cooperative localization system, since the traditional centralized structure has limitations in computing and communication ability, we adopt a decentralized cooperative structure. The use of a decentralized cooperative structure not only reduces the computing and communication pressure of the vehicle network, but is also more suitable for dynamic vehicle networks. In the following, a conclusion of the main subjects discussed in each chapters of this thesis is given.

In chapter 1, we provide an overview of the history and current status of cooperative localization in MSMVs and analyzes current unresolved challenges. Compared with the traditional self-localization algorithm, the cooperative vehicle localization algorithm based on V2V communication technique has higher efficiency. However, in the MSMV cooperative localization system, there are two problems that need to be addressed: The first problem is that there is a data incest problem when vehicles use its relative estimates provided by neighboring vehicles for relative positioning, which leads to inconsistent data fusion results; The second problem is that the traditional split covariance intersection filter (SCIF) algorithm has high computational overhead in the relative positioning stage, caused by complicated state update iteration. In this background, the context and motivation of our thesis have been discussed. In addition, the main aims of our thesis are to propose a new consistent data fusion algorithm, named interval split covariance intersection filter (ISCIF), and give its theoretical consistency proof. Then, ISCIF incorporating interval constraint propagation (ICP) method is applied to the cooperative localization of the MSMV system. Finally, in order to enhance the robustness of the system, the fault detection and exclusion method is used in our system.

In chapter 2, the survey of the state-of-the-art vehicle localization techniques is highlighted. We analyze the comprehensive performance of existing advanced vehicle localization techniques and discuss their challenges. Firstly, we analyze the self-localization methods based on active and passive sensors. The results show that, the light detection and ranging (LiDAR)

and vision-based localization techniques can reach high accuracy. However, they have high computational complexity. Only using the inertial measurement unit (IMU), global positioning system (GPS), radar, and ultrasonic sensors may not realize localization result with high accuracy. Then, we discuss V2X-based cooperative localization methods, analyze the multi-sensor based localization techniques and compare the comprehensive performance among all methods. Although the artificial intelligence (AI) techniques can effectively enhance the efficiency of vision-based localization algorithms, the high computational complexity still should be considered. In addition, since the IMU, GPS, radar, and ultrasonic sensors have good performance in terms of the availability, reliability, scalability, and cost-effectiveness, they can be used as auxiliary sensors to achieve good comprehensive performance through data fusion techniques. Finally, we analyze the performances of different kind of vehicle localization techniques, propose the challenges of these techniques and our research questions.

In chapter 3, firstly, we give an overview of the intelligent transportation system (ITS), including its architecture and communication techniques. Then, the related techniques for cooperative vehicle localization are presented in section 3.3. In order to address the data incest problem in the MSMV localization system, a new data fusion algorithm named ISCIF is proposed, and the generic consistency proof of the ISCIF is provided. Furthermore, the proposed ISCIF is implemented in both absolute and relative positioning stages in a decentralized MSMV localization system. Noting that in the relative positioning stage, since there are multiple relative estimates, which reduces the localization accuracy and increases the computational overhead, the ICP method is employed to mitigate the impact caused by the multiple relative position estimates and provide input data for ISCIF. In addition, the KLD based FDE method is implemented to increase the robustness of the MSMV localization systems.

Moreover, the main reasons why the ICP method can output accurate results include: accurate modeling and constraint propagation. In terms of accurate modeling, the ICP method can precisely infer the possible ranges of variables by considering the relationships between constraints and variables. Additionally, constraint propagation is employed to narrow down

the ranges of variables, effectively reducing the solution space and achieving accurate vehicle positioning. Regarding the proposed ISCIF algorithm, it addresses the impact of relative estimation among neighbors by utilizing interval analysis techniques, allowing it to provide state estimation intervals instead of traditional point estimates. This allows the algorithm to more comprehensively represent the uncertainty of state variables and mitigate the impact of state estimation uncertainty. Furthermore, interval arithmetic operations, compared to traditional numerical computations, can reduce rounding errors to some extent, thereby yielding more accurate results.

The proposed method is evaluated through simulation tests with two different scenarios, and the results are illustrated in chapter 4. Firstly, we set up correlated coefficients in equations (3.52) and (3.55) based on ten experiments. In simulation 1, we compare our proposed method with extended Kalman filter (EKF), cubature kalman filter (CKF), adaptive cubature kalman filter (ACKF), and split covariance intersection filter (SCIF) in terms of localization accuracy. When all vehicles in the system have the same absolute positioning ability, as shown in paragraph 4.2.1. Simulation results show that our method demonstrates an approximate reduction in the RMSE by 8.9%, 12.8%, 40.6%, and 18.7% compared to the SCIF, ACKF, EKF, and CKF methods, respectively. Moreover, when vehicle has the excellent absolute positioning ability, as shown in paragraph 4.2.2, Our method showcases reductions in the RMSE of 15.5%, 41.1%, 58.2%, and 45.0% compared to the SCIF, ACKF, EKF, and CKF methods, respectively. In addition, the simulation results in paragraph 4.2.3 shows the advantages when we implement Kullback–Leibler divergence (KLD)-based fault detection and exclusion (FDE) method in our system. When a sensor failure occurs within the system, we are able to detect it in time and execute relevant mechanisms to mitigate the impact of the sensor failure on the vehicle localization accuracy within the system.

Additionally, in order to further investigate the localization accuracy of our proposed method, another simulation scenario with more complex trajectory is designed in section 4.3. In this chapter, we compare our proposed method with single localization method (SL), interval con-

straint propagation method (ICP), and split covariance intersection filter (SCIF) in terms of localization accuracy. When all vehicles have the same absolute positioning ability, as shown in paragraph 4.3.1, our method reduces the RMSE by about 65%, 11%, and 43% compared to the ICP, SCIF, and SL method, respectively. Furthermore, When vehicle one has the excellent absolute positioning ability, as shown in paragraph 4.3.2, our method reduces the RMSE by about 22%, 21%, and 67% compared to the ICP, SCIF, and SL method, respectively. Based on the results obtained from the simulations, our proposed method can achieve reasonable accuracy. Compared with state of the art methods, our proposed approach significantly reduces RMSE in both scenarios. Moreover, the true vehicle position can be included in the intervals outputted by our method almost all the time, which means that our method can be implemented in the interval non-linear system. Furthermore, based on the computation burden analysis, our proposed method implemented in MSMV cooperative vehicle localization has a lower computational costs.

Finally, in our future work, we aim to propose an algorithm suitable for GPS-denied scenarios, as GPS signals can easily be affected by satellite transmission signal strength in the real world. Additionally, we intend to test the performance of our proposed method using real-world data.

Bibliography

[1] X. Shan, A. Cabani, and H. Chafouk, "Cooperative vehicle localization in multi-sensor multi-vehicle systems based on an interval split covariance intersection filter with fault detection and exclusion," Vehicles, vol. 6, no. 1, pp. 352–373, 2024.

[2] E. Zhang and N. Masoud, "Increasing gps localization accuracy with reinforcement learning," IEEE Transactions on Intelligent Transportation Systems, vol. 22, no. 5, pp. 2615–2626, 2020.

[3] J. K. Suhr, J. Jang, D. Min, and H. G. Jung, "Sensor fusion-based low-cost vehicle localization system for complex urban environments," IEEE Transactions on Intelligent Transportation Systems, vol. 18, no. 5, pp. 1078–1086, 2016.

[4] Y. Xu, V. John, S. Mita, H. Tehrani, K. Ishimaru, and S. Nishino, "3d point cloud map based vehicle localization using stereo camera," in 2017 IEEE intelligent vehicles symposium (IV), pp. 487–492, IEEE, 2017.

[5] W. Zhao, R. He, B. Ai, Z. Zhong, and H. Zhang, "Vehicle localization based on hypothesis test in nlos scenarios," IEEE Transactions on Vehicular Technology, vol. 71, no. 2, pp. 2198–2203, 2021.

[6] M. Randriamasy, A. Cabani, H. Chafouk, and G. Fremont, "Geolocation process to perform the electronic toll collection using the its-g5 technology," IEEE Transactions on Vehicular Technology, vol. 68, no. 9, pp. 8570–8582, 2019.

[7] M. Randriamasy, A. Cabani, H. Chafouk, and G. Fremont, "Reliable vehicle location in electronic toll collection service with cooperative intelligent transportation systems," in 2017 IEEE 28th Annual International Symposium on Personal, Indoor, and Mobile Radio Communications (PIMRC), pp. 1–7, 2017.

[8] Y. Han, C. Wei, R. Li, J. Wang, and H. Yu, "A novel cooperative localization method based on imu and uwb," Sensors, vol. 20, no. 2, p. 467, 2020.

[9] X. Shan, A. Cabani, and H. Chafouk, "Cooperative localization based on gps correction and ekf in urban environment," in 2022 2nd International Conference on Innovative Research in Applied Science, Engineering and Technology (IRASET), pp. 1–8, IEEE, 2022.

[10] C. Huang and X. Wu, "Cooperative vehicle tracking using particle filter integrated with interacting multiple models," in ICC 2019-2019 IEEE International Conference on Communications (ICC), pp. 1–6, IEEE, 2019.

[11] X. Shan, A. Cabani, and H. Chafouk, "A survey of vehicle localization: Performance analysis and challenges," IEEE Access, 2023.

[12] T. Yang, A. Cabani, and H. Chafouk, "A survey of recent indoor localization scenarios and methodologies," Sensors, vol. 21, no. 23, 2021.

[13] N. Karam, Agrégation de données décentralisées pour la localisation multi-véhicules. PhD thesis, Université Blaise Pascal-Clermont-Ferrand II, 2009.

[14] M. Abu Bakr and S. Lee, "Distributed multisensor data fusion under unknown correlation and data inconsistency," Sensors, vol. 17, no. 11, p. 2472, 2017.

[15] B. Khaleghi, A. Khamis, F. O. Karray, and S. N. Razavi, "Multisensor data fusion: A review of the state-of-the-art," Information fusion, vol. 14, no. 1, pp. 28–44, 2013.

[16] H. Li and F. Nashashibi, "Cooperative multi-vehicle localization using split covariance intersection filter," IEEE Intelligent transportation systems magazine, vol. 5, no. 2, pp. 33–44, 2013.

[17] T.-K. Chang, K. Chen, and A. Mehta, "Resilient and consistent multirobot cooperative localization with covariance intersection," IEEE Transactions on Robotics, vol. 38, no. 1, pp. 197–208, 2021.

[18] Y. Lu, H. Ma, E. Smart, and H. Yu, "Real-time performance-focused localization techniques for autonomous vehicle: A review," IEEE Transactions on Intelligent Transportation Systems, 2021.

[19] A. Motwani, S. Sharma, R. Sutton, and P. Culverhouse, "Interval kalman filtering in navigation system design for an uninhabited surface vehicle," The Journal of Navigation, vol. 66, no. 5, pp. 639–652, 2013.

[20] J. Rohn and R. Farhadsefat, "Inverse interval matrix: a survey," The Electronic Journal of Linear Algebra, vol. 22, pp. 704–719, 2011.

[21] X. Shan, A. Cabani, and H. Chafouk, "A survey of vehicle localization: Performance analysis and challenges," IEEE Access, 2023.

[22] J. Xiong, J. W. Cheong, Z. Xiong, A. G. Dempster, S. Tian, R. Wang, and J. Liu, "Fault-tolerant relative navigation based on kullback–leibler divergence," International Journal of Advanced Robotic Systems, vol. 17, no. 6, p. 1729881420979125, 2020.

[23] S. Eguchi and J. Copas, "Interpreting kullback–leibler divergence with the neyman–pearson lemma," Journal of Multivariate Analysis, vol. 97, no. 9, pp. 2034–2040, 2006.

[24] M. Wu, H. Ma, and X. Zhang, "Decentralized cooperative localization with fault detection and isolation in robot teams," Sensors, vol. 18, no. 10, p. 3360, 2018.

[25] J. A. Hage, M. E. El Najjar, and D. Pomorski, "Collaborative localization for multi-robot system with fault detection and exclusion based on the kullback-leibler divergence," Journal of Intelligent & Robotic Systems, vol. 87, pp. 661–681, 2017.

[26] S. Kuutti, S. Fallah, K. Katsaros, M. Dianati, F. Mccullough, and A. Mouzakitis, "A survey of the state-of-the-art localization techniques and their potentials for autonomous vehicle applications," IEEE Internet of Things Journal, vol. 5, no. 2, pp. 829–846, 2018.

[27] K.-W. Kim and G.-I. Jee, "Free-resolution probability distributions map-based precise vehicle localization in urban areas," Sensors, vol. 20, no. 4, p. 1220, 2020.

[28] J.-H. Im, S.-H. Im, and G.-I. Jee, "Extended line map-based precise vehicle localization using 3d lidar," Sensors, vol. 18, no. 10, p. 3179, 2018.

[29] K.-W. Kim, J.-H. Im, M.-B. Heo, and G.-I. Jee, "Precise vehicle position and heading estimation using a binary road marking map," Journal of Sensors, vol. 2019, 2019.

[30] R. W. Wolcott and R. M. Eustice, "Robust lidar localization using multiresolution gaussian mixture maps for autonomous driving," The International Journal of Robotics Research, vol. 36, no. 3, pp. 292–319, 2017.

[31] Z. Ren and L. Wang, "Accurate real-time localization estimation in underground mine environments based on a distance-weight map (dwm)," Sensors, vol. 22, no. 4, p. 1463, 2022.

[32] N. Akai, L. Y. Morales, T. Yamaguchi, E. Takeuchi, Y. Yoshihara, H. Okuda, T. Suzuki, and Y. Ninomiya, "Autonomous driving based on accurate localization using multilayer lidar and dead reckoning," in 2017 IEEE 20th International Conference on Intelligent Transportation Systems (ITSC), pp. 1–6, IEEE, 2017.

[33] A. Schaefer, D. Büscher, J. Vertens, L. Luft, and W. Burgard, "Long-term urban vehicle localization using pole landmarks extracted from 3-d lidar scans," in 2019 European Conference on Mobile Robots (ECMR), pp. 1–7, IEEE, 2019.

[34] C. Shi, J. Li, J. Gong, B. Yang, and G. Zhang, "An improved lightweight deep neural network with knowledge distillation for local feature extraction and visual localization using images and lidar point clouds," ISPRS Journal of Photogrammetry and Remote Sensing, vol. 184, pp. 177–188, 2022.

[35] H. Yin, Y. Wang, X. Ding, L. Tang, S. Huang, and R. Xiong, "3d lidar-based global localization using siamese neural network," IEEE Transactions on Intelligent Transportation Systems, vol. 21, no. 4, pp. 1380–1392, 2019.

[36] A. Charroud, K. El Moutaouakil, V. Palade, and A. Yahyaouy, "Xdll: Explained deep learning lidar-based localization and mapping method for self-driving vehicles," Electronics, vol. 12, no. 3, p. 567, 2023.

[37] F. Ghallabi, G. El-Haj-Shhade, M.-A. Mittet, and F. Nashashibi, "Lidar-based road signs detection for vehicle localization in an hd map," in 2019 IEEE Intelligent Vehicles Symposium (IV), pp. 1484–1490, IEEE, 2019.

[38] C.-M. Hsu and C.-W. Shiu, "3d lidar-based precision vehicle localization with movable region constraints," Sensors, vol. 19, no. 4, p. 942, 2019.

[39] T. Zhou, M. Yang, K. Jiang, H. Wong, and D. Yang, "Mmw radar-based technologies in autonomous driving: A review," Sensors, vol. 20, no. 24, p. 7283, 2020.

[40] X. Wang, M. Huang, C. Shen, and D. Meng, "Robust vehicle localization exploiting two based stations cooperation: A mimo radar perspective," IEEE Access, vol. 6, pp. 48747–48755, 2018.

[41] L. Zhaoyu, Z. Wenli, Z. Jingyue, G. Shisheng, C. Guolong, K. Lingjiang, and L. Kun, "Non-los target localization via millimeter-wave automotive radar," Journal of Systems Engineering and Electronics, 2023.

[42] K. Yoneda, N. Hashimoto, R. Yanase, M. Aldibaja, and N. Suganuma, "Vehicle localization using 76ghz omnidirectional millimeter-wave radar for winter automated driving," in 2018 IEEE Intelligent Vehicles Symposium (IV), pp. 971–977, IEEE, 2018.

[43] T. Ort, I. Gilitschenski, and D. Rus, "Autonomous navigation in inclement weather based on a localizing ground penetrating radar," IEEE Robotics and Automation Letters, vol. 5, no. 2, pp. 3267–3274, 2020.

[44] L. Narula, P. A. Iannucci, and T. E. Humphreys, "Automotive-radar-based 50-cm urban positioning," in 2020 IEEE/ION Position, Location and Navigation Symposium (PLANS), pp. 856–867, IEEE, 2020.

[45] L. R. Cenkeramaddi, P. K. Rai, A. Dayal, J. Bhatia, A. Pandya, J. Soumya, A. Kumar, and A. Jha, "A novel angle estimation for mmwave fmcw radars using machine learning," IEEE Sensors Journal, vol. 21, no. 8, pp. 9833–9843, 2021.

[46] Y. Wang, Z. Jiang, X. Gao, J.-N. Hwang, G. Xing, and H. Liu, "Rodnet: Radar object detection using cross-modal supervision," in Proceedings of the IEEE/CVF Winter Conference on Applications of Computer Vision, pp. 504–513, 2021.

[47] L. Yang, X. Feng, J. Zhang, and X. Shu, "Multi-ray modeling of ultrasonic sensors and application for micro-uav localization in indoor environments," Sensors, vol. 19, no. 8, p. 1770, 2019.

[48] J. H. Rhee and J. Seo, "Low-cost curb detection and localization system using multiple ultrasonic sensors," Sensors, vol. 19, no. 6, p. 1389, 2019.

[49] M. Moussa, A. Moussa, and N. El-Sheimy, "Ultrasonic based heading estimation for aiding land vehicle navigation in gnss denied environment.," International Archives of the Photogrammetry, Remote Sensing & Spatial Information Sciences, 2018.

[50] M. Elhousni and X. Huang, "A survey on 3d lidar localization for autonomous vehicles," in 2020 IEEE Intelligent Vehicles Symposium (IV), pp. 1879–1884, IEEE, 2020.

[51] X. Yu and M. Marinov, "A study on recent developments and issues with obstacle detection systems for automated vehicles," Sustainability, vol. 12, no. 8, p. 3281, 2020.

[52] M. Brossard, A. Barrau, and S. Bonnabel, "Ai-imu dead-reckoning," IEEE Transactions on Intelligent Vehicles, vol. 5, no. 4, pp. 585–595, 2020.

[53] K. Eckenhoff, P. Geneva, and G. Huang, "Mimc-vins: A versatile and resilient multi-imu multi-camera visual-inertial navigation system," IEEE Transactions on Robotics, vol. 37, no. 5, pp. 1360–1380, 2021.

[54] M. Zhang, X. Xu, Y. Chen, and M. Li, "A lightweight and accurate localization algorithm using multiple inertial measurement units," IEEE Robotics and Automation Letters, vol. 5, no. 2, pp. 1508–1515, 2020.

[55] K. Eckenhoff, P. Geneva, and G. Huang, "Sensor-failure-resilient multi-imu visual-inertial navigation," in 2019 International Conference on Robotics and Automation (ICRA), pp. 3542–3548, IEEE, 2019.

[56] A. Al-Radaideh and L. Sun, "Observability analysis and bayesian filtering for self-localization of a tethered multicopter in gps-denied environments," in 2019 International Conference on Unmanned Aircraft Systems (ICUAS), pp. 1041–1047, IEEE, 2019.

[57] Y. Yang, W. Gao, S. Guo, Y. Mao, and Y. Yang, "Introduction to beidou-3 navigation satellite system," NAVIGATION, Journal of the Institute of Navigation, vol. 66, no. 1, pp. 7–18, 2019.

[58] X. Li, Z. Shen, X. Li, G. Liu, Y. Zhou, S. Li, H. Lyu, and Q. Zhang, "Continuous decimeter-level positioning in urban environments using multi-frequency gps/bds/galileo ppp/ins tightly coupled integration," Remote Sensing, vol. 15, no. 8, p. 2160, 2023.

[59] S. Park, S. Ryu, J. Lim, and Y.-S. Lee, "A real-time high-speed autonomous driving based on a low-cost rtk-gps," Journal of Real-Time Image Processing, vol. 18, pp. 1321–1330, 2021.

[60] S. Misra, B. Wang, K. Sundar, R. Sharma, and S. Rathinam, "Single vehicle localization and routing in gps-denied environments using range-only measurements," IEEE Access, vol. 8, pp. 31004–31017, 2019.

[61] T. Welsh, S. M. Marks, and A. Pronschinske, "Gps-denied vehicle localization for augmented reality using a road-aided particle filter and rgb camera," in 2023 IEEE/ION Position, Location and Navigation Symposium (PLANS), pp. 1363–1372, IEEE, 2023.

[62] G. Bassma, S. Tayeb, et al., "Support vector machines for improving vehicle localization in urban canyons," in MATEC Web of Conferences, vol. 200, p. 00004, EDP Sciences, 2018.

[63] Y.-L. Hsueh and H.-C. Chen, "Map matching for low-sampling-rate gps trajectories by exploring real-time moving directions," Information Sciences, vol. 433, pp. 55–69, 2018.

[64] G. R. Jagadeesh and T. Srikanthan, "Online map-matching of noisy and sparse location data with hidden markov and route choice models," IEEE Transactions on Intelligent Transportation Systems, vol. 18, no. 9, pp. 2423–2434, 2017.

[65] S. Lynen, B. Zeisl, D. Aiger, M. Bosse, J. Hesch, M. Pollefeys, R. Siegwart, and T. Sattler, "Large-scale, real-time visual–inertial localization revisited," The International Journal of Robotics Research, vol. 39, no. 9, pp. 1061–1084, 2020.

[66] M. Adjrad and P. D. Groves, "Enhancing least squares gnss positioning with 3d mapping without accurate prior knowledge," NAVIGATION, Journal of the Institute of Navigation, vol. 64, no. 1, pp. 75–91, 2017.

[67] D. Lu, V. C. Jammula, S. Como, J. Wishart, Y. Chen, and Y. Yang, "Carom-vehicle localization and traffic scene reconstruction from monocular cameras on road infrastructures," in 2021 IEEE International Conference on Robotics and Automation (ICRA), pp. 11725–11731, IEEE, 2021.

[68] K. Lu, R. Xu, J. Li, Y. Lv, H. Lin, and Y. Liu, "A vision-based detection and spatial localization scheme for forest fire inspection from uav," Forests, vol. 13, no. 3, p. 383, 2022.

[69] A. Thomas, V. Leboucher, A. Cotinat, P. Finet, and M. Gilbert, "Uav localization using panoramic thermal cameras," in Computer Vision Systems: 12th International Conference, ICVS 2019, Thessaloniki, Greece, September 23–25, 2019, Proceedings 12, pp. 754–767, Springer, 2019.

[70] A. Gupta and X. Fernando, "Simultaneous localization and mapping (slam) and data fusion in unmanned aerial vehicles: Recent advances and challenges," Drones, vol. 6, no. 4, p. 85, 2022.

[71] S. Fang, H. Li, and M. Yang, "Lidar slam based multivehicle cooperative localization using iterated split cif," IEEE Transactions on Intelligent Transportation Systems, vol. 23, no. 11, pp. 21137–21147, 2022.

[72] H. Kim, K. Granström, L. Svensson, S. Kim, and H. Wymeersch, "Pmbm-based slam filters in 5g mmwave vehicular networks," IEEE Transactions on Vehicular Technology, vol. 71, no. 8, pp. 8646–8661, 2022.

[73] J. Cheng, L. Zhang, Q. Chen, X. Hu, and J. Cai, "A review of visual slam methods for autonomous driving vehicles," Engineering Applications of Artificial Intelligence, vol. 114, p. 104992, 2022.

[74] A. Macario Barros, M. Michel, Y. Moline, G. Corre, and F. Carrel, "A comprehensive survey of visual slam algorithms," Robotics, vol. 11, no. 1, p. 24, 2022.

[75] P. Schmuck and M. Chli, "Ccm-slam: Robust and efficient centralized collaborative monocular simultaneous localization and mapping for robotic teams," Journal of Field Robotics, vol. 36, no. 4, pp. 763–781, 2019.

[76] T. Taketomi, H. Uchiyama, and S. Ikeda, "Visual slam algorithms: a survey from 2010 to 2016," IPSJ Transactions on Computer Vision and Applications, vol. 9, no. 1, pp. 1–11, 2017.

[77] K. Yoneda, R. Yanase, M. Aldibaja, N. Suganuma, and K. Sato, "Mono-camera based vehicle localization using lidar intensity map for automated driving," Artificial Life and Robotics, vol. 24, no. 2, pp. 147–154, 2019.

[78] S. Houben, M. Neuhausen, M. Michael, R. Kesten, F. Mickler, and F. Schuller, "Park marking-based vehicle self-localization with a fisheye topview system," Journal of Real-Time Image Processing, vol. 16, no. 2, pp. 289–304, 2019.

[79] R. P. D. Vivacqua, M. Bertozzi, P. Cerri, F. N. Martins, and R. F. Vassallo, "Self-localization based on visual lane marking maps: An accurate low-cost approach for autonomous driving," IEEE Transactions on Intelligent Transportation Systems, vol. 19, no. 2, pp. 582–597, 2017.

[80] G. Huang, Z. Hu, Q. Tao, F. Zhang, and Z. Zhou, "Improved intelligent vehicle self-localization with integration of sparse visual map and high-speed pavement visual odometry," Proceedings of the Institution of Mechanical Engineers, Part D: Journal of Automobile Engineering, vol. 235, no. 1, pp. 177–187, 2021.

[81] S. Chen, J. Hu, Y. Shi, Y. Peng, J. Fang, R. Zhao, and L. Zhao, "Vehicle-to-everything (v2x) services supported by lte-based systems and 5g," IEEE Communications Standards Magazine, vol. 1, no. 2, pp. 70–76, 2017.

[82] K. Kiela, V. Barzdenas, M. Jurgo, V. Macaitis, J. Rafanavicius, A. Vasjanov, L. Kladovscikov, and R. Navickas, "Review of v2x–iot standards and frameworks for its applications," Applied sciences, vol. 10, no. 12, p. 4314, 2020.

[83] S. Zhang, J. Chen, F. Lyu, N. Cheng, W. Shi, and X. Shen, "Vehicular communication networks in the automated driving era," IEEE Communications Magazine, vol. 56, no. 9, pp. 26–32, 2018.

[84] S. Gyawali, S. Xu, Y. Qian, and R. Q. Hu, "Challenges and solutions for cellular based v2x communications," IEEE Communications Surveys & Tutorials, vol. 23, no. 1, pp. 222–255, 2020.

[85] W. Wang, D. Marelli, and M. Fu, "Multiple-vehicle localization using maximum likelihood kalman filtering and ultra-wideband signals," IEEE Sensors Journal, vol. 21, no. 4, pp. 4949–4956, 2020.

[86] E. I. Adegoke, J. Zidane, E. Kampert, C. R. Ford, S. A. Birrell, and M. D. Higgins, "Infrastructure wi-fi for connected autonomous vehicle positioning: A review of the state-of-the-art," Vehicular Communications, vol. 20, p. 100185, 2019.

[87] A. Motroni, A. Buffi, and P. Nepa, "A survey on indoor vehicle localization through rfid technology," IEEE Access, vol. 9, pp. 17921–17942, 2021.

[88] H. Kim, S. H. Lee, and S. Kim, "Cooperative localization with constraint satisfaction problem in 5g vehicular networks," IEEE Transactions on Intelligent Transportation Systems, vol. 23, no. 4, pp. 3180–3189, 2020.

[89] M. A. G. Al-Sadoon, R. Asif, Y. I. A. Al-Yasir, R. A. Abd-Alhameed, and P. S. Excell, "Aoa localization for vehicle-tracking systems using a dual-band sensor array," IEEE Transactions on Antennas and Propagation, vol. 68, no. 8, pp. 6330–6345, 2020.

[90] J. Tiemann and C. Wietfeld, "Scalable and precise multi-uav indoor navigation using tdoa-based uwb localization," in 2017 international conference on indoor positioning and indoor navigation (IPIN), pp. 1–7, IEEE, 2017.

[91] N. Saeed, W. Ahmad, and D. M. S. Bhatti, "Localization of vehicular ad-hoc networks with rss based distance estimation," in 2018 International Conference on Computing, Mathematics and Engineering Technologies (iCoMET), pp. 1–6, IEEE, 2018.

[92] H. Sallouha, M. M. Azari, A. Chiumento, and S. Pollin, "Aerial anchors positioning for reliable rss-based outdoor localization in urban environments," IEEE Wireless Communications Letters, vol. 7, no. 3, pp. 376–379, 2017.

[93] F. B. Günay, E. Öztürk, T. Çavdar, Y. S. Hanay, et al., "Vehicular ad hoc network (vanet) localization techniques: a survey," Archives of Computational Methods in Engineering, vol. 28, no. 4, pp. 3001–3033, 2021.

[94] M. Brambilla, M. Nicoli, G. Soatti, and F. Deflorio, "Augmenting vehicle localization by cooperative sensing of the driving environment: Insight on data association in urban traffic scenarios," IEEE Transactions on Intelligent Transportation Systems, vol. 21, no. 4, pp. 1646–1663, 2019.

[95] L. Rivoirard, M. Wahl, P. Sondi, D. Gruyer, and M. Berbineau, "A cooperative vehicle ego-localization application using v2v communications with cbl clustering," in 2018 IEEE Intelligent Vehicles Symposium (IV), pp. 722–727, IEEE, 2018.

[96] H. Kim, K. Granström, L. Gao, G. Battistelli, S. Kim, and H. Wymeersch, "5g mmwave cooperative positioning and mapping using multi-model phd filter and map fusion," IEEE Transactions on Wireless Communications, vol. 19, no. 6, pp. 3782–3795, 2020.

[97] M. Randriamasy, A. Cabani, H. Chafouk, and G. Fremont, "Formally validated of novel tolling service with the its-g5," IEEE Access, vol. 7, pp. 41133–41144, 2019.

[98] H. Wang, L. Wan, M. Dong, K. Ota, and X. Wang, "Assistant vehicle localization based on three collaborative base stations via sbl-based robust doa estimation," IEEE Internet of Things Journal, vol. 6, no. 3, pp. 5766–5777, 2019.

[99] R. Chen, X. Huang, Y. Zhou, Y. Hui, and N. Cheng, "Uhf-rfid-based real-time vehicle localization in gps-less environments," IEEE Transactions on Intelligent Transportation Systems, 2021.

[100] J. Zhang, X. Wang, Z. Yu, Y. Lyu, S. Mao, S. C. Periaswamy, J. Patton, and X. Wang, "Robust rfid based 6-dof localization for unmanned aerial vehicles," IEEE Access, vol. 7, pp. 77348–77361, 2019.

[101] S. Huang, Y. Guo, S. Zha, F. Wang, and W. Fang, "A real-time location system based on rfid and uwb for digital manufacturing workshop," Procedia Cirp, vol. 63, pp. 132–137, 2017.

[102] A. J. Alami, K. El-Sayed, A. Al-Horr, H. Artail, and J. Guo, "Improving the car gps accuracy using v2v and v2i communications," in 2018 IEEE International Multidisciplinary Conference on Engineering Technology (IMCET), pp. 1–6, IEEE, 2018.

[103] H. Qin, Y. Peng, and W. Zhang, "Vehicles on rfid: Error-cognitive vehicle localization in gps-less environments," IEEE Transactions on Vehicular Technology, vol. 66, no. 11, pp. 9943–9957, 2017.

[104] P. Bonnifait, I. Fantoni, et al., "Cooperative localization with reliable confidence domains between vehicles sharing gnss pseudoranges errors with no base station," IEEE Intelligent Transportation Systems Magazine, vol. 9, no. 1, pp. 22–34, 2017.

[105] J. Al Hage, M. E. El Najjar, and D. Pomorski, "Multi-sensor fusion approach with fault detection and exclusion based on the kullback–leibler divergence: Application on collaborative multi-robot system," Information Fusion, vol. 37, pp. 61–76, 2017.

[106] M. Á. de Miguel, F. García, and J. M. Armingol, "Improved lidar probabilistic localization for autonomous vehicles using gnss," Sensors, vol. 20, no. 11, p. 3145, 2020.

[107] D. Kang and D. Kum, "Camera and radar sensor fusion for robust vehicle localization via vehicle part localization," IEEE Access, vol. 8, pp. 75223–75236, 2020.

[108] J. Nubert, S. Khattak, and M. Hutter, "Graph-based multi-sensor fusion for consistent localization of autonomous construction robots," in 2022 International Conference on Robotics and Automation (ICRA), pp. 10048–10054, IEEE, 2022.

[109] Y. A. Almansoub, M. Zhong, Z. Hu, G. Huang, M. A. Al-qaness, and A. A. Abbasi, "Multi-scale vehicle localization in underground parking lots by integration of dead reckoning, wi-fi and vision," in 2020 6th International Conference on Big Data Computing and Communications (BIGCOM), pp. 41–49, IEEE, 2020.

[110] Z. Zhang, J. Zhao, C. Huang, and L. Li, "Learning visual semantic map-matching for loosely multi-sensor fusion localization of autonomous vehicles," IEEE Transactions on Intelligent Vehicles, vol. 8, no. 1, pp. 358–367, 2022.

[111] W. Liu, Y. Liu, and R. Bucknall, "A robust localization method for unmanned surface vehicle (usv) navigation using fuzzy adaptive kalman filtering," IEEE Access, vol. 7, pp. 46071–46083, 2019.

[112] W. Farag, "Real-time autonomous vehicle localization based on particle and unscented kalman filters," Journal of Control, Automation and Electrical Systems, vol. 32, no. 2, pp. 309–325, 2021.

[113] Q. Xu, X. Li, and C.-Y. Chan, "A cost-effective vehicle localization solution using an interacting multiple model- unscented kalman filters (imm-ukf) algorithm and grey neural network," Sensors, vol. 17, no. 6, p. 1431, 2017.

[114] Q.-b. Zhang, P. Wang, and Z.-h. Chen, "An improved particle filter for mobile robot localization based on particle swarm optimization," Expert Systems with Applications, vol. 135, pp. 181–193, 2019.

[115] F. Hu and G. Wu, "Distributed error correction of ekf algorithm in multi-sensor fusion localization model," IEEE Access, vol. 8, pp. 93211–93218, 2020.

[116] W. Liu, Z. Li, S. Sun, M. K. Gupta, H. Du, R. Malekian, M. A. Sotelo, and W. Li, "Design a novel target to improve positioning accuracy of autonomous vehicular navigation system in gps denied environments," IEEE Transactions on Industrial Informatics, vol. 17, no. 11, pp. 7575–7588, 2021.

[117] Y. Yan, B. Zhang, J. Zhou, Y. Zhang, and X. Liu, "Real-time localization and mapping utilizing multi-sensor fusion and visual–imu–wheel odometry for agricultural robots in unstructured, dynamic and gps-denied greenhouse environments," Agronomy, vol. 12, no. 8, p. 1740, 2022.

[118] S. Plangi, A. Hadachi, A. Lind, and A. Bensrhair, "Real-time vehicles tracking based on mobile multi-sensor fusion," IEEE Sensors Journal, vol. 18, no. 24, pp. 10077–10084, 2018.

[119] B. Suwandi, T. Kitasuka, and M. Aritsugi, "Low-cost imu and gps fusion strategy for apron vehicle positioning," in TENCON 2017-2017 IEEE Region 10 Conference, pp. 449–454, IEEE, 2017.

[120] H. Kim and I. Lee, "Localization of a car based on multi-sensor fusion," International Archives of the Photogrammetry, Remote Sensing & Spatial Information Sciences, vol. 42, no. 1, 2018.

[121] J. M. Kang, T. S. Yoon, E. Kim, and J. B. Park, "Lane-level map-matching method for vehicle localization using gps and camera on a high-definition map," Sensors, vol. 20, no. 8, p. 2166, 2020.

[122] S. Goel, A. Kealy, V. Gikas, G. Retscher, C. Toth, D.-G. Brzezinska, and B. Lohani, "Cooperative localization of unmanned aerial vehicles using gnss, mems inertial, and uwb sensors," Journal of Surveying Engineering, vol. 143, no. 4, p. 04017007, 2017.

[123] M. Hossain, I. Elshafiey, A. Al-Sanie, et al., "Cooperative vehicle positioning with multi-sensor data fusion and vehicular communications," Wireless Networks, vol. 25, no. 3, pp. 1403–1413, 2019.

[124] D. Wang, H. Zhang, and B. Ge, "Adaptive unscented kalman filter for target tacking with time-varying noise covariance based on multi-sensor information fusion," Sensors, vol. 21, no. 17, p. 5808, 2021.

[125] L. Li and M. Yang, "Joint localization based on split covariance intersection on the lie group," IEEE Transactions on Robotics, vol. 37, no. 5, pp. 1508–1524, 2021.

[126] A. Lima, P. Bonnifait, V. Cherfaoui, and J. Al Hage, "Data fusion with split covariance intersection for cooperative perception," in 2021 IEEE International Intelligent Transportation Systems Conference (ITSC), pp. 1112–1118, IEEE, 2021.

[127] Y. Yao, M. Xu, C. Choi, D. J. Crandall, E. M. Atkins, and B. Dariush, "Egocentric vision-based future vehicle localization for intelligent driving assistance systems," in 2019 International Conference on Robotics and Automation (ICRA), pp. 9711–9717, IEEE, 2019.

[128] W.-C. Ma, I. Tartavull, I. A. Bârsan, S. Wang, M. Bai, G. Mattyus, N. Homayounfar, S. K. Lakshmikanth, A. Pokrovsky, and R. Urtasun, "Exploiting sparse semantic hd maps for self-driving vehicle localization," in 2019 IEEE/RSJ International Conference on Intelligent Robots and Systems (IROS), pp. 5304–5311, IEEE, 2019.

[129] S. B. Cruz, T. E. Abrudan, Z. Xiao, N. Trigoni, and J. Barros, "Neighbor-aided localization in vehicular networks," IEEE Transactions on Intelligent Transportation Systems, vol. 18, no. 10, pp. 2693–2702, 2017.

[130] G. Wan, X. Yang, R. Cai, H. Li, Y. Zhou, H. Wang, and S. Song, "Robust and precise vehicle localization based on multi-sensor fusion in diverse city scenes," in 2018 IEEE International Conference on Robotics and Automation (ICRA), pp. 4670–4677, IEEE, 2018.

[131] R. Zhang, F. Yan, W. Xia, S. Xing, Y. Wu, and L. Shen, "An optimal roadside unit placement method for vanet localization," in GLOBECOM 2017-2017 IEEE Global Communications Conference, pp. 1–6, IEEE, 2017.

[132] I. Hofstetter, M. Sprunk, F. Schuster, F. Ries, and M. Haueis, "On ambiguities in feature-based vehicle localization and their a priori detection in maps," in 2019 IEEE Intelligent Vehicles Symposium (IV), pp. 1192–1198, IEEE, 2019.

[133] B. Yang, L. Guo, R. Guo, M. Zhao, and T. Zhao, "A novel trilateration algorithm for rssi-based indoor localization," IEEE Sensors Journal, vol. 20, no. 14, pp. 8164–8172, 2020.

[134] J. Luomala and I. Hakala, "Adaptive range-based localization algorithm based on trilateration and reference node selection for outdoor wireless sensor networks," Computer Networks, vol. 210, p. 108865, 2022.

[135] C.-H. Ou, B.-Y. Wu, and L. Cai, "Gps-free vehicular localization system using roadside units with directional antennas," Journal of Communications and Networks, vol. 21, no. 1, pp. 12–24, 2019.

[136] J. Fayyad, M. A. Jaradat, D. Gruyer, and H. Najjaran, "Deep learning sensor fusion for autonomous vehicle perception and localization: A review," Sensors, vol. 20, no. 15, p. 4220, 2020.

[137] K. Makkawi, N. Ait-Tmazirte, M. El Badaoui El Najjar, and N. Moubayed, "Adaptive diagnosis for fault tolerant data fusion based on α-rényi divergence strategy for vehicle localization," Entropy, vol. 23, no. 4, p. 463, 2021.

[138] F. Wen and T. Svensson, "Collaborative localization with truth discovery for heterogeneous and dynamic vehicular networks," in 2020 IEEE 91st Vehicular Technology Conference (VTC2020-Spring), pp. 1–5, IEEE, 2020.

[139] M. Barth and M. Todd, "Intelligent transportation system architecture for a multi-station shared vehicle system," in ITSC2000. 2000 IEEE Intelligent Transportation Systems. Proceedings (Cat. No. 00TH8493), pp. 240–245, IEEE, 2000.

[140] X. Yan, H. Zhang, and C. Wu, "Research and development of intelligent transportation systems," in 2012 11th International Symposium on Distributed Computing and Applications to Business, Engineering & Science, pp. 321–327, IEEE, 2012.

[141] Y. Deng, D. Kim, Z. Li, and Y.-J. Choi, "Implementing distributed tdma using relative distance in vehicular networks," IEEE Transactions on Vehicular Technology, vol. 69, no. 7, pp. 7295–7305, 2020.

[142] Z. Wang and A. Lambert, "A low-cost consistent vehicle localization based on interval constraint propagation," Journal of Advanced Transportation, vol. 2018, 2018.

[143] A. Gning and P. Bonnifait, "Constraints propagation techniques on intervals for a guaranteed localization using redundant data," Automatica, vol. 42, no. 7, pp. 1167–1175, 2006.

[144] S. J. Julier and J. K. Uhlmann, "Using covariance intersection for slam," Robotics and Autonomous Systems, vol. 55, no. 1, pp. 3–20, 2007.

[145] P. Wang, L. Mihaylova, P. Bonnifait, P. Xu, and J. Jiang, "Feature-refined box particle filtering for autonomous vehicle localisation with openstreetmap," Engineering Applications of Artificial Intelligence, vol. 105, p. 104445, 2021.

[146] H. Li, F. Nashashibi, and M. Yang, "Split covariance intersection filter: Theory and its application to vehicle localization," IEEE Transactions on Intelligent Transportation Systems, vol. 14, no. 4, pp. 1860–1871, 2013.

[147] W. Niehsen, "Information fusion based on fast covariance intersection filtering," in Proceedings of the Fifth International Conference on Information Fusion. FUSION 2002.(IEEE Cat. No. 02EX5997), vol. 2, pp. 901–904, IEEE, 2002.

[148] P. Yang, D. Duan, C. Chen, X. Cheng, and L. Yang, "Multi-sensor multi-vehicle (msmv) localization and mobility tracking for autonomous driving," IEEE transactions on vehicular technology, vol. 69, no. 12, pp. 14355–14364, 2020.

[149] L. Wei, C. Cappelle, Y. Ruichek, and F. Zann, "Intelligent vehicle localization in urban environments using ekf-based visual odometry and gps fusion," IFAC Proceedings Volumes, vol. 44, no. 1, pp. 13776–13781, 2011.

[150] I. Arasaratnam and S. Haykin, "Cubature kalman filters," IEEE Transactions on automatic control, vol. 54, no. 6, pp. 1254–1269, 2009.

[151] J. Geng, L. Xia, and D. Wu, "Attitude and heading estimation for indoor positioning based on the adaptive cubature kalman filter," Micromachines, vol. 12, no. 1, p. 79, 2021.

Abstract

Data incest problem causes inter-estimate correlation during data fusion process, which yields inconsistent data fusion result. Especially in the multi-sensor multi-vehicle (MSMV) cooperative localization system, the data incest problem is serious due to multiple relative position estimations, which not only leads to pessimistic estimation, but also causes additional computational overhead. In order to address the data incest problem, we propose a new data fusion method named interval split covariance intersection filter (ISCIF). The general consistency of the ISCIF is proven, serving as a supplementary proof for the split covariance intersection filter (SCIF). Moreover, a decentralized MSMV localization system including absolute and relative positioning stages is designed. In the absolute positioning stage, each vehicle uses the ISCIF algorithm to update its own position based on absolute measurements. In the relative position stage, the interval constraint propagation (ICP) method is implemented to preprocess multiple relative position estimates and prepare input data for ISCIF at first. Then, the proposed ISCIF algorithm is employed to realize relative positioning. Furthermore, in order to enhance the robustness of the proposed localization method in MSMV systems, a Kullback–Leibler divergence (KLD)-based fault detection and exclusion (FDE) method is implemented in our system. In addition, comparative simulations demonstrate that the proposed method can achieve accurate, robust and low-cost results compared with the state of the art methods.

Keywords— Data incest; multi-sensor multi-vehicle (MSMV) system; cooperative localization; fault detection and exclusion(FDE); split intersection filter (SCIF)

Résumé

Le problème de consanguinité des données ou data incest en anglais provoque une corrélation entre les estimations pendant le processus de fusion de données, ce qui donne des résultats de fusion de données incohérents. En particulier la localisation coopérative dans le système multi-capteurs multi-véhicules (MSMV) met en evidence le problème deconsanguinité des données qui est grave en raison de multiples estimations de positions relatives, qui ne conduit pas seulement à une estimation pessimiste, mais entraîne également une surcharge de calcul supplémentaire. Afin de résoudre le problème de consanguinité des données, nous proposons une nouvelle méthode de fusion de données appelée filtre d'intersection de covariance divisée par intervalles (ISCIF). La cohérence générale de l'ISCIF est prouvée, servant comme preuve supplémentaire pour le filtre d'intersection de covariance divisée (SCIF). De plus, un système de localisation MSMV décentralisé comprenant des étapes de positionnement absolu et relatif est conçu. Dans l'étape de positionnement absolu, chaque véhicule utilise l'algorithme ISCIF pour mettre à jour sa propre position sur la base de mesures absolues. Au cours de l'étape de position relative, la méthode de propagation par contrainte d'intervalle (ICP) est mise en œuvre pour prétraiter plusieurs estimations de position relative et préparer les données d'entrée pour l'ISCIF. Ensuite, l'algorithme ISCIF proposé est utilisé pour réaliser le positionnement relatif. De plus, pour augmenter la robustesse de la méthode de localisation proposée dans les systèmes MSMV, une méthode de détection et d'exclusion de défauts (FDE) basée sur la divergence Kullback-Leibler (KLD) est implémentée dans notre système. Des simulations comparatives démontrent que la méthode proposée peut obtenir des résultats précis, robustes et peu coûteux par rapport aux méthodes de l'état de l'art.

Mots-clés— Consanguinité des données ; système multi-capteurs multi-véhicules ; localisation coopérative ; détection et exclusion de défauts ; SCIF